UNCLASSIFIED

AD 444111

DEFENSE DOCUMENTATION CENTER

FOR

SCIENTIFIC AND TECHNICAL INFORMATION

CAMERON STATION, ALEXANDRIA, VIRGINIA

UNCLASSIFIED

411411

A STUDY OF DYNAMICALLY LOADED COMPOSITE MEMBERS

TECHNICAL DOCUMENTARY REPORT NO. AFWL TDR-64-35

July 1964

DDC

AUG 1 7 1964

DDC-IRA   C
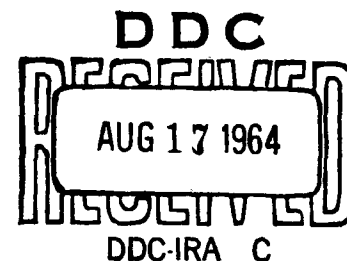
Research and Technology Division
AIR FORCE WEAPONS LABORATORY
Air Force Systems Command
Kirtland Air Force Base
New Mexico

Research and Technology Division
Air Force Systems Command
AIR FORCE WEAPONS LABORATORY
Kirtland Air Force Base
New Mexico

DDC AVAILABILITY NOTICE

FOREWORD

This is the final research report for the Air Force Weapons Laboratory under Contract No. AF 29(601)-5837. The objective of this contract was to extend the basic information on the behavior of concrete beams reinforced with steel plates when subjected to dynamic loadings. Welded steel-stud shear connectors were used at the concrete-steel interface to transfer the shear.

This study resulted in the determination of the increase in flexural resistance of beams loaded dynamically over companion beams loaded statically. The stud capacities for different stud diameters and concrete strengths were determined also. Another important result in this study was the determination of the relationship of stud capacities from dynamic push-out tests with those from beam tests.

On behalf of the authors, I wish to express appreciation to the staff of the Air Force Weapons Laboratory for their assistance in carrying out this investigation. Appreciation is also extended to Professor Hudson Matlock for his assistance with the theory and mathematics involved in this study.

Directing Staff:

J. Neils Thompson, Director and Professor of Civil Engineering

E. A. Ripperger, Associate Director and Professor of Engineering Mechanics

Phil M. Ferguson, Research Engineer (Faculty) and Professor of Civil Engineering

Ned H. Burns, Research Engineer (Faculty) and Assistant
    Professor of Civil Engineering

Ervin S. Perry, Research Engineer Associate I

Larry J. Kilgore, Research Engineer Assistant II

James T. Houston, Research Engineer Assistant I

J. Neils Thompson
Director
Structural Mechanics Research Laboratory
The University of Texas
Austin, Texas

January 1, 1964

ABSTRACT
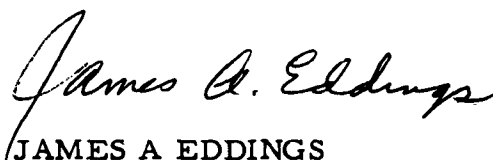
The purpose of this study was to extend the basic information on the behavior of concrete beams reinforced with steel plates and loaded both statically and dynamically at their center lines. The test beams had a steel plate either on the bottom serving as tensile reinforcement or on the top serving as compression reinforcement. Steel studs welded to the plate were used to transfer the shear at the concrete-steel interface. Stud behavior was determined from special push-out tests loaded both statically and dynamically. Comparisons of behavior as obtained from beam and push-out tests were made. The principal variables studied were stud diameter, concrete strength, number of studs per shear span, and type of load.

Dynamic loads were obtained by dropping a mass onto a cushioning material resting on the specimen which provided load pulses with two positive slopes. An initial rise time of 3 to 9 milliseconds and a total duration up to 120 milliseconds, and loads up to 80 kips were obtained.

The results of this study indicate that beams loaded dynamically have approximately a 50 percent greater flexural resistance than companion beams loaded statically. The results from dynamic push-out tests and beam tests with web reinforcement compared favorably and indicated that stud capacities vary directly with stud diameter and concrete strength. Various recommendations for use in beam design are presented.

PUBLICATION REVIEW
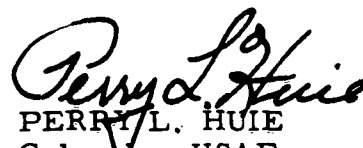
This report has been reviewed and is approved.

James A. Eddings

JAMES A EDDINGS
Lieutenant   USAF
Project Officer

Thomas J. Lowry, Jr.

THOMAS J. LOWRY, JR
Colonel   USAF
Chief, Civil Engineering Branch

Perry L. Huie

PERRY L. HUIE
Colonel   USAF
Chief, Research Division

CONTENTS

CONTENTS
(Cont'd)

CONTENTS
(Cont'd)

LIST OF FIGURES

LIST OF FIGURES
(Cont'd)

LIST OF FIGURES
(Cont'd)

LIST OF TABLES

LIST OF SYMBOLS

The following symbols are used in this report. Other symbols not listed below are defined where they are used.

A = Beam cross-sectional area, in.^{2}

C = Compressive force in plate, lb

d = Stud diameter, in.

$\Delta_{\mathfrak{C}}$ = Beam deflection at center line, in.

E_c = Young's Modulus of concrete, lb/in.^{2}

E_s = Young's Modulus of steel, lb/in.^{2}

f'_c = Ultimate compressive concrete strength, lb/in.^{2}

I = Moment of inertia, in.^{4}

k = Initial slope of load pulse, lb/sec

k_1 = Final slope of load pulse, lb/sec

L = Beam length, in.

M = Beam moment, in. -lb

m = Variable in summation of series

N = Number of studs per shear span

n = Number of modes of vibration

ω_n = Fundamental frequency of vibration, rad/sec

P = Total force on beam, lb

π = Mathematical constant

R = Average force per stud, lb

R_{dc} = Ultimate dynamic stud capacity, lb

$R_{d_{0.02}}$ = Dynamic stud capacity at slip of 0.02 in., lb

$R_{d_{0.04}}$ = Dynamic stud capacity at slip of 0.04 in., lb

$R_{d_{0.06}}$ = Dynamic stud capacity at slip of 0.06 in., lb

R_e = Highest load per stud which permits essentially all beam deflection to be recovered upon removal of the load, lb

ρ = Mass per unit volume, $\dfrac{\text{lb} - \text{sec}^2}{\text{in.}^4}$

s = Shear span, in.

t = Time, sec

t_d = Load pulse duration, sec

t_r = Load pulse rise time, sec

T_n = Fundamental period of vibration, sec/cycle

T = Tensile force in plate, lb

θ = Slope of beam

V = Vertical shear in beam, lb

x = Distance along beam, in.

x' = Distance along beam to point of load application, in.

y = Beam deflection, in.

SECTION 1. INTRODUCTION

1.1   General Remarks and Background

In various underground protective construction, such as the
Minuteman Missile Silos in use by the United States Air Force, plate
steel is being used as a liner on one side of the concrete. The most
efficient structural use of the materials is obtained when the concrete
and steel act compositely. To develop composite action, an adequate
shear connection must be provided at the concrete-steel interface.
Numerous types of shear connections are available such as welded
stud shear connectors, welded wire fabric, and the use of epoxy to
bond the steel and concrete together at the interface.

A study at the University of Illinois[1] revealed that welded stud
shear connectors are more economical and satisfactory than welded
wire fabric when used in composite beams tested statically. In that
study, basic information concerning stud capacities in composite
beams and composite beam response under static loadings was also
determined. The investigation reported herein was undertaken to
determine similar information for dynamic loadings. Studies were
included in the investigation at the University of Illinois[1] concerning
the analysis and applicability of welded studs to the design of flat
slabs. Even though the purposes of performing the investigation

1

reported herein do not include an application to flat slab design, the findings should be applicable to slabs as well as beams.

1.2 Object

The main objective of this research effort was to extend the basic information on and understanding of the behavior of concrete beams reinforced with steel plates to include the effects of dynamic loadings.

Specific objectives were:

1. To investigate the phenomena associated with the increase of flexural strength of composite members.

2. To study the critical parameters associated with the analysis and design of composite members subject to dynamic loads.

3. To interpret the laboratory test results theoretically and formulate design theories and techniques therefrom.

4. To determine basic data on dynamic capacities of studs for use in design.

In addition to the objectives mentioned above, an analytical study has been performed to determine the elastic deflection response of the type of beam studied in this investigation.[2] Using the method of solution presented in the analytical study, the effect of the shape of the load pulse on the response of the elastic beam was studied. This effect is discussed in Section 3 of this report.

2

1.3 Scope

This investigation consisted of testing statically and dynamically, (1) simply supported composite beams with a concentrated load at midspan, and (2) push-out specimens of the type tested by Viest.[3] The beam tests included: (1) beams with a steel plate at the bottom acting as tensile reinforcement and (2) beams with a steel plate at the top acting as compressive reinforcement. Two beams were reinforced concrete beams tested without a steel plate in either tension or compression. A break-down of the types of tests performed follows in Table 1.1. A detailed listing of specimen data is given in Table A-1 in Appendix A.

TABLE 1.1

SUMMARY OF TESTS PERFORMED

Type of Specimen	Static Test	Dynamic Tests
Beams with a plate in tension	3	13
Beams with a plate in compression	3	5
Beams without a plate	1	1
Push-Out Specimens	2	12
TOTAL	9	31

The two main variables studied in this investigation were stud diameter and concrete strength. Two sizes of studs were studied: 1/2-in. dia. and 5/8-in. dia. studs. The ultimate compressive strengths of the concretes used in the specimens varied from 2500 psi to 6150 psi. Most of the specimens can be grouped according to concrete strengths into two categories: (1) specimens with concrete compressive strength approximately 3000 psi and (2) specimens with concrete compressive strength approximately 5000 psi.

This investigation also included a study of: (1) type of loading, (2) number of studs per shear span, (3) web reinforcement in the beams, and (4) successive dynamic loadings.

A correlation between stud capacities as found from beam tests and as found from push-out-specimen tests is also given.

4

SECTION 2. DESCRIPTION OF TEST SPECIMENS AND TEST PROCEDURES

2.1 General Remarks

As stated in Section 1, the main objective of this investigation was to extend the basic information on and understanding of the behavior of concrete beams reinforced with steel plates to include the effects of dynamic loadings. To this end, beams reinforced with a steel plate at the bottom on the outer side of the concrete and connected to the concrete with welded steel studs were tested both statically and dynamically. These beams will hereafter be referred to as the plate-in-tension series. Beams, having the same size as the beams in the plate-in-tension series, but reinforced with a steel plate at the top on the outer side of the concrete were also tested both statically and dynamically. These beams will subsequently be referred to as the plate-in-compression series.

After this investigation was started, it was determined that to understand fully the behavior of dynamically loaded composite beams, the dynamic capacity of the steel studs needed to be obtained for various concrete compressive strengths and stud sizes. To accomplish this, a type of direct shear specimen similar to the specimen tested by Viest[3] was tested dynamically. These specimens will subsequently be referred to in this report as push-out specimens.

2.2 Explanation of Test Specimen Numbering System

At the beginning of this investigation, a specimen numbering system consisting of a Roman numeral, an Arabic number, a letter, and another Arabic number, in that order, was tentatively adopted. Two examples follow:

```
       I              4              S              5
        \             ↑              ↑               \
         \            |              |                \
                  Specimen        Type of       Approx. f'c in
  Phase I         Number           Test            Kips per
                                 Static or          sq in.
                                 Dynamic
         /            |              |                /
        ↓            ↓              ↓                ↓
       I              9              D              3
```
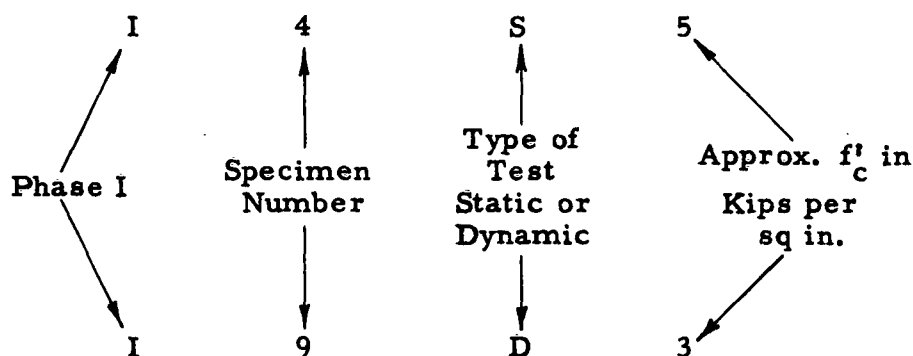
Later, it became desirable to have a numbering system that would give more details about the specimens. Consequently, a numbering system was adopted consisting of either five or six entries using alternately Arabic numbers and letters. Two examples of this numbering system along with an explanation of the entries follow:

```
    10            D            5            A            9
    ↑             ↑             \            \            \
    |             |              \            \            \
 Specimen     Type of      Approx. f'c in            Number of      Push-Out
 Number        Test          Kips per      Stud      Studs per      Specimen
             Static or        sq in.       Size     Shear Span
             Dynamic
    |             |              /            /            /            /
    ↓             ↓             ↓            ↓            ↓            ↓
    23            D            3            A            4            P
```

6
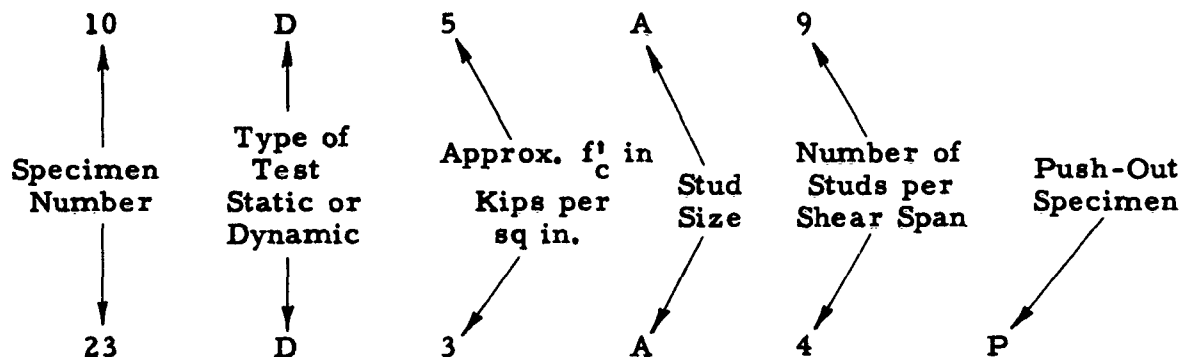
First Entry   --   Specimen identification number

Second Entry   --   S. . . . . . Static Test

                       D. . . . . . Dynamic Test

Third Entry   --   3. . . . . . . f'_c = approximately 3000 psi

                       5. . . . . . . f'_c = approximately 5000 psi

Fourth Entry   --   A. . . . . . 1/2-in.-dia. studs, plate in tension

                       B. . . . . . 5/8-in.-dia. studs, plate in tension

                       C. . . . . . 1/2-in.-dia. studs, plate in compression

                       D. . . . . . 5/8-in.-dia. studs, plate in compression

Fifth Entry   --   Number of studs per shear span or total number of studs in push-out specimens

Sixth Entry   --   P. . . . . . Indicate push-out specimens only.

The latter specimen-numbering system will be used throughout this report. However, the first numbering system will be seen in some photographs.

2.3 Test Specimens

Beams. The general geometric properties common to all beams tested in both the plate-in-tension series and the plate-in-compression series are shown in Fig. 2.1. Specific dimensions such as stud spacing and stirrup spacing for each individual specimen are shown in Fig. A-1 through Fig. A-3 in Appendix A. The dimensions shown in Fig. 2.1 were selected to give the best combination for existing metal forms and the test facility. According to Howland and Egger[4] the increase in the

7

STEEL PLATE

CONCRETE

LOAD

6" — 36" — 36" — 6"

12"

8"

4"

SIMPLE
SUPPORT

SIMPLE
SUPPORT

1/4"

2"

PLATE-IN-TENSION BEAM

STEEL PLATE

CONCRETE

LOAD

6" — 36" — 36" — 6"

1/4"

2"

6"

8"

4"

2-NO.8 BARS

12"

SIMPLE
SUPPORT

SIMPLE
SUPPORT

END ANCHOR PLATE
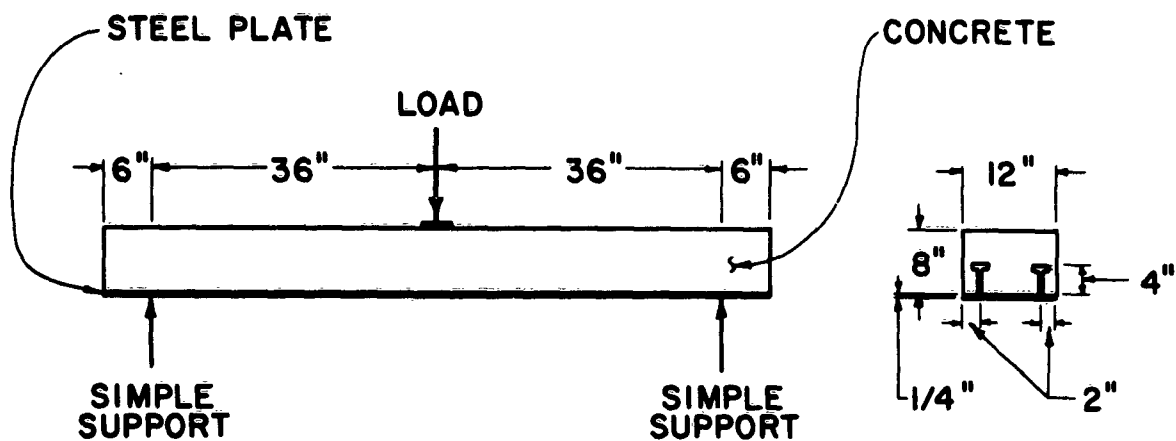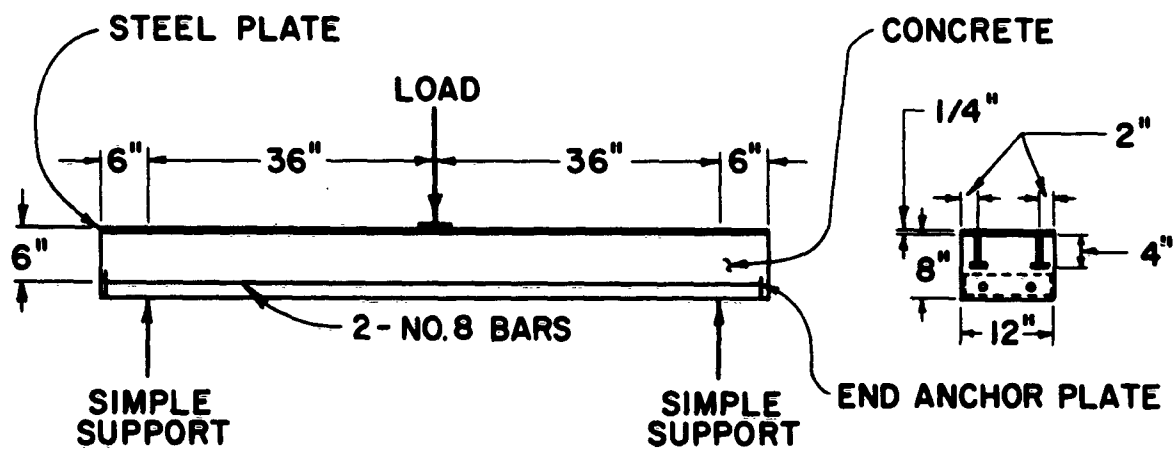
PLATE-IN-COMPRESSION BEAM

FIG. 2.1. GENERAL GEOMETRIC PROPERTIES OF BEAMS
FOR PLATE-IN-TENSION SERIES, AND BEAMS
FOR PLATE-IN-COMPRESSION SERIES.

8

dynamic fully plastic resistance over the static fully plastic resistance for steel beams is a function of the specimen material and not the conformation of the specimen. Assuming that this same reasoning is valid for members composed of materials which act compositely, only one size of beam specimen was believed to be necessary. A shear span of 36 in. was chosen to match the shear span used in the Illinois tests. [1]

Push-out specimens. All push-out specimens had the same general size as shown in Fig. 2.2. The only geometric difference between specimens was the location of the studs on the section of 8 WF 24. The steel 8 WF 24 section shown in Fig. 2.2 was reused in several tests. Due to difficulties experienced in welding studs in exactly the same location as previously welded, each specimen had stud locations slightly different. The difference in locations varied only vertically.

Materials. The cement used in this investigation was Type III (high early strength). The steel plates consisted of A-7 steel and the steel reinforcing bars were high strength bars with a static yield strength of approximately 70,000 psi. A detailed description of each of the materials used in the test specimens is given in Appendix B.

Specimen preparation. Metal forms 9 in. deep and 8 ft long were used in casting all beam specimens. The width of these forms was adjustable. All beams were cast with a 1/4-in.-thick, 12-in.-wide steel plate, fabricated with the welded studs, placed in the bottom of the form on top of a piece of 3/4-in.-thick plywood. The steel plate served as the bottom of the form. The total depth of the beam was thus accurately

9

CONCRETE

8WF24 STEEL SECTION

12"

APPROX. 8"

2"

8" 8" 8"

ELEVATION

$3\frac{3}{4}$"

$6\frac{1}{2}$"

$4\frac{1}{2}$"

$3\frac{3}{4}$"
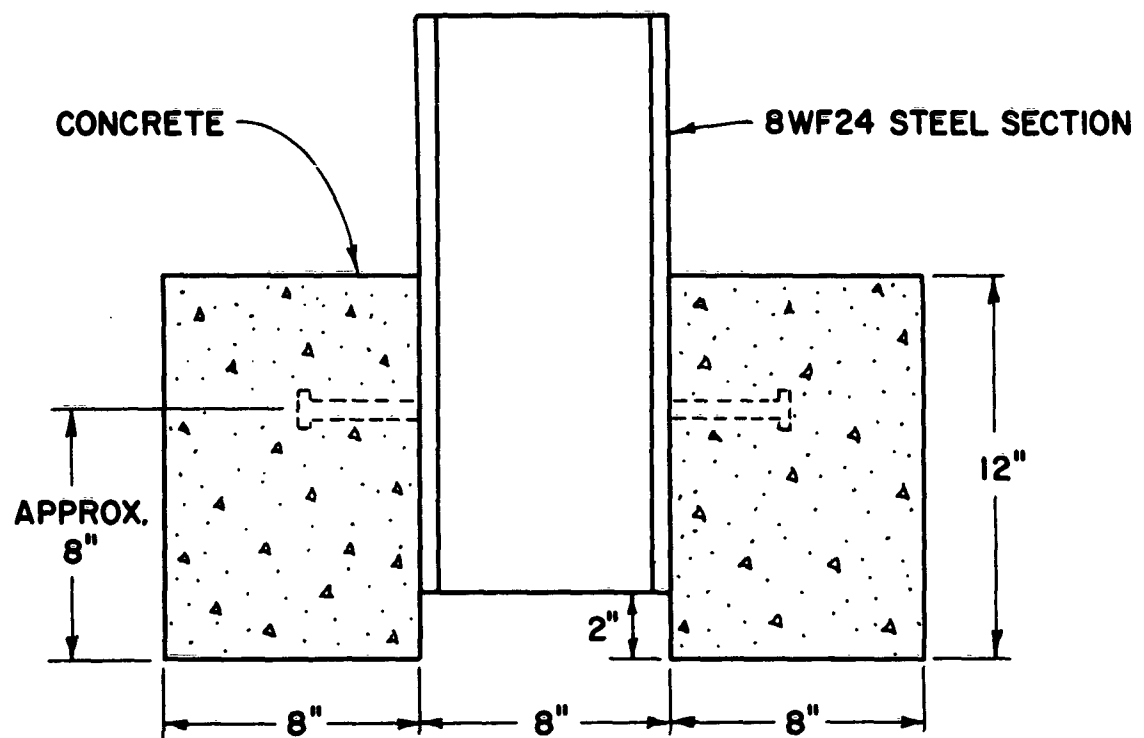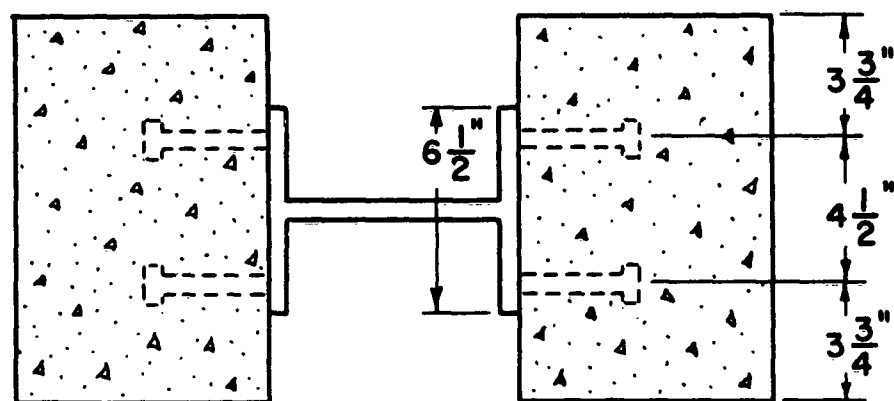
PLAN VIEW

FIG. 2.2. GENERAL DIMENSIONS OF PUSH-OUT SPECIMENS

10

controlled to 8-1/4 inches. Since all of the beams were cast with a plate at the bottom, the beams in the plate-in-compression series were cast in an upside down position. The tensile reinforcing bars and stirrups were supported on chairs to correctly position them.

All concrete was mixed either in a 14-cu-ft capacity or 11-cu-ft capacity mixer. This permitted each specimen to be cast from one batch. When push-out specimens were cast with beam specimens, they too, along with at least three cylinders for compressive strength determinations, were cast from the same batch.

Strain gages were mounted on the steel plates at or near the center line of the steel plate as shown in Fig. A-3 before the plates were placed in the forms. These gages were metal foil gages and were mounted in the usual way using epoxy, until some difficulty in getting the gages to stick was experienced. The usual procedure as recommended by the gage manufacturer was then altered to include lightly sand blasting the back of the gage before mounting. After sand blasting the back of the gages, no bonding trouble was experienced.

All studs were welded to the steel plates in the Structural Mechanics Research Laboratory at The University of Texas using the procedures recommended by the Nelson Stud Manufacturers. One very important step in the procedure was to grind all of the mill scale off the plate at the spot where the studs were to be welded. This was necessary to obtain an adequate weld. All studs were checked visually, and those appearing

to have weak welds were struck briskly with a hammer. If the stud broke off at the weld when tapped, a new stud was welded in that position.

The wire-type, paper-backed strain gages which were put on the concrete were attached according to the gage manufacturer's recommendations with Duco cement. They were cured at least 24 hours before testing. No difficulties were experienced in bonding the gages to the surface of the concrete as the concrete surfaces were very carefully prepared before applying the gages.

All push-out specimens were cast in specially prepared wooden forms which were reusable. No special preparation was necessary for the push-out specimens since no strain gages were attached.

Specimen curing. All specimens, including push-out specimens, were stripped of their forms the next day after casting (approximately 24 hours). The specimens were then carefully wrapped and taped in a reinforced plastic material obtained from the Griffolyn Company in Houston, Texas. This material is specifically designed for curing concrete. All specimens remained wrapped in this plastic material until one day before testing. This material appeared to have effectively prohibited moisture from leaving the specimen due to evaporation.

2.4 Test Setups and Instrumentation

Static tests. A 200,000-lb-capacity Young Testing Machine in the Civil Engineering Laboratory at The University of Texas was used in testing all beams that were tested statically. All beams were simply

12

supported with the applied load concentrated at the center of the beam. The center-line deflection was measured by a dial gage. All strain-gage outputs were fed into switch and balance units and measured by a strain indicator.

One of the static push-out tests was performed using the 200,000-lb Young testing machine and the other one using a 400,000-lb Riehle Testing Machine. Dial gages were mounted on the 8 WF 24 section to measure the slip between the steel and concrete. During the first static push-out test, two slip devices (see Fig. 2.5) were used in addition to the dial gages so that their performance could be checked with the readings from the dial gages.

Measurements taken in dynamic tests. The measurements taken during the dynamic beam tests consisted of:

1. Force on beam at center line.

2. Center line deflection of beam.

3. Reactions at the ends of the beam.

4. Slip between concrete and steel 6 in. inside of the reactions.

5. Strain in steel plate at center line of beams with the plate in tension.

6. Strain in steel plate 3-1/2 in. from center line of beams with the plate in compression.

7. Strain at top fiber of concrete 3-1/2 in. from center line of beams with the plate in tension.

8. Strain in steel reinforcing bars at center line of beams with the plate in compression.

13

Only one end reaction was measured for most beam tests. After comparing the two end reactions in some early tests, it was decided to record only one, thus freeing one channel for use on some other measurement. (Examples of the two reaction measurements can be seen in Figs. 3.3 and 3.4.)

Dynamic beam tests. Figure 2.3 shows a schematic diagram of the test setup used in all dynamic beam tests. Notice that a guided falling mass fell onto a cushioning material which loaded the beam through a plate resting on a load spreader. The cushioning material between the falling mass and the beam was used to shape the load pulse that the beam received. This method of shaping the load pulse was very effective, and it could be controlled adequately within the limits of magnitude and duration desired. The beam was supported at each end by dynamometers which were bolted to a steel base plate. The base plate rested on a concrete base. The two blocks shown under the beam were placed there to catch the beam in case of excessive deflection. This prevented damage to the center line deflection device placed under the beam at the center line (not shown in Fig. 2.3). The straps shown across the ends of the beam held the beam firmly against the supports and prevented the beam from jumping off the supports. This strap offered no resistance to beam rotation at the end.

An accelerometer was mounted on the top of the mass shown in Fig. 2.3 to indicate the mass deceleration, from which the load on the beam at the center line was obtained. A first glance at this setup might

14

GUIDED MASS (STEEL AND LEAD) FALLING FROM VARIABLE DROP HEIGHTS

g

VERMICULITE CONCRETE USED AS CUSHIONING MATERIAL

4" O.D. HEAVY-DUTY PIPE WITH BASE PLATE RIGIDLY ATTACHED

HEAVY-DUTY CONFINING PIPE

DYNAMOMETERS ATTACHED TO STEEL ARMOR PLATE

STEEL PLATE RESTING ON LOAD SPREADER

STRAP HOLDING BEAM ON SUPPORT

BEAM SPECIMEN

BLOCKS TO CATCH BEAM

MASSIVE STEEL ARMOR PLATE RESTING ON CONCRETE BASE

FIG. 2.3.   SCHEMATIC DIAGRAM OF BEAM SETUP FOR DYNAMIC TESTS

15

cause a feeling that there is a serious delay time between the time the
accelerometer senses a deceleration and the time the beam receives
the corresponding force. Tests performed at the Structural Mechanics
Research Laboratory which were similar to these except dynamometers
were placed under the cushioning material, have shown excellent agree-
ment in force measurements as recorded from the accelerometer and
the dynamometers. Further, it can be reasoned that the wave propagation
times for the mass and cushion are approximately equal, which causes
the accelerometer to sense a deceleration at about the same time that
the beam receives the corresponding force.

The weight of the cushioning material, confining equipment, and
plate was approximately one-twentieth of the weight of the mass. The
additional force on the beam due to the inertia of the mass of the
cushioning assembly was therefore neglected. However, this additional
force, along with the inertial forces due to the weight of the beam, was
recorded in the reactions.

The cushioning material shown in Fig. 2.3 is lightweight vermiculite
concrete. Vermiculite concrete was used for all tests except three. A
material made of aluminum and designated as Spiralgrid (see Appendix B
for description) was used in the other three tests. Spiralgrid resulted
in a somewhat smoother load pulse than that obtained with vermiculite
concrete. However, the vermiculite concrete was less expensive than
the Spiralgrid and could be fabricated in the Civil Engineering Materials
Laboratory. The vermiculite concrete was loaded by a heavy-duty pipe

16

with a base plate rigidly attached at the bottom, as shown in Fig. 2.3. This pipe and base plate assembly will be subsequently called the plunger. The base plate on the plunger was varied in diameter to give the desired magnitude of load needed for the different tests.

The mass weighed 2274 lb for all tests. Variable energy transmitted to the beam was attained by dropping the mass from different heights. A complete description of the drop facility is given in Ref. 5.

Dynamic push-out tests. A schematic diagram of the test setup used in all dynamic push-out tests is shown in Fig. 2.4. Notice that the method of loading is very similar to that previously described and used in the dynamic beam tests.

The type of specimen used in these tests was the same as that used by Viest[3] in his static tests. For general dimensions of the specimen, refer to Fig. 2.2.

As the wide flange section was loaded, a shearing action was forced on the studs causing them to shear off, crush the concrete directly under the studs, or a combination of the two. This same basic shearing action is the type of action that exists between the studs and concrete in composite members.

The only measurements that were made in the dynamic push-out tests were (1) total force transmitted to the wide flange section (shearing force on studs) as a function of time, and (2) slip between the concrete and steel on both sides of the specimen as a function of time. These measurements permitted force-slip information to be obtained.

17

MASS (STEEL AND LEAD)
GUIDED DOWN FROM
VARIABLE DROP HEIGHTS

g

4" O.D. HEAVY-DUTY PIPE
WITH BASE RIGIDLY ATTACHED

VERMICULITE CONCRETE
USED AS CUSHIONING
MATERIAL

HEAVY-DUTY CONFINING
PIPE

STEEL PLATE

SECTION OF 8WF24

ARMOR PLATE
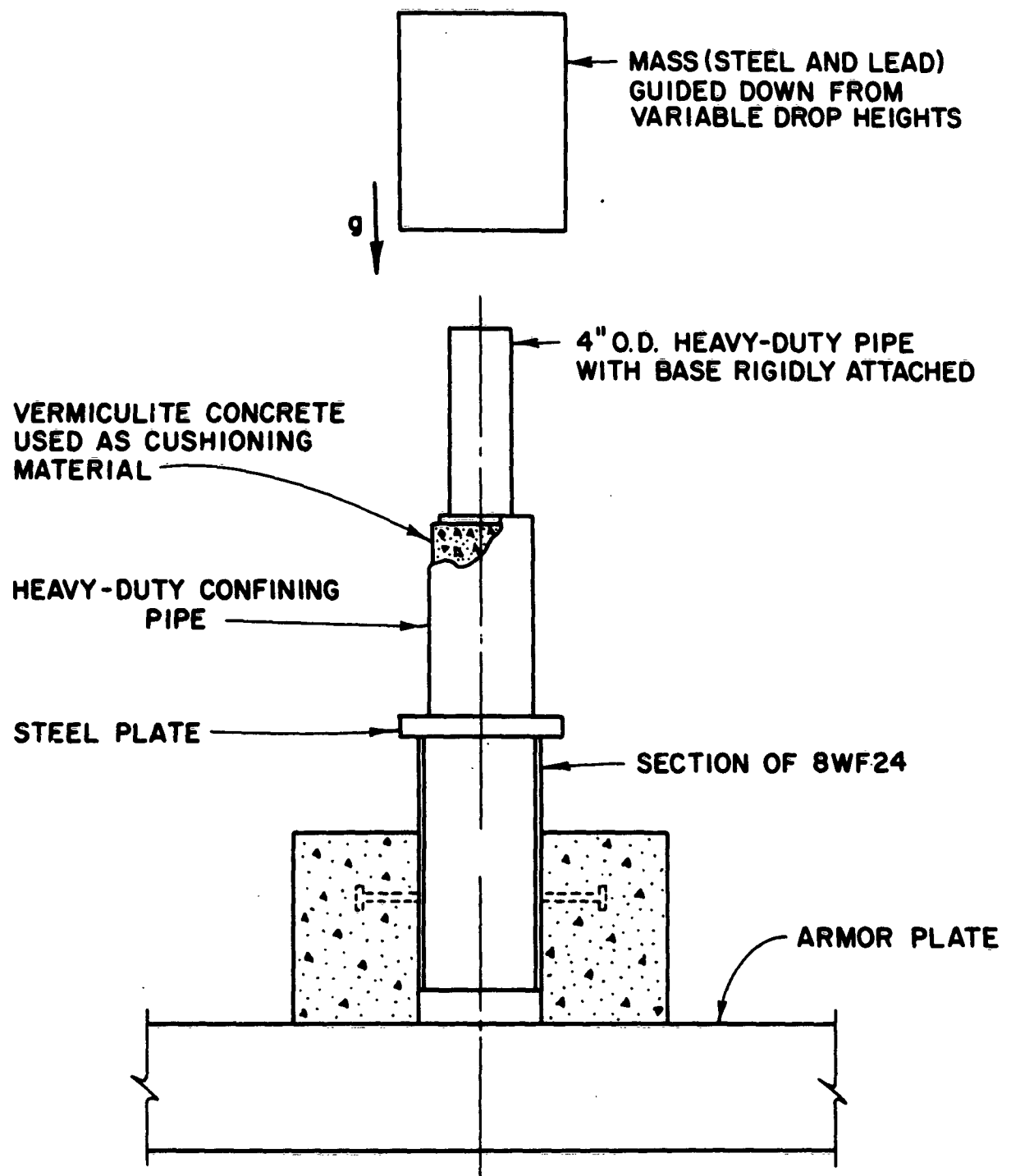
FIG. 2.4.   SETUP FOR DYNAMIC PUSH-OUT TESTS

18

Measuring devices. Various devices were used in making the measurements. These included an accelerometer, dynamometers, a linear potentiometer, slip devices, and strain gages. All of these devices except the slip devices were made by various manufacturers and are described in Appendix B.

The slip devices were conceived, designed, and fabricated in the Structural Mechanics Research Laboratory at The University of Texas. Figure 2.5 shows a slip device along with the way it was attached and used on the beam. The $1/2 \times 3/16$-in. cantilever in the slip device was made from Brown and Sharpe precision-ground tool steel, which had a tensile yield stress of 82, 500 psi.

The slip device was attached to the steel plate by screws. The cantilever was thus attached to the steel plate and positioned vertically along the side of the concrete beam. An adjustable base containing an adjusting screw was attached to the concrete on the side of the beam with epoxy. This adjusting screw was used to deflect the cantilever a predetermined distance before the test. As slip took place, the cantilever was thus deflected back to its equilibrium position. This procedure was used to prevent yielding of the cantilever in the event more slip took place than was anticipated. The measured slip was the value of slip between the concrete and steel.

This type of slip device was used because it was easily adaptable to both static and dynamic tests for the measurement of slip. This device was also used in the push-out tests. Resolutions of $1/1000$-in. slip were easily obtained with this device.

19

$\frac{1}{2} \times \frac{3}{16}$" HIGH-STRENGTH STEEL CANTILEVER

STRAIN GAGES(TWO TRANS-VERSE AND TWO LONGITUDINAL FORMING FULL EXTERNAL BRIDGE CIRCUIT)

HOLES TO ATTACH SLIP DEVICE TO STEEL ON SPECIMEN

SECTION OF $3\frac{1}{2} \times 2\frac{1}{2} \times \frac{1}{4}$" ANGLE

(a) SLIP DEVICE

CONCRETE

BASE ATTACHED TO CONCRETE WITH EPOXY

ADJUSTING SCREW

STEEL PLATE WITH STUDS ATTACHED

END SUPPORT

SLIP DEVICE BOLTED TO STEEL PLATE ON BEAM
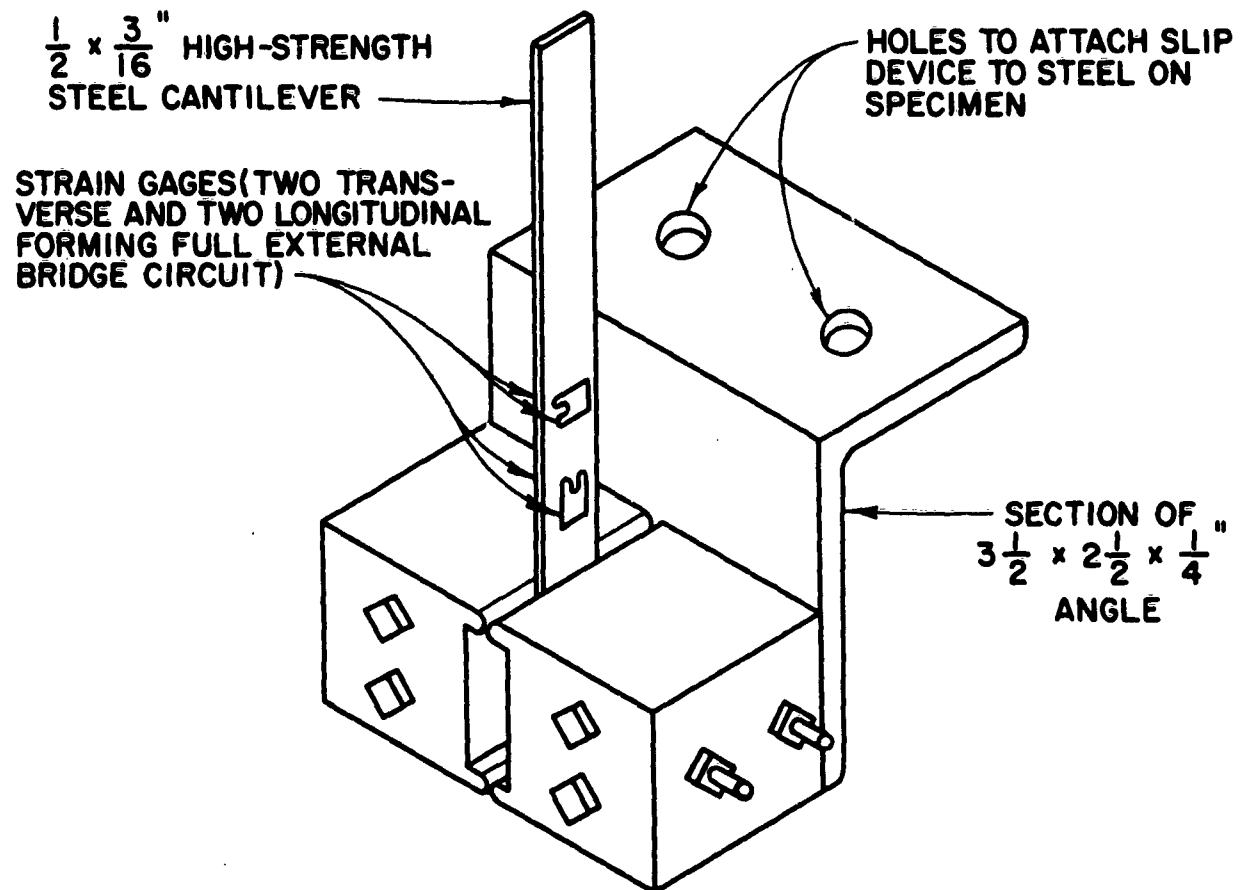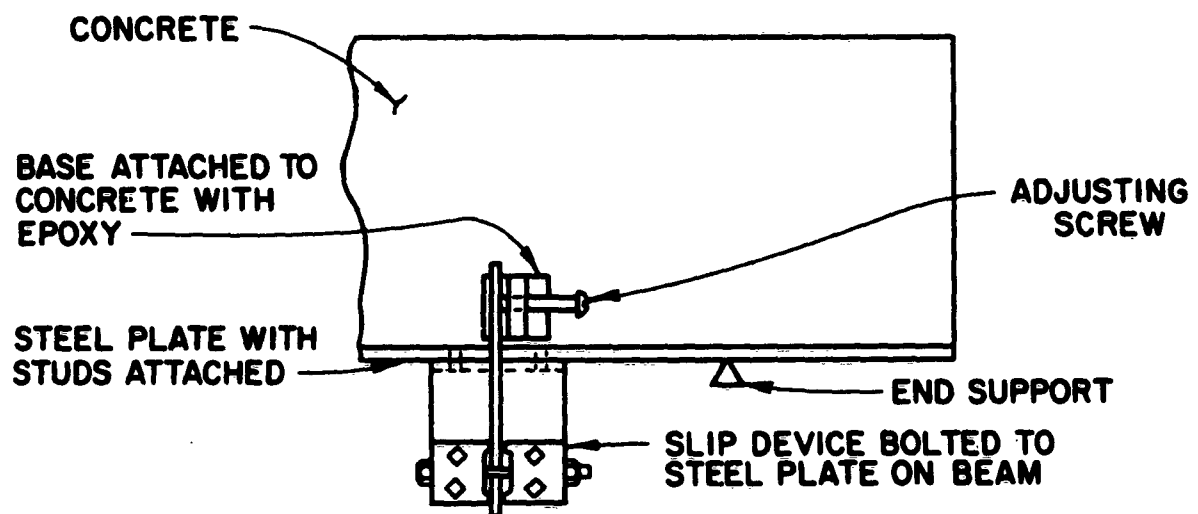
(b) SLIP DEVICE ATTACHED TO CONCRETE BEAM

FIG. 2.5. SLIP DEVICE AND ATTACHMENT

20

The fundamental frequency of one of the cantilevers in the slip device as it was positioned in its supports was 150 cps. The other one had a fundamental frequency of 140 cps. These frequency responses were higher than the fundamental frequency of beam specimen and should have given reliable slip measurements.

Recording equipment. A six-channel Visicorder, an oscilloscope with Polaroid camera, and a high-speed movie camera were used to record the measurements from the dynamic tests. A description of each of these items of equipment is given in Appendix B.

In some of the dynamic beam tests, a total of eight different measurements were made, which required equipment for recording the two additional measurements that the Visicorder could not handle. A dual beam oscilloscope with a polaroid camera attached was used to record these measurements. In all other beam tests in which only seven measurements were made, the six-channel Visicorder and a single beam oscilloscope were used. Since only three different measurements were made in all push-out tests, only the Visicorder was necessary for these tests.

A high-speed movie camera recorded beam action during most tests of beams loaded dynamically. This was done to observe crack development during beam failure. A constant-velocity motor with a dail attached to its shaft was used to indicate the elapsed time during a test.

Calibrations. All measuring devices were calibrated before starting the test program. In general, a bridge arrangement was used to balance the circuits of the various measuring devices. Various shunts were applied across the bridge to deflect the galvonometer which measured

21

the output from the bridge. However, in each case, the physical quantity corresponding to the deflection of the galvanometer had to be determined.

Due to differences in battery voltages supplied to the bridge over a period of time, each measuring device was calibrated by applying known shunts across the bridge immediately before each test. Thus, the calibration marks were recorded on each record for that particular test.

The accelerometer used in this investigation was calibrated by its manufacturer. The calibration data are given in Appendix B. In addition, an automatic calibration could be obtained with each test. Since the accelerations during the tests were small, the one g acceleration resulting from the release of the hook, which held the mass, was comparatively large. This acceleration showed up on the Visicorder record if the Visicorder was started before release of the hook. The accelerometer thus gave an automatic calibration on the Visicorder trace.

The dynamometers were calibrated statically by loading the dynamometers in a testing machine to deflect the galvanometer in the visicorder to correspond to the deflection of the galvanometer due to various shunts.

The linear potentiometer, which was used to measure the center line deflection of the beam, was calibrated by deflecting the potentiometer a known amount before each test, and recording the value of the deflection shown by the galvanometer in the Visicorder.

22

The setup used in calibrating a slip device is shown in Fig. 2.6. The calibration procedure consisted of deflecting the cantilever on the slip device with the adjusting screw the degree necessary to produce the same deflection of the galvanometer in the Visicorder as that produced by various shunts. This actual movement of the cantilever was measured by the dial gage shown in Fig. 2.6.

Calibration data for the strain gages used for measuring strains in the steel plate, concrete, and steel reinforcing bar are given in Appendix B.

Data reduction. The raw data as received from the recording equipment were in the form of Polaroid photographs and traces on Visicorder paper. All quantities were traced with time as the abscissa. A typical Visicorder record and Polaroid photograph are shown in Fig. 2.7. The calibrations for the various measurements are shown on the records.

An Oscar Oscillographic Record Reader and Digitizer was used to digitize the information on the Visicorder traces. These digitized data were then manually plotted on graph paper. A Telecomputing Corporation Telereader was used to replot the Polaroid prints to a larger scale on graph paper.

2.5 Reliability of Measurements

Various checks were made on the measurements taken throughout the test program. Checks on calibration and recalibration were made repeatedly.

23
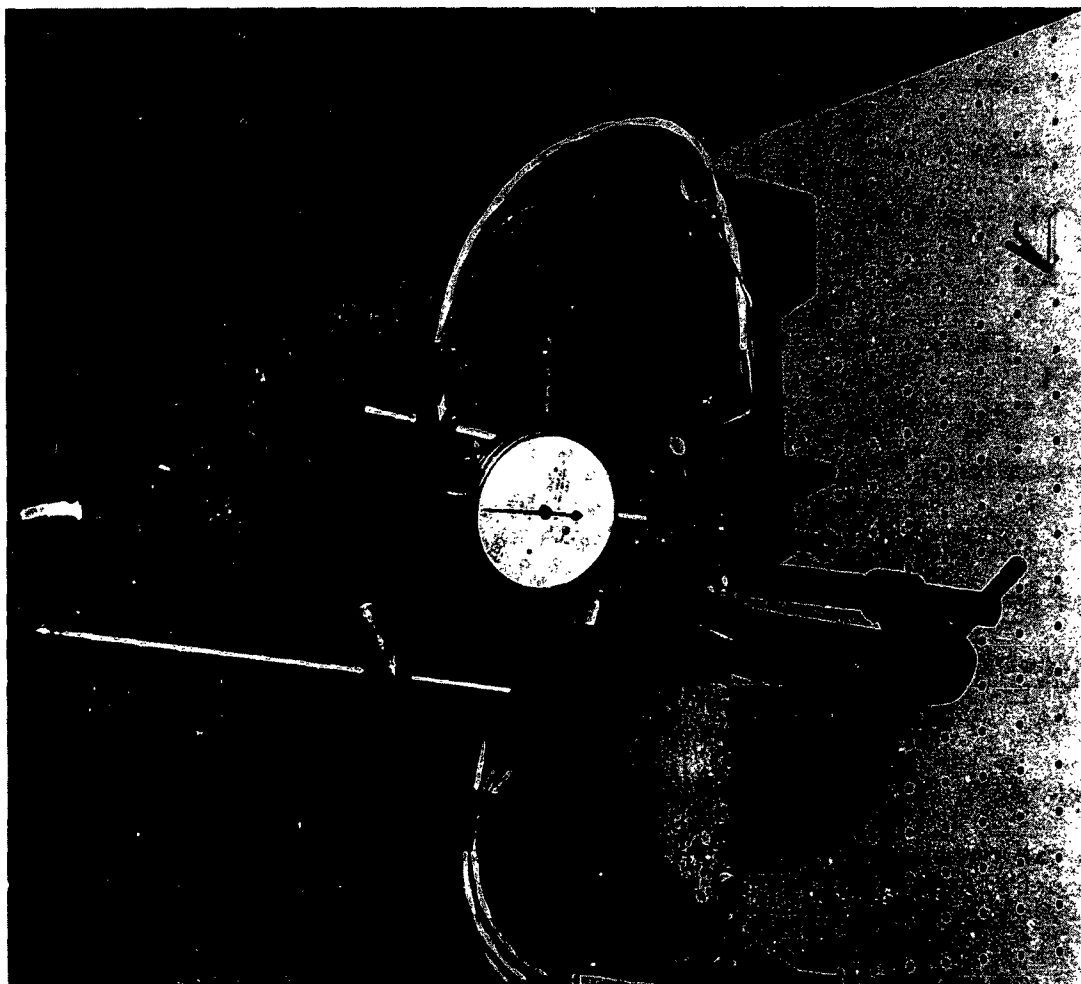
FIG. 2.6. SETUP USED IN CALIBRATING SLIP DEVICES

24

CALIBRATION
MARKS

DROP 16
903 A 6

SOUTH SLIP

0.0601"

CENTER LINE
DEFLECTION

0.50"

NORTH SLIP

SOUTH
DYNAMOMETER

11,400#   0.055"

NORTH
DYNAMOMETER

11,550#

10.1 g

MASS
ACCELERATION

|— 10 MS

VISICORDER   RECORD

CENTER LINE CONCRETE STRAIN

CENTER LINE STEEL STRAIN

STEEL STRAIN
CALIBRATION

0.00231

CONCRETE STRAIN
CALIBRATION

0.00233

|—20 MS
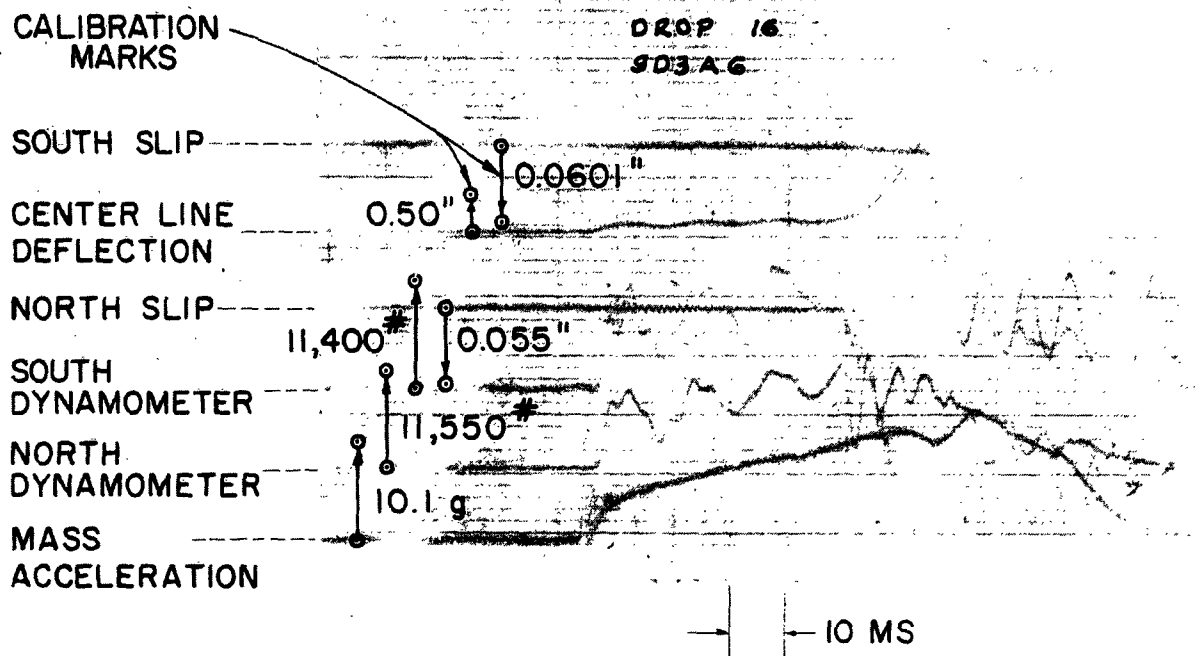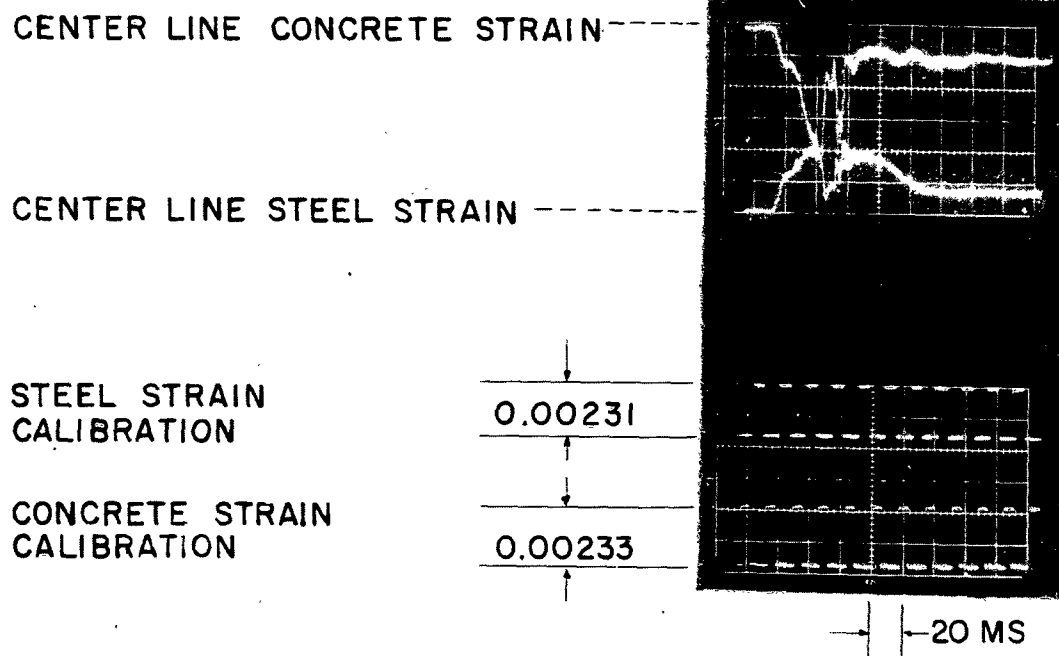
POLAROID PHOTOGRAPH   (DROP NO. 30)

FIG. 2.7. TYPICAL VISICORDER RECORD AND POLAROID
          PHOTOGRAPH

25

As a check on the accelerometer, the acceleration data from the accelerometer were integrated twice,with respect to time, to obtain deformations of the cushioning material. The final deformations thus obtained from various tests were compared with the final measured deformation. These deformations were found to be within 10 percent of each other with the majority being less than 5 percent different.

There were no simple ways of checking the validity of the measurements from the potentiometer, slip devices, and strain gages. Therefore, extreme caution was exercised in making calibrations for these measurements.

SECTION 3. SHAPE OF LOAD PULSE

3.1 Theoretical Considerations

The shape of the load pulse used to impact a beam will change the beam's dynamic deflection response i.e., the ratio of dynamic deflection to static deflection.[*] A study[2] was performed at The University of Texas on the effects of the shapes of load pulses on the deflection response of a simply supported, uniform, elastic beam subjected to a dynamic load pulse at the center line. That study considered shapes of load pulses which could be made up from two distinct slopes as seen in Fig. 3.1.
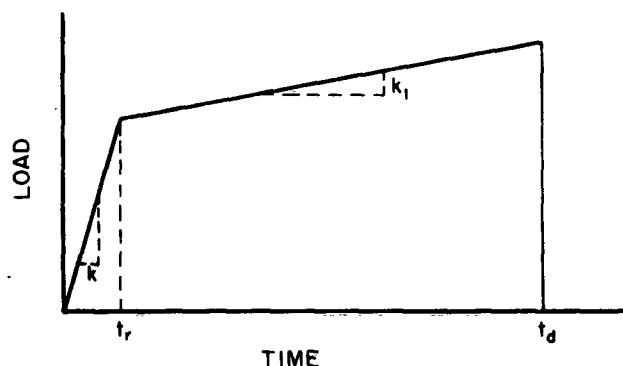
FIG. 3.1. SHAPE OF LOAD PULSE USED
IN ANALYTICAL STUDY

where

k = Initial slope of pulse

k_1 = Final slope of pulse

---

[*]Static deflection as used here denotes the deflection that would be produced by a static load equal in magnitude to that of the dynamic load at the time of interest.

27

t_r = Pulse rise time

t_d = Pulse duration

Of the parameters studied in that investigation, rise time and final slope had the greatest effects on deflection response. Some important effects are given in the following paragraphs for beams in which damping is not considered. It should be remembered while reading the following, which was taken from Ref. 2, that the term response as used herein is defined as a ratio of dynamic to static deflection where both deflections are computed at the time of interest. The dynamic portion is the actual deflection of the point of the beam, while the static portion refers to the deflection which would occur under the same load if no dynamic effects existed.

3.2 Effect of Rise Time

A flat-top load pulse (final slope = zero) of varying rise time will produce a varying maximum response in the beam. The largest maximum ratio of dynamic deflection to static deflection is 2.0 for this type pulse and occurs when the pulse has an instantaneous rise time (t_r = 0), in effect, a rectangular load pulse. If the load pulse has a rise time equal to an integral multiple of the natural period of the beam, the beam will not vibrate after the load becomes constant, i.e., after time $t = t_r$. [2]

3.3 Effect of Final Slope

Positive final slope. A load pulse with an instantaneous initial value and a positive final slope will produce a first maximum response less than 2.0. General trends indicate that the larger the positive final slope, the smaller the maximum response. As the final slope approaches zero, the first maximum response approaches, as an upper limit, the value 2.0.

28

If the final slope is positive, the maximum response, or ratio of dynamic to static deflections at successive peaks will decrease with time. The actual value of the amount of overshoot, or oscillations about the static-deflection curve, does not change from peak to peak.

Rate of decay. The rate of decay of a traingular load pulse with an instantaneous initial value and a linear decay will affect the first maximum response of an elastic beam. General trends indicate that the faster the decay, the larger the first maximum response. As the rate of decay decreases, or as the pulse approaches a rectangular shape, the first maximum response approaches, as a lower limit, the value of 2.0.

For a pulse with a negative final slope, the maximum response at successive peaks will increase with time. Again, the actual amount of overshoot, or oscillation about the static deflection does not change from peak to peak. [2]

From the above effects, it can be seen that rise time of the load pulse is of extreme importance. If the rise time is short enough, dynamic deflections nearly twice the static deflections can be expected, thus causing nearly twice the static stresses if the pulse is long enough. Since steel and concrete exhibit only about a 50 percent increase in yield strength as a maximum when subjected to high rates of strain, it is possible that dynamic yield strengths of materials in beams may be exceeded due solely to a short rise time. Theoretically, a load pulse with the same magnitude but with a longer rise time, can be applied to the beam and not cause the yield strengths to be exceeded.

In general, a rectangular load pulse ($t_r = 0$, $k_1 = 0$) is easier to work with mathematically, but it is very difficult to produce exactly in experimental practice. Therefore, modifications of the rectangular pulse are usually used.

29

3.4 Load Pulse Used

In this investigation, a load pulse with a duration long enough to eventually cause beam failure was desired. It was further desired to have a load pulse which maintained a constant amplitude ($k_1 = 0$) or had a small positive final slope. Since vermiculite concrete (the main cushioning material used) inherently has a small positive final slope in its dynamic stress-strain characteristics, the shape of load pulse shown in Fig. 3.2 was adopted for use throughout this investigation.
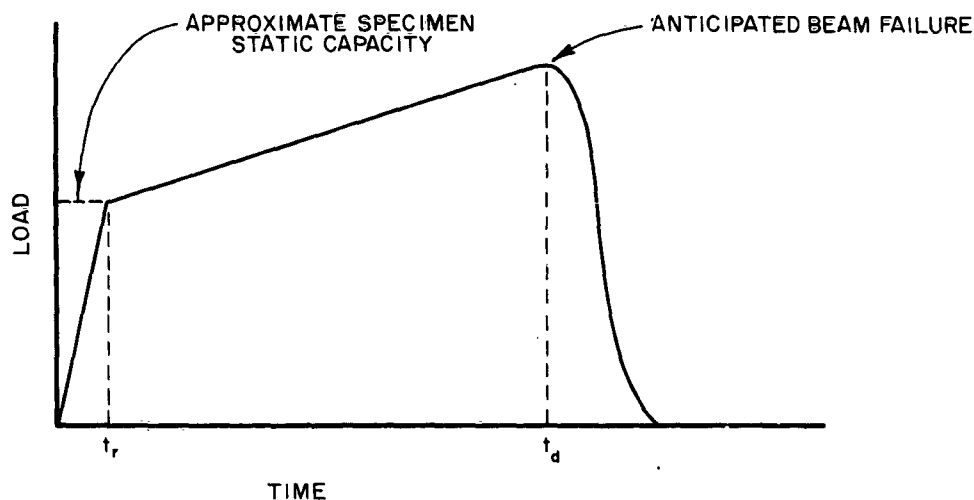
FIG. 3.2. SHAPE OF LOAD PULSE USED IN EXPERIMENTAL STUDY

The rise time varied from approximately 3 to 9 milliseconds and the duration to beam failure varied from about 20 to 120 milliseconds. The majority of the beams failed after a load duration of 40 to 70 milliseconds.

The fundamental period of most beams was approximately 10 milliseconds. The fundamental periods of the beams were computed using a transformed area of the steel and assuming an uncracked

30

section. Measured periods before beam tests verified these results. An effort was made to control the rise time of the load pulse to less than 10 milliseconds. On the other hand, a rise time as long as possible was desired to eliminate some of the ringing[*] inherent in the loading system due to fast rise times. In general, it was desired to have a load-pulse duration longer than twice the fundamental period of the specimen. Due to the tremendous damping quality of composite steel and concrete beams, most oscillations of the beams were damped out completely before two beam periods had elapsed. Therefore, a more accurate beam failure load could be obtained by using the type of load pulse indicated in Fig. 3.2.

Two typical examples of the load pulse used in this investigation are shown in Figs. 3.3 and 3.4. Figure 3.3 is an example of the type of load pulse which was produced when the mass was cushioned by vermiculite concrete. The original record for this load pulse can be seen in Fig. 2.7. Notice that the pulse as presented in Fig. 3.3 has been smoothed at the beginning. It is believed that the ringing present in Fig. 2.7 is due mainly to ringing in the plunger assembly. The dip in the force curve seen in Fig. 3.3 at about 60 milliseconds is due to the beam failing at that time resulting in decreased resistance. The beam resistance increased again after the beam deflected and hit the supports directly under the beam. (See Fig. 2.3.) The mass still had energy to be delivered to the beam at the time the beam hit the supports.

---

[*] The term ringing is used here to denote the oscillations that take place as a result of the impact and the characteristics of the system.

31
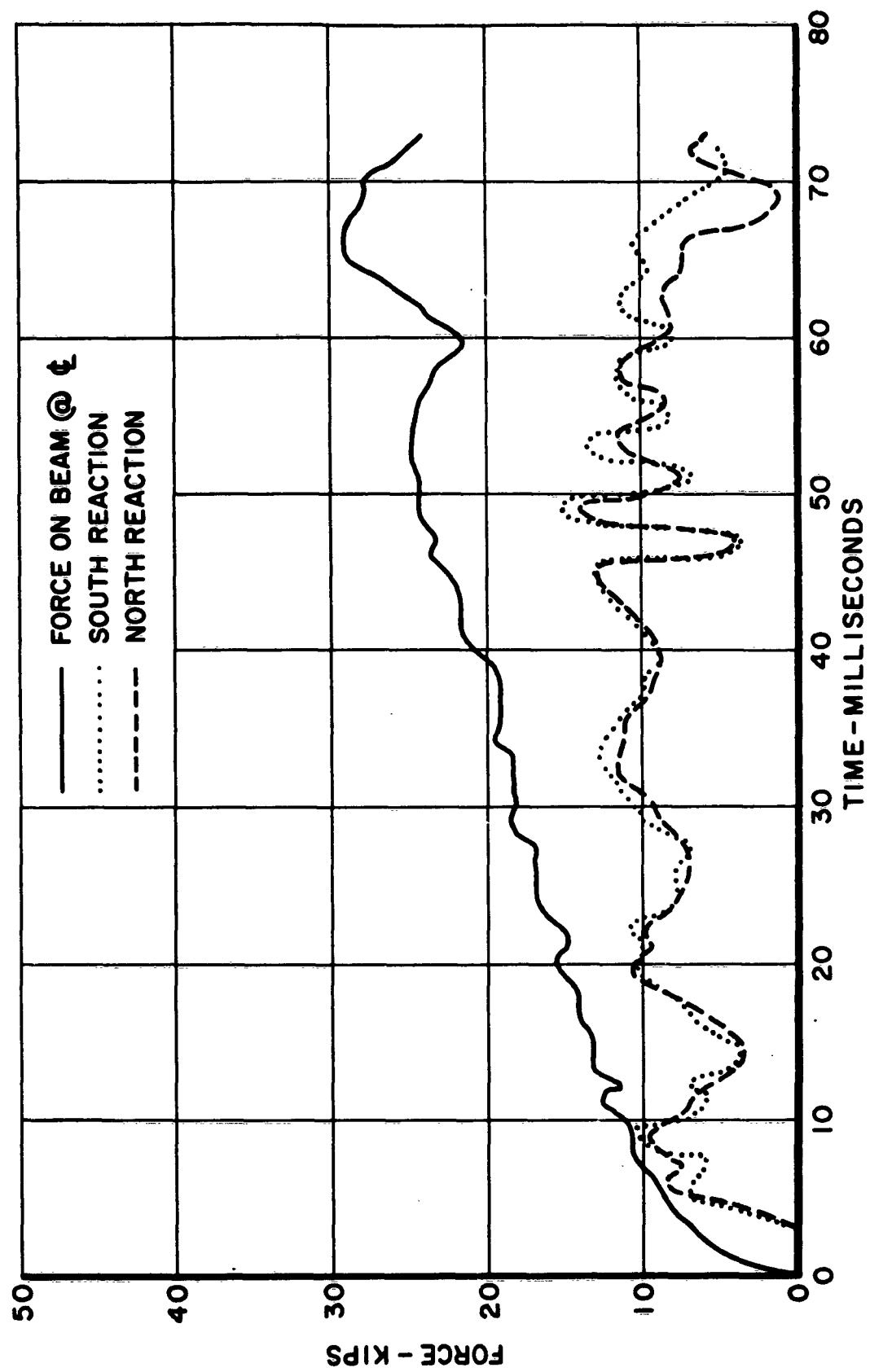
FIG. 3.3. TYPICAL LOAD PULSE USING VERMICULITE CONCRETE AS CUSHION

32
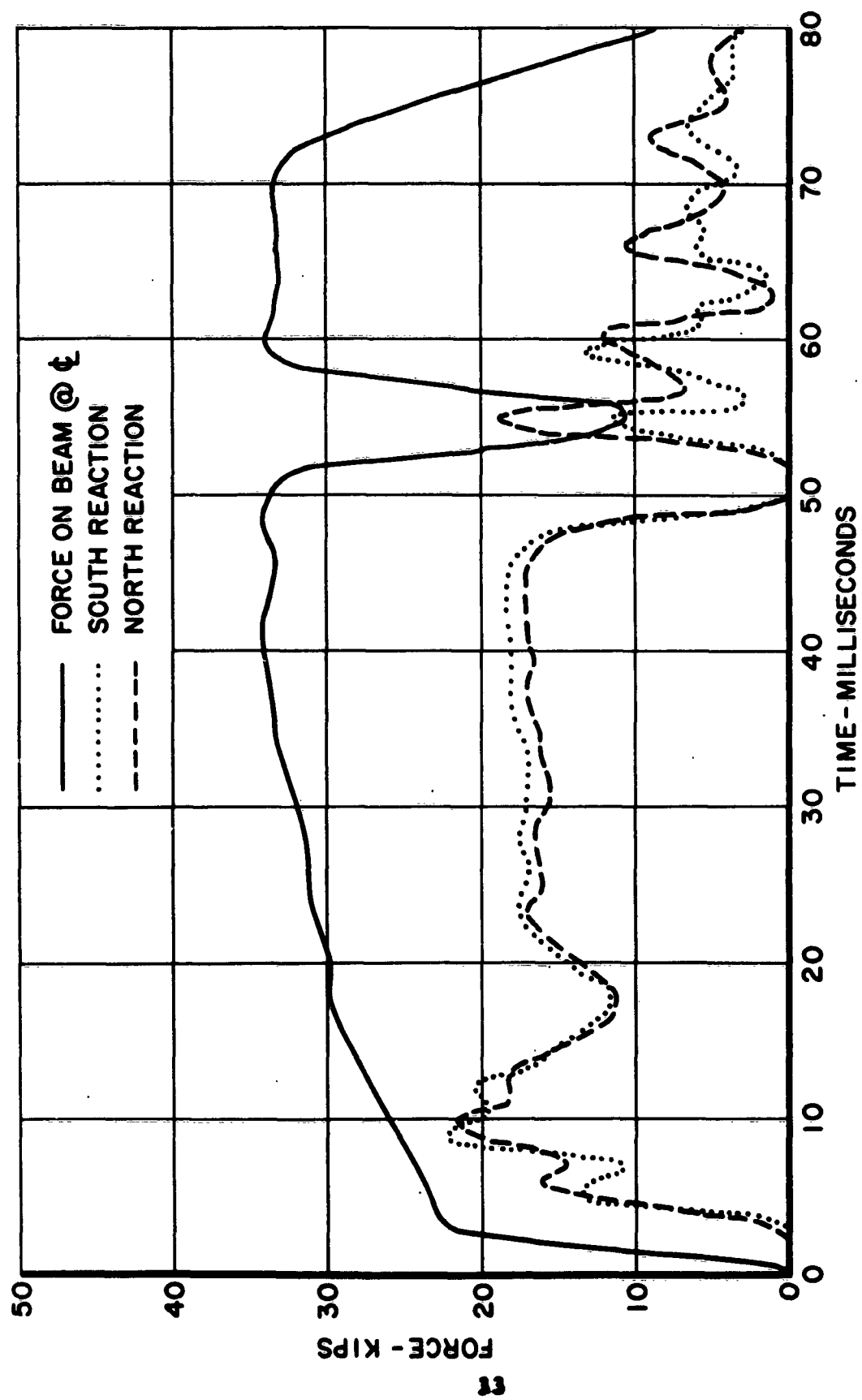
FIG. 3.4. TYPICAL LOAD PULSE USING SPIRALGRID AS CUSHION

Legend:
FORCE ON BEAM @ ₵
SOUTH REACTION
NORTH REACTION

TIME - MILLISECONDS

FORCE - KIPS

33

Figure 3.4 is an example of the type of load pulse obtained when Spiralgrid was used to cushion the mass. Again, notice the dip at about 53 milliseconds denoting beam failure.[*] This force curve has not been smoothed (see Fig. 3.5) as the curve for vermiculite concrete was. Spiralgrid was used for only three dynamic tests. This material could not be altered at the time of test to give a higher or lower force level. Therefore, the beams had to be manufactured to fit the force level produced by the Spiralgrid. However, Spiralgrid is now manufactured with different crushing strengths. Vermiculite concrete offered much more flexibility in this respect.

As seen in Figs. 3.3 and 3.4, the reactions lagged behind the load pulse by 2 or 3 milliseconds at the beginning. Apparently, a short time was required for the beam to deflect and the reactions did not receive any force until some deflection occurred. The wave propagation time in these beams was believed to be very small and therefore had little effect in causing this time lag.

Figure 3.6 shows a typical original visicorder record from a push-out test. The load pulse was of the same general form as those used for the beam tests.

---

[*] The dip in the load pulse was dependent upon the beam resistance as it was failing and also, the beam deflection which had taken place before failure. This accounts for the differences in the dips as seen in Figs. 3.3 and 3.4.

34
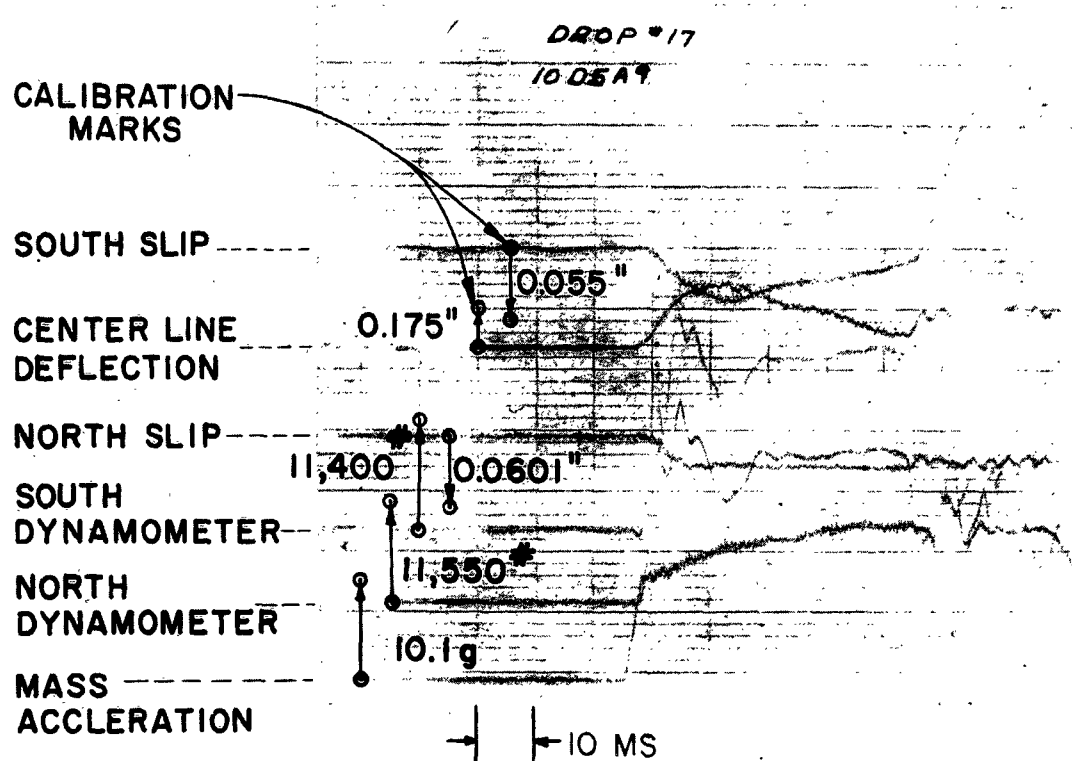
FIG. 3.5. ORIGINAL VISICORDER RECORD USING SPIRALGRID
AS CUSHION
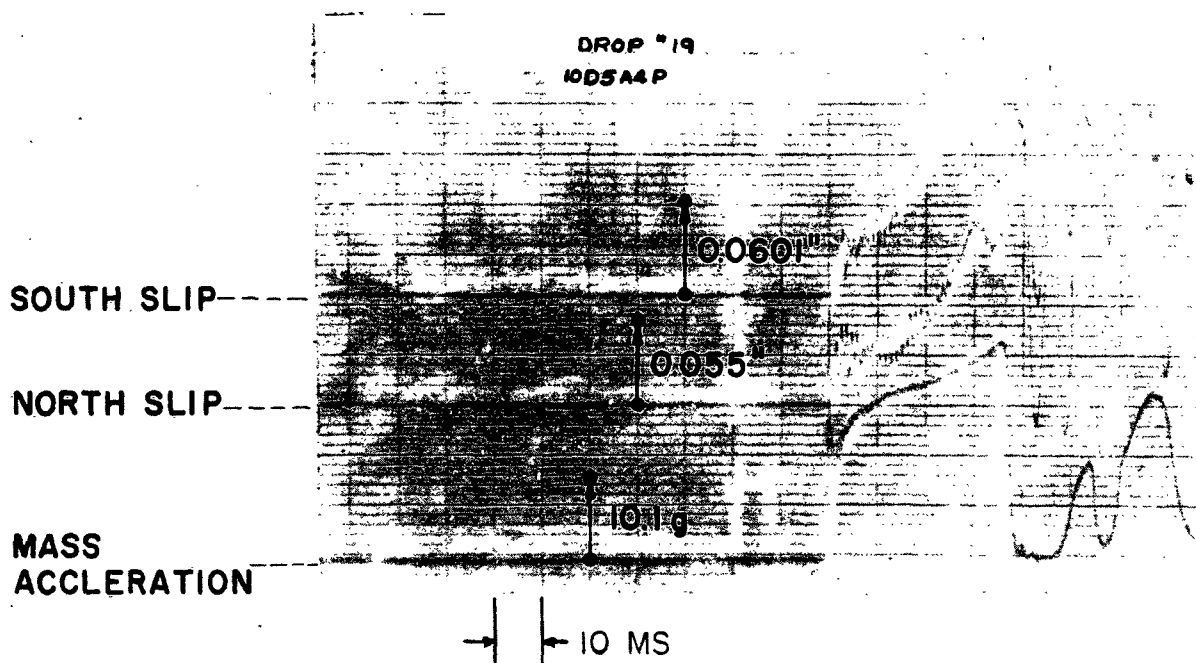
FIG. 3.6. ORIGINAL VISICORDER RECORD OF
PUSHOUT TEST

SECTION 4. RESULTS OF PLATE-IN-TENSION SERIES

4.1 General Remarks

This section contains the results of the tests on 16 specimens with
the steel plate acting as tension reinforcement. Since one of the major
objectives was to study stud capacities, the results are presented in the
form of force per stud vs deflection, and force per stud vs slip curves.
The deflection relationships are beam deflections at the center line.
The slip measurements were made 6 in. inside the supports between
the steel plate and concrete. Force per stud is related to the total load
on the beam by Eq. (4.1).
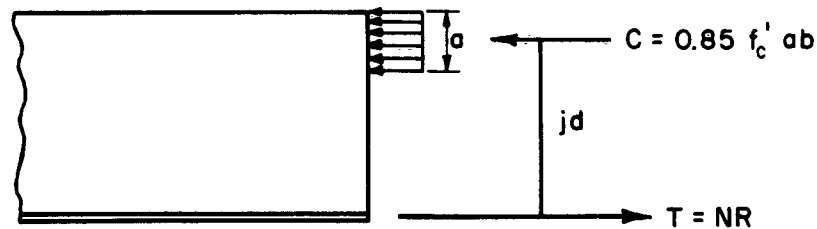
$$R = \frac{Vs}{jdN} = \frac{Ps}{2jdN} \qquad \text{- - - - -} \quad (4.1)$$

where

        R = the average force per stud, lb

        V = the vertical shearing force, lb. For all beams in this
           study $V = P/2$

36

P = the total load on the beam

s = the shear span = 36 in. for all beams in this study

jd = the moment arm, in inches, taken as 7.0 in. for all beams in this study .

N = the total number of studs per shear span

a = the depth of the stress block

b = the width of the beam, in.

T = the tensile force in the plate, lb

C = the compressive force on the concrete, lb

A value of 7.0 in. for jd was used throughout this series because computations revealed that for extreme cases, jd varied from about 8.0 in. to 6.0 inches. At beam failure, jd was approximately 7.0 in. for most of these beams. These values were based upon static analysis, but since for fast rates of straining the steel plate tensile yield strength and the concrete compressive strength increase approximately proportionately, the value of jd remains virtually unchanged.

Equation (4.1) was based upon the assumption that all studs share the horizontal shear equally. This assumption seems valid since the vertical shear was equal throughout the shear span. However, for dynamic loads, it is possible that the studs near the center of the beam will receive a very small force before the studs near the end of the beam. At beam failure, after some plastic flow has occurred, it is believed that all studs share the shear load equally.

Throughout this section, the effects of the various parameters are presented by comparing the results from tests as similar to each other

as possible. Small differences such as concrete compressive strengths
existed, but these differences did not significantly alter the trends
involved.

4.2 Effect of Concrete Strength

Figure 4.1 shows the effect that concrete compressive strength
had on the deflection response of two companion beams with concrete
strengths of approximately 2800 psi and 4000 psi, respectively. These
curves indicate a trend of decreasing deflection with increase in concrete
strengths for identical loads. This trend shows up better for the 5/8-in.-
dia. studs (beams No. 8 and 11) than for the 1/2-in.-dia. studs (beams
No. 10 and 13).*

All curves shown in Fig. 4.1 were cut off at a point where the
beam suddenly broke or at the point where the beam hit the block supports
underneath the center of the beam. Nevertheless, Fig. 4.1 indicates
more ductility in the beams with the higher concrete compressive strengths.

It appears that concrete strength should have a greater effect on
slip between the plate and concrete than on the deflection. Figure 4.2
is a plot of the force-slip curves for the same specimens shown in
Fig. 4.1. Figure 4.2 clearly shows higher forces per stud with the
higher concrete strengths for the same values of slip. The magnitude
of this increase in force per stud varies approximately from 15 to 30
per cent. This increase is the result of an increase in concrete strength

---

*This trend is indicated best for the two tests in which the concrete
strengths were closer. This is probably due to normal experimental
scatter in results.

38
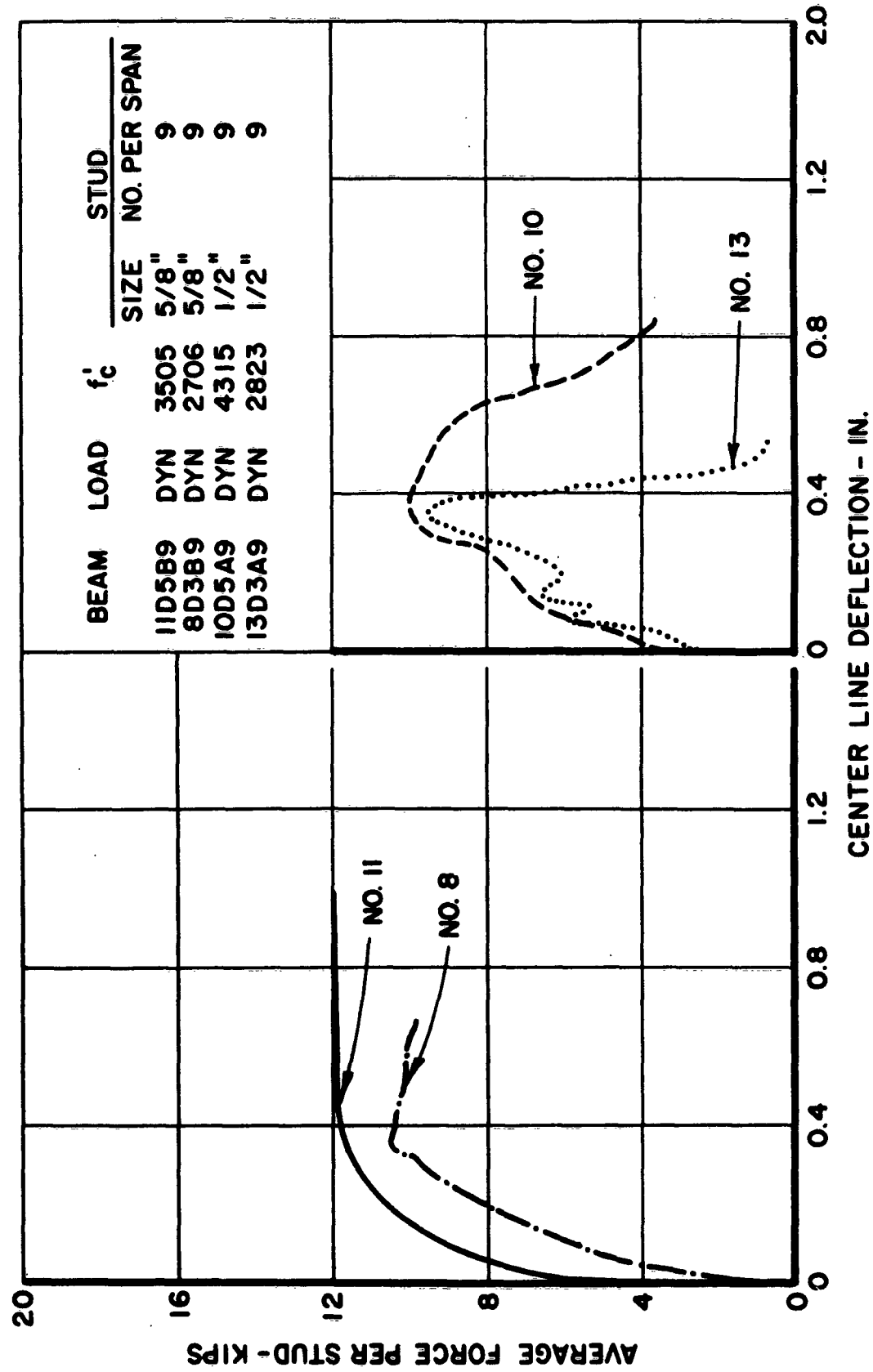
FIG. 4.1. EFFECT OF CONCRETE STRENGTH ON DEFLECTION, PLATE IN TENSION
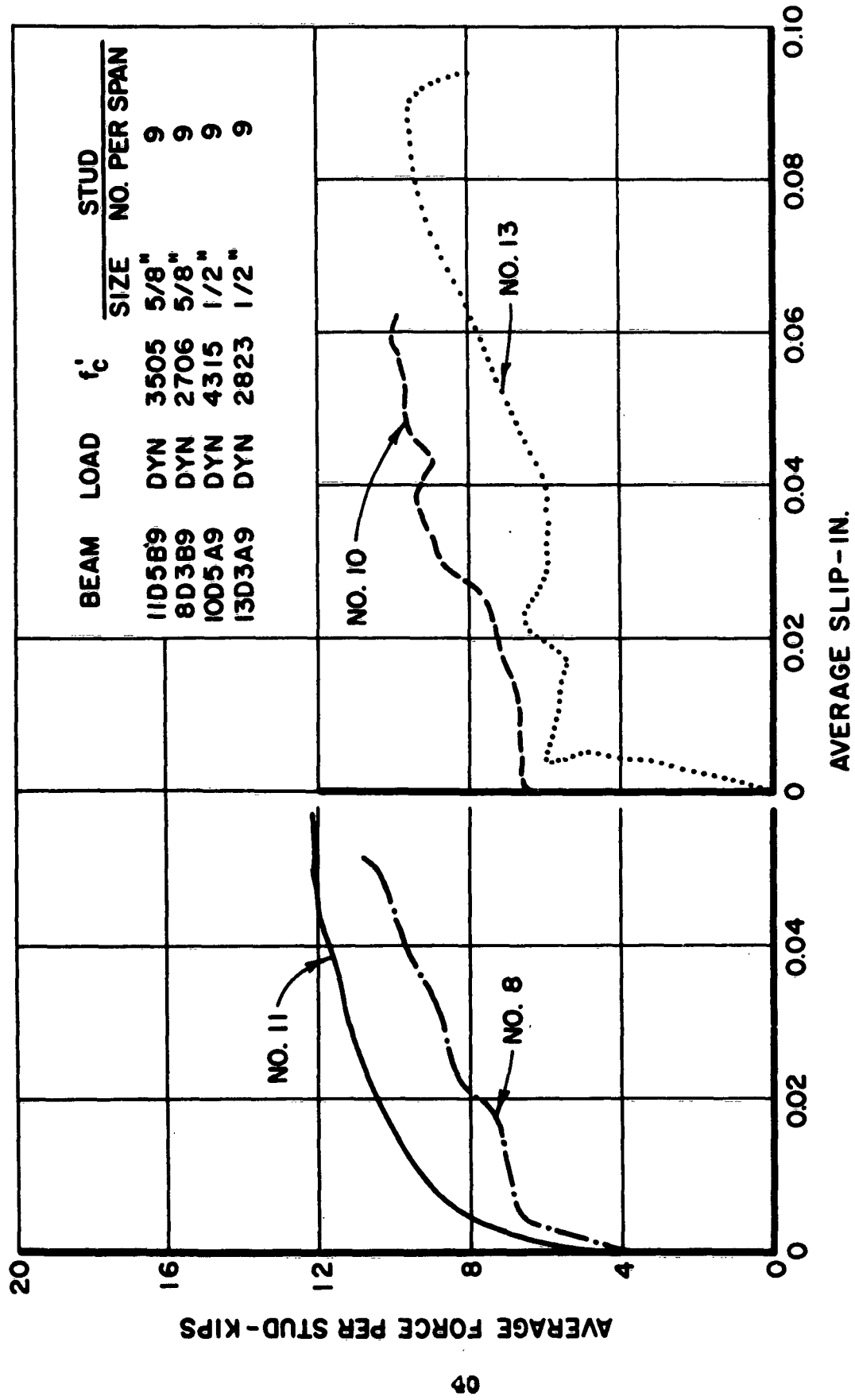
FIG. 4.2. EFFECT OF CONCRETE STRENGTH ON SLIP, PLATE IN TENSION

from approximately 2800 psi to 4000 psi, which is an increase in square roots from a value of 53 to 63. This suggests that the stud capacities vary directly with the square root of the concrete compressive strength.

Even though this section is not devoted to the effect of stud size, Figs. 4.1 and 4.2 show higher forces per stud for the larger studs than for the smaller studs. This is true for both deflection response as well as slip response.

4.3 Effect of Stud Size

In addition to the differences noted in Figs. 4.1 and 4.2 concerning stud size, Fig. 4.3 shows the same trend of higher forces per stud for the larger studs for the same beam deflection. This is to be expected, however, for the larger studs. This trend is more clearly seen in Fig. 4.4. From all of the tests involved in the plate-in-tension series, and also the push-out tests, (discussed in Section 6), it appears that approximately a 50 or 60 per-cent increase was the average value. This increase corresponds to the increase in the square of the diameter of 5/8-in. studs over the square of the diameter of 1/2-in. studs. From these tests and tests performed at the University of Illinois,[1] it appears that forces per stud vary with the cross-sectional area of the studs or the square of stud diameters and the square root of concrete compressive strengths.

Other than the trend mentioned above, stud diameter seemingly has little or no other effect on beam response. Beam ductility is apparently not affected by stud diameter.

41
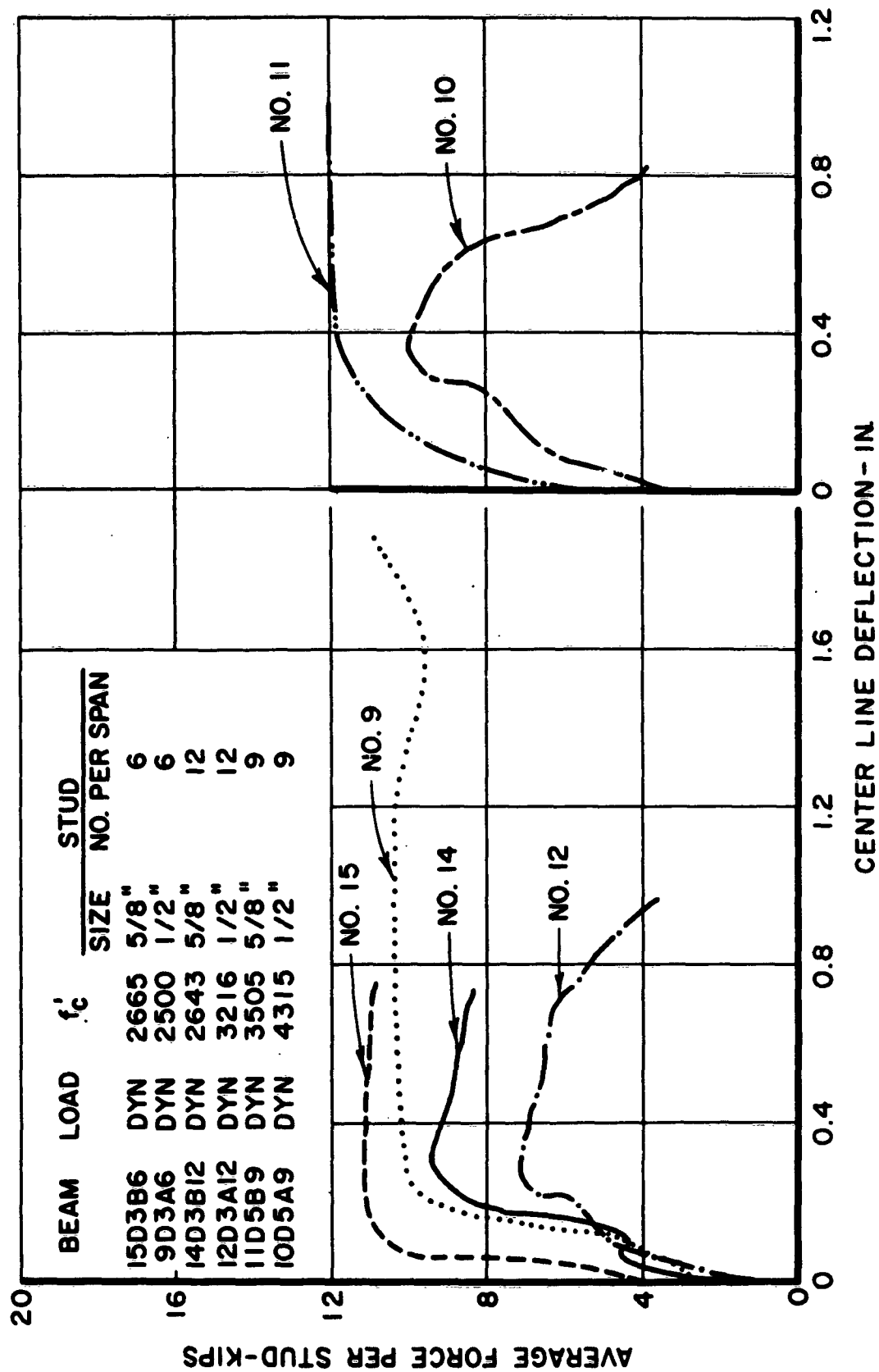
FIG. 4.3. EFFECT OF STUD SIZE ON DEFLECTION, PLATE IN TENSION

42
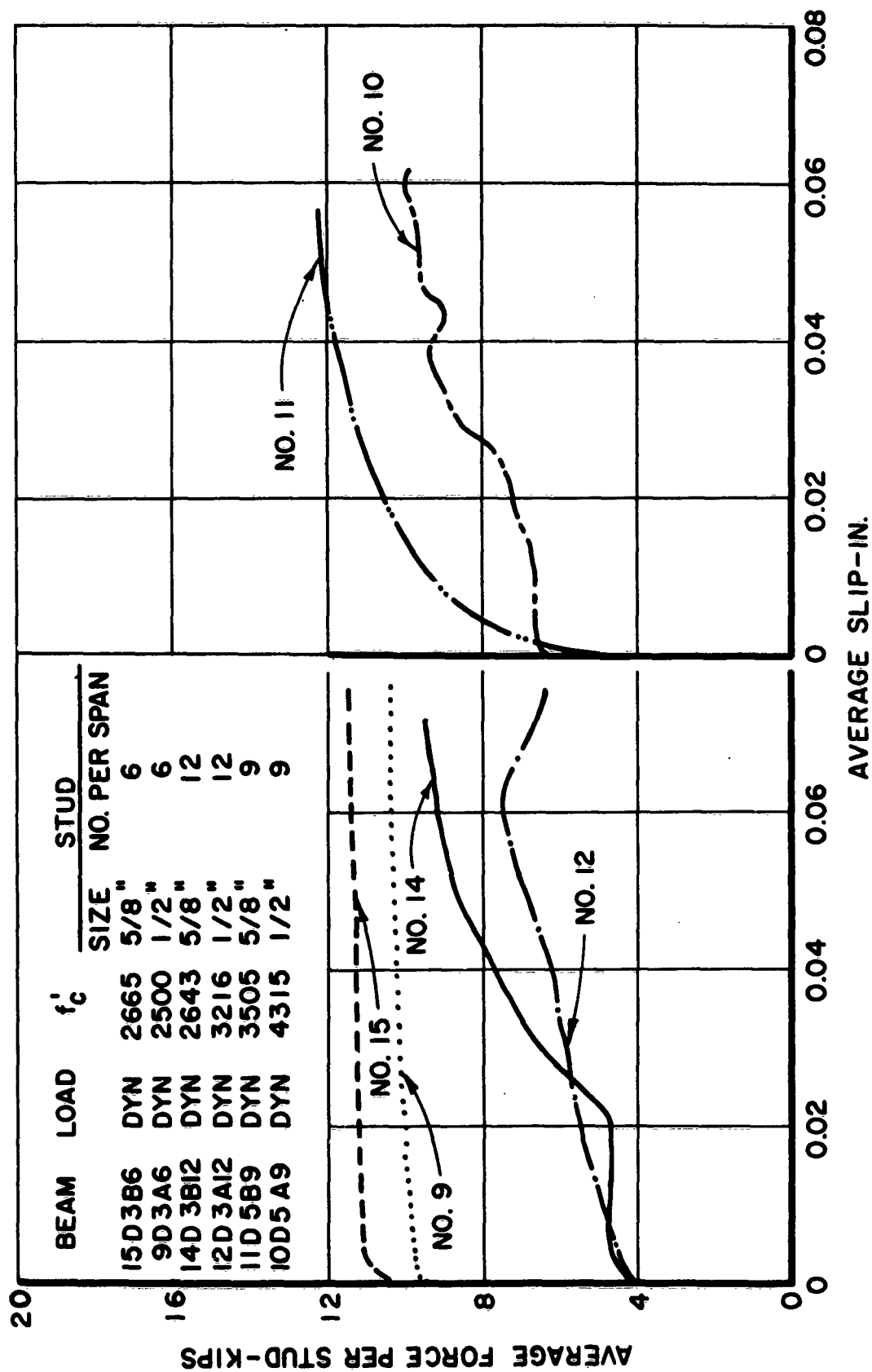
FIG. 4.4. EFFECT OF STUD SIZE ON SLIP, PLATE IN TENSION

43

4.4 Effect of Number of Studs Per Shear Span and Shear Reinforcement

The effect of the number of studs per shear span was studied by comparing force-deflection relationships for 6, 9, and 12 studs per shear span for both 1/2-in., and 5/8-in.-dia. studs. In terms of number of studs per square foot of plate, 6, 9, and 12 studs per shear span corresponds to 2, 3, and 4 studs, respectively.

Figure 4.5 shows the effect of the number of studs per shear span for 1/2-in.-dia. studs. The same effect for 5/8-in.-dia. studs is shown in Fig. 4.6. In Fig. 4.5, the curves for beams No. 9, 12, and 13 show that by increasing the number of studs per shear span, the maximum force per stud decreased. This same trend is present for 5/8-in.-dia. studs as shown by the curves for beams No. 8, 14, and 15 in Fig. 4.6.

A study of the curves in Figs. 4.5 and 4.6 revealed that all the beams studied up to this point had approximately the same ultimate load capacity, regardless of the number of studs per shear span, providing all other variables were the same. This led to a conclusion that the studs were possibly not reaching their ultimate capacities in the beams because of the beams failing prematurely in some other way except primary stud failure. A study of the Fastax movies and the ruptured beams after failure revealed that all beams tested up to this point (and all beams previously mentioned in this section) had failed by diagonal cracks across the beams. Therefore, it was believed that these beams were inherently weak in shear. Since one of the main objectives of this study was to determine stud capacities, shear

44
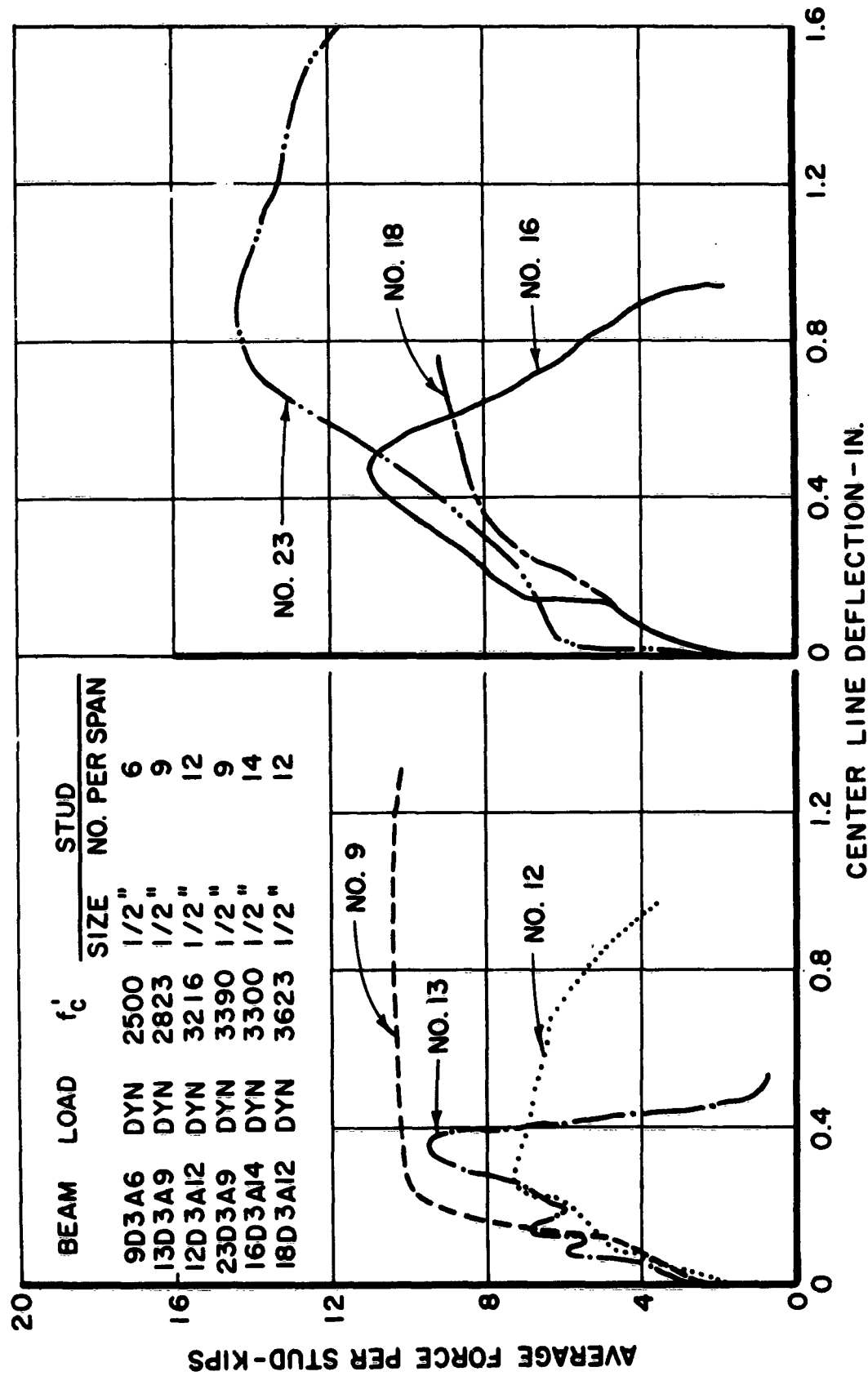
FIG. 4.5. EFFECT OF NUMBER OF STUDS PER SHEAR SPAN AND SHEAR
REINFORCEMENT, 1/2-IN. STUDS, PLATE IN TENSION

45
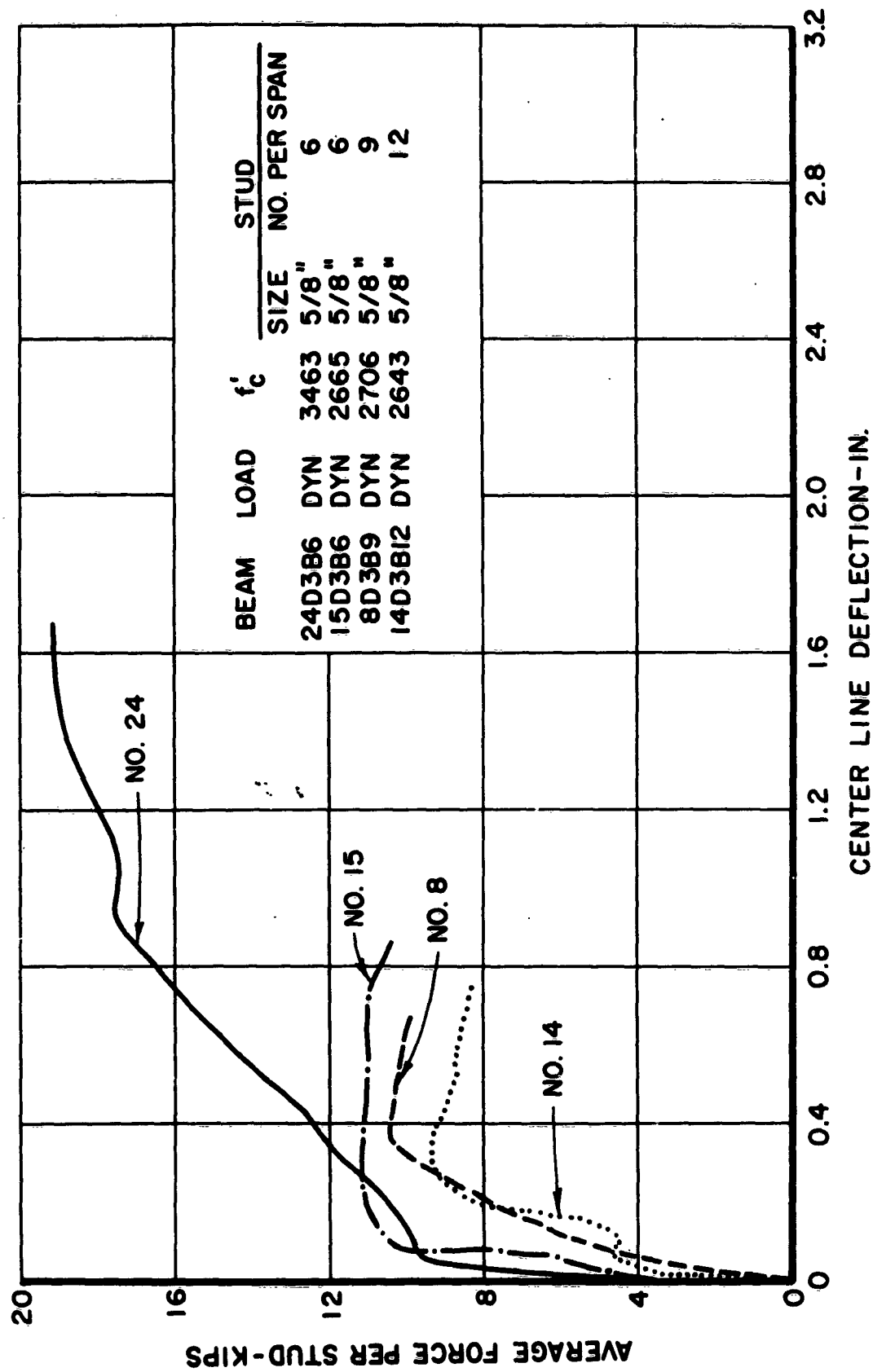
FIG. 4.6. EFFECT OF NUMBER OF STUDS PER SHEAR SPAN AND SHEAR REINFORCEMENT, 5/8" STUDS, PLATE IN TENSION

reinforcement in the form of closed stirrups was added to all succeeding beams to see if higher forces per stud could be obtained.

Stirrups were first put in beam No. 18 within the region of the beam where the diagonal cracks had been prevalent. When beam No. 18 was tested, the same type of diagonal cracks formed, but outside of the region where stirrups were (see Fig. 4.12 and A-2). Stirrups were then put over the entire length of the remaining beams.

A definite increase in force per stud can be seen in Figs. 4.5 and 4.6 as represented by the curves for beams No. 23 and 24. The addition of stirrups not only increased the observed forces per stud but also the ductility of the beams.

It can be noted also that the curve for beam No. 16 in Fig. 4.5 does not fall into the pattern where an increased number of studs yields decreasing forces per stud. Beam No. 16 had 14 studs per shear span and apparently if enough studs are put in the shear span, some of these studs become effective in intercepting some of the diagonal cracks. This will tend to give an increased force per stud at beam failure.

In view of the above comments, it is not conclusive that by increasing the number of studs per shear span, the capacity per stud is reduced. Rather, it is believed that the number of studs per square foot of plate has little or no influence upon stud capacities. However, this study of number of studs per shear span did help to uncover a weakness in the test beams.

47

In order to obtain the full dyanmic capacities of the studs in a beam with the cross section and shear span used in this study, it was necessary to add shear reinforcement. It is not known, however, what effect the confining action of closed stirrups such as those used herein had upon the dynamic capacities of the studs.

4.5 Effect of Type of Loading

Two sets of beam tests having similar beams were chosen to study the comparison between static and dynamic loadings. Figure 4.7 shows the comparison for both 1/2 and 5/8-in.-dia. studs. In general, the force-deflection curves follow each other up to a certain point for both static and dynamic tests, indicating approximately the same beam resistance. This suggests that the inertial effects of the beam loaded dynamically are probably less than expected in the early loading stage.

Beams No. 7 and 8 are probably more realistic than beams No. 4 and 10 in determining the true difference between static and dynamic loadings. Beam No. 8, which was loaded dynamically, shows a definite increase in ultimate capacity over beam No. 7. Also, more ductility was observed in the dynamic test. The increased capacity was believed to be due to the increase in yield capacities of the materials subjected to high rates of straining. It is possible that the ratios of t_r/T_n and t_d/T_n could have affected this increase. (See footnote on page 50).

It is believed that the force-deflection curve for beam No. 10 would have exhibited an increase in capacity over beam No. 4, as was the case for the 5/8-in. studs, if beam No. 10 had not failed early due to shear.
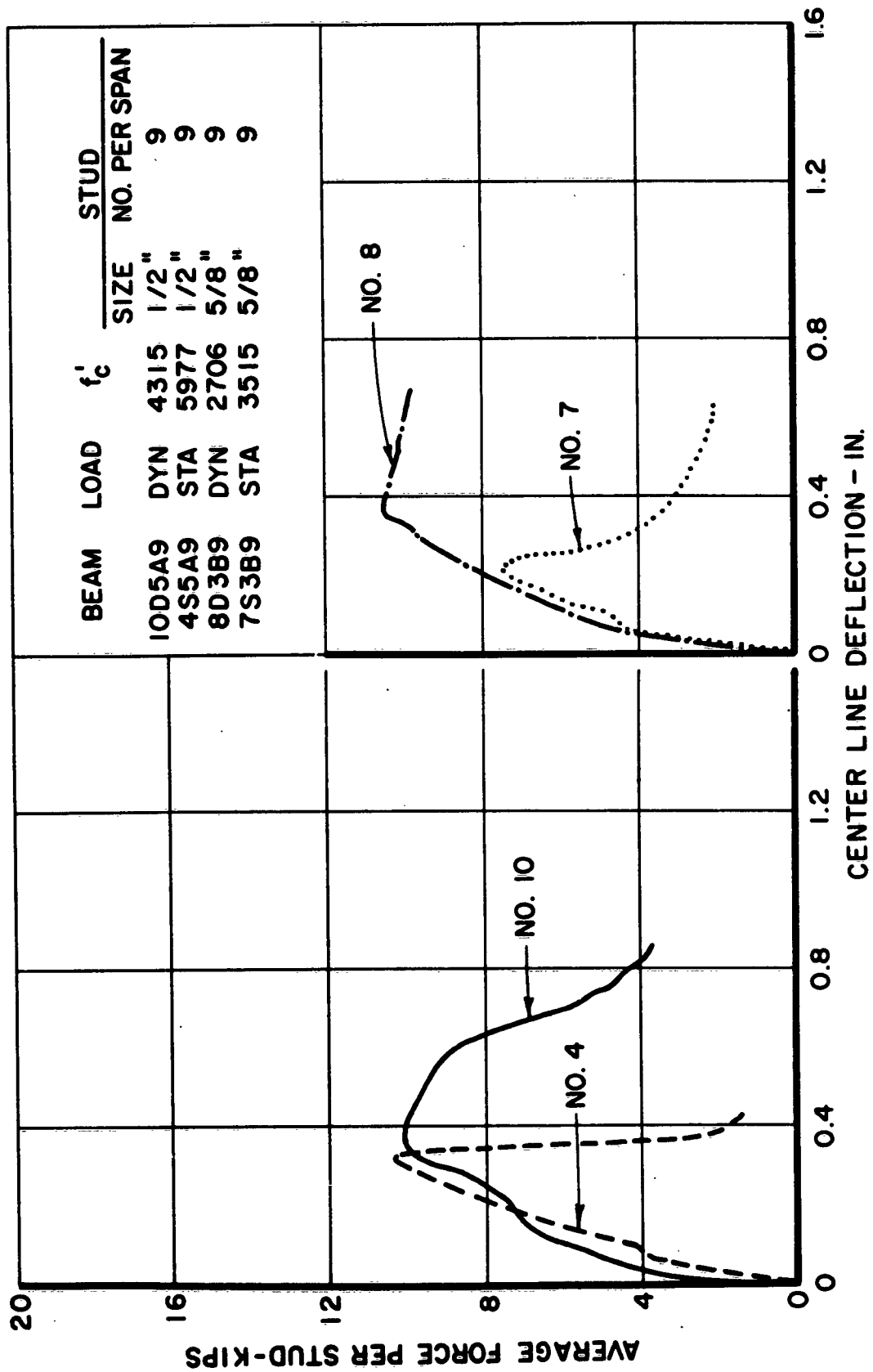
FIG. 4.7. EFFECT OF THE TYPE OF LOADING, PLATE IN TENSION

Apparently, the dynamic shear strength of concrete does not increase in the same ratio as dynamic compressive strength due to high straining rates.

In general, it is believed that the dynamic capacity of a beam loaded with the type of load pulse used in this study is increased over the static capacity in proportion to the increase in strength of the different materials caused by high straining rates, provided the beam is adequately reinforced for shear.[*] This includes a strength increase of the studs also. This means the increase in strength varies up to approximately 50 per cent over the static strength. The dynamic yield deflection is increased also. (See Beams No. 7 and 8 of Fig. 4.7.)

4.6 Effect of Successive Dynamic Loadings

Some of the beams did not collapse completely during the first drop of the mass onto the beam. All beams were loaded to complete collapse, requiring two or three drops on some beams. All beams without shear reinforcement collapsed under the first drop except beam No. 17. Beam No. 17 apparently was not damaged to any great extent during the first drop, because, when the load was removed, the center-line deflection and slips returned to zero. This beam was loaded to only about one-half of its final collapse capacity during the first drop. Two diagonal cracks about 4 to 6 in. long were observed in the concrete on each side of the beam after the first drop.

---

[*]The response of a flexural member subjected to an initially peaked, decaying force pulse, such as that resulting from a nuclear weapon depends to a large extent on the ratios t_r/T_n and t_d/T_n.

Figure 4.8 shows the force-deflection curves of two successive drops on two different beams, having 1/2 and 5/8-in.-dia. studs. Notice how much deflection was recovered after the first drop on each specimen. The force-deflection curve for the second drop in each case was started at the point the first curve returned to zero force. Upon reloading the specimen, the initial portion of the curve follows approximately the same slope as the initial portion of the curve for the first drop. Notice in the second drop that after the maximum force obtained in the first drop was reached, the curve continues with approximately the same slope as the final portion of the loading stage of the first drop. In effect, the two curves form a somewhat continuous response in which an envelope can be drawn to the two curves indicating the over-all response. (See the solid line in Fig. 4.8.) All other beams loaded more than once in the plate-in-tension series exhibited this same type of action.

Successive dynamic loadings on a beam might cause progressive effects leading to collapse under a load less than some previous loading. It appears that all slip is not recoverable after the load is removed. If deflection is thought of as an index to slip, notice the permanent set in Fig. 4.8 after the first drop. This apparently permits the cracks to propagate more and more under each loading, thus reducing the beam stiffness.

All force-deflection curves shown in this report involving more than one drop are curves of the over-all response (obtained by drawing an envelope to the individual curves) of the specimen.

51
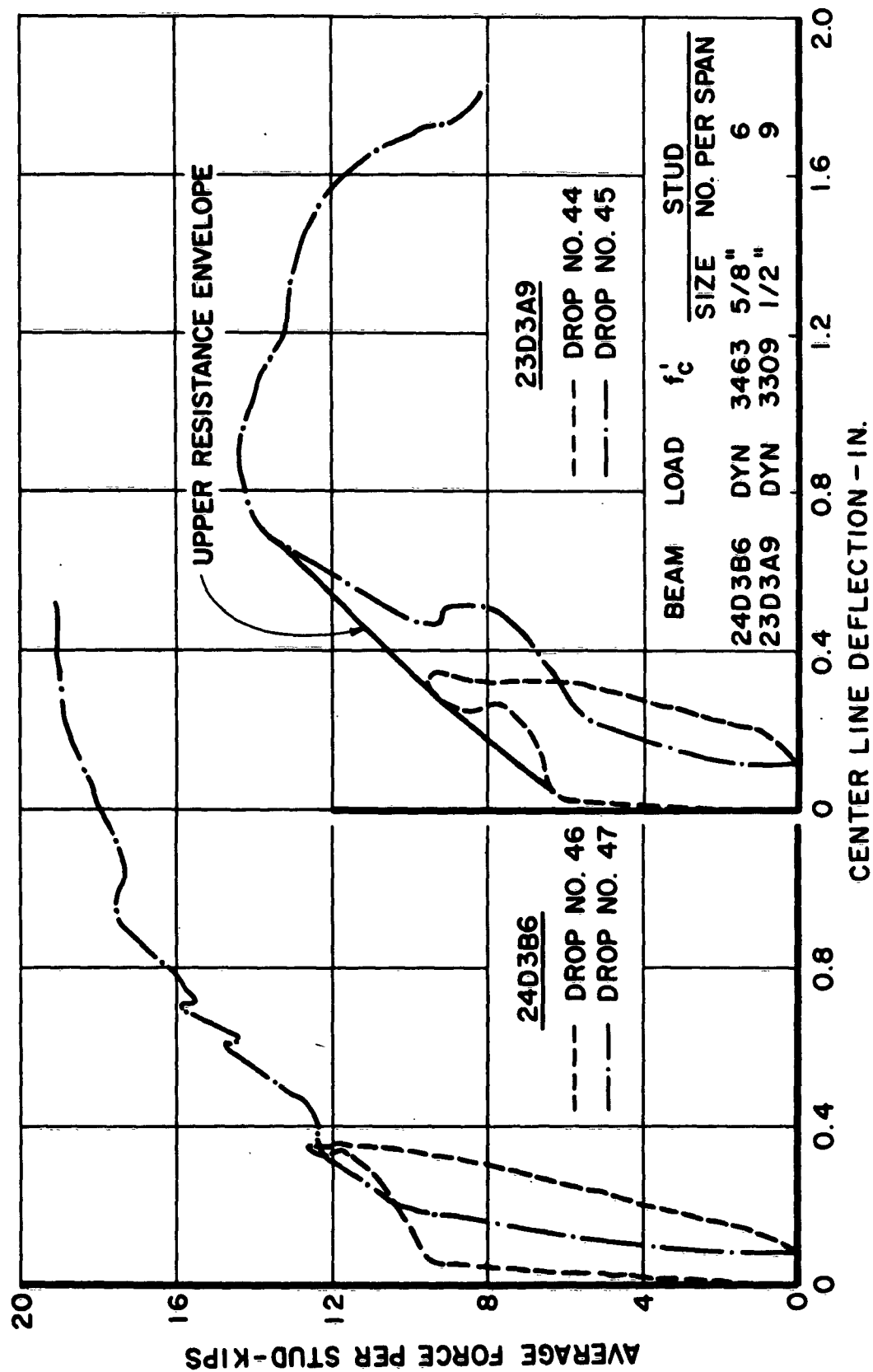
FIG. 4.8. EFFECT OF SUCCESSIVE DYNAMIC LOADINGS ON 24D3B6 AND 23D3A9

4.7 Behavior of Beams During Testing

Static tests. The behavior of the beams tested statically was somewhat dependent upon the number of studs per shear span. In general, the first crack was noticed and the first significant slip appeared simultaneously. The first observed cracks were short (2 to 3 in.) flexural cracks near the center line of the beam. These were accompanied by a slight decrease in machine load and increase in center-line deflection. As the load was increased, the center-line deflection and slip varied almost linearly with the load up to a point at which the slip began to increase at a faster rate than the load. The number of studs per shear span seemingly influenced the above-mentioned action in that the crack patterns were altered. In the three static tests performed, cracks always started vertically at or very near the position of a stud. In beam No. 3, which had 18 studs per shear span, the cracks remained vertical until the top of the studs was reached. At this point, the cracks started to turn inward toward the load. Beams No. 4 and 7 which had 9 studs per shear span had fewer cracks, but the cracks were more inclined than those in beam No. 3. Therefore, the cracking patterns in composite beams are apparently affected by the spacing of the studs.

The behavior discussed above corresponds to three well-defined stages of beam deformation: (1) an essentially elastic stage during which the concrete was uncracked with zero slip, (2) an inelastic stage during which the concrete was cracked and slip started, but in which the shear transfer between the concrete and steel plate was intact, and (3) a final

53

stage in which slip became increasingly greater, and cracks propagated faster until the beam collapsed. These three stages were also mentioned in the Illinois study.[1]

Dynamic tests. Because of the nature of the dynamic tests, it was impossible to observe and analyze different stages in the loading process. Beam behavior in the dynamic tests was obtained by studying the different time dependent measurements taken during the tests. This was further enhanced by studying the Fastax movies of some of the tests.

As the mass was dropped on the beam, the beam started deflecting with the deflection lagging the load slightly during the first few milli-seconds. After the load passed over its first peak indicating the end of the rise time, the deflection became almost constant with a very slight increase with time. During the time the deflection was essentially constant, small oscillations generally occurred. Slip between the concrete and steel plate also started during this time. In some cases, the slip became approximately constant with small oscillations. As the load was increased, the deflection usually increased slightly until a point was reached at which the deflection started to increase very rapidly. Usually this was accompanied by a sharp decrease in load and a rapid increase in slip. These three things usually denoted beam collapse.

As the beam was loaded, the concrete strain in the top fiber of the beam and the steel plate strain increased very rapidly at first, but lagged the load slightly. After this initial rapid rise the strains tended to become essentially constant until the beam collapsed. The steel-plate

54

strain then increased rapidly while the concrete strain decreased. The decrease in concrete strain was caused by a crack or cracks which propagated to the top of the beam, thus relieving stress.

When the beam was first impacted, the ends of the beam tended to kick up, imparting a negative reaction. These reactions became positive, however, after 1 or 2 milliseconds.

It is not known definitely just when the cracks started in the concrete and how they propagated with load. An attempt was made to determine this by studying successive frames in a Fastax movie. Figure 4.9 shows photographs taken from a Fastax movie showing the formation of cracks. The pictures reading from the top downward were taken about 3 frames apart. This means that approximately one-half of a millisecond of time elapsed between the frames shown. It appears as though the cracks propagated almost the entire depth of the beam instantaneously. As time passed and the load was increased, the cracks opened wider until the beam finally failed. It is believed that these cracks started to appear a very short time (5 to 10 milliseconds) after the beam was impacted. These cracks possibly could not be seen in the Fastax movie until they had opened up fairly wide.

The beam shown in Fig. 4.9 was a beam without shear reinforcement. Fastax movies taken of beams with shear reinforcement did not show any visible cracks. However, examination of these specimens after the tests revealed numerous cracks which did not open wide enough to be seen in the movies.

55
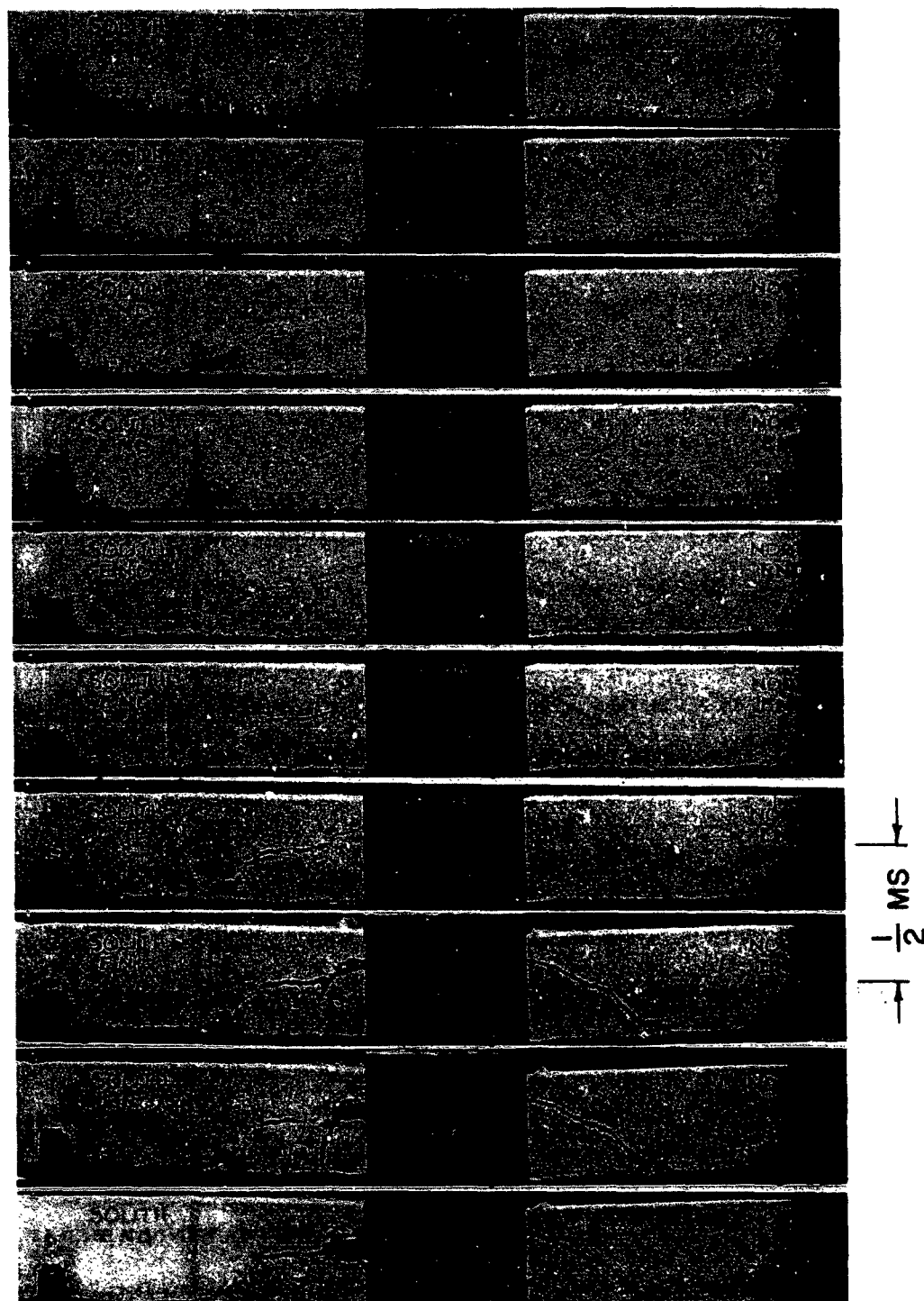
FIG. 4.9. PHOTOGRAPHS TAKEN FROM FASTAX MOVIE
SHOWING CRACK DEVELOPMENT DURING DYNAMIC
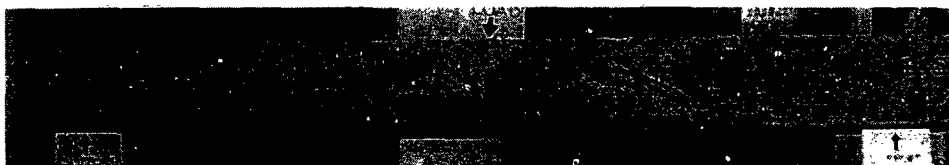TEST

4.8 Modes of Failure

Static tests. Beams No. 4 and 7 exhibited what has been termed a bond-shear failure.[1] This type of failure is so termed because excessive slip between the concrete and steel plate breaks down the bond, thus triggering shear cracks and shear failure. The primary failure appears not to be due directly to shear because beam No. 3 which had 18 studs per shear span failed by yielding of the plate and simultaneous crushing of the concrete in the top fiber. Enough studs to retard or prevent slip would apparently cause the beam to develop its full flexural strength potential without resulting into primary shear failure. Figure 4.10 shows the modes of failure of static tests. The cracks were marked at different values of load.

Dynamic tests. There were two types of failures in the dynamic tests. All beams without shear reinforcement exhibited a shear failure. These beams are shown after failure in Fig. 4.11. Since the exact slip-crack relationship is not known for all of the dynamic tests, the failures cannot be classified directly as bond-shear failures as in the static tests. In most beams, a significant amount of slip had taken place before failure, which could have caused the type of bond-shear failure mentioned above. However, in beam No. 9, no slip occurred until beam failure. Slip and beam collapse occurred simultaneously.

Beams with shear reinforcement exhibited a failure consisting of excessive slip between the concrete and steel plate and crushing of the concrete in the top fiber. Figure 4.12 shows the failure patterns of the three beams in the plate-in-tension series with shear reinforcement. It should be remembered that beam No. 18 had stirrups only over the middle 36 inches. In view of the excessive slips in these beams before failure, it is believed that the maximum stud capacities were reached.

57
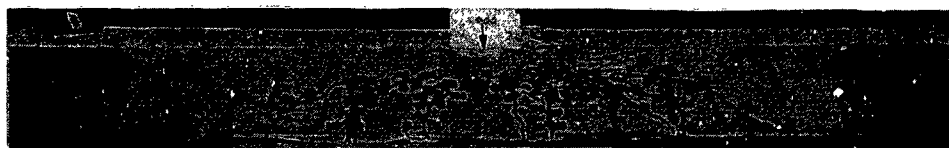
3 S5 AI8

4S5A9

7S3B9

FIG. 4.10. MODES OF FAILURE OF STATIC TESTS
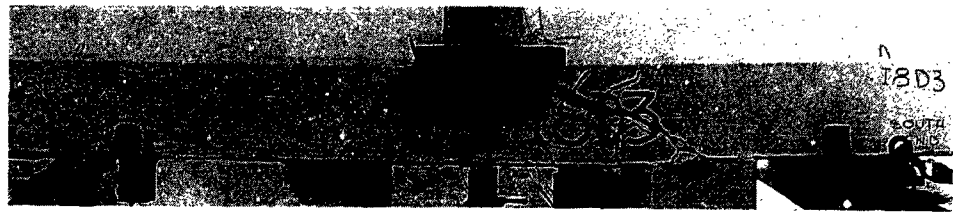
8D3B9
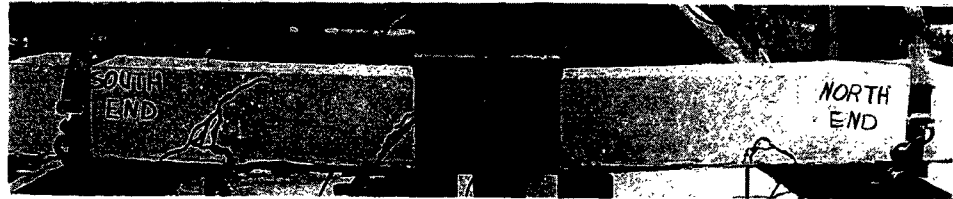
9D3A6

10D5B9
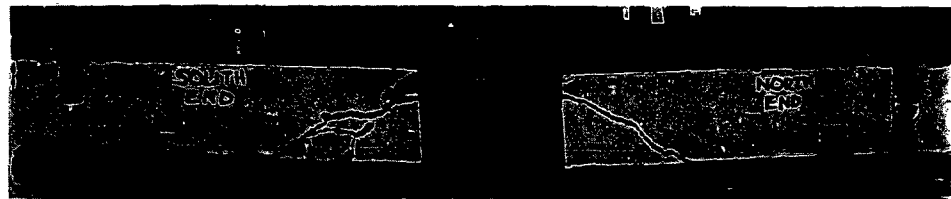
11D5B9

12D3A12

FIG.4.11.   MODES OF FAILURE OF DYNAMIC TESTS, BEAMS
WITHOUT SHEAR REINFORCEMENT
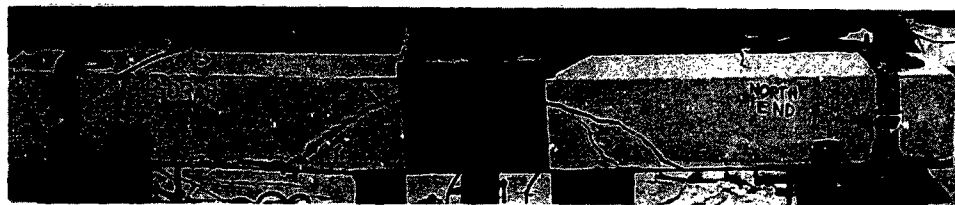
13D3A9

14D3B12
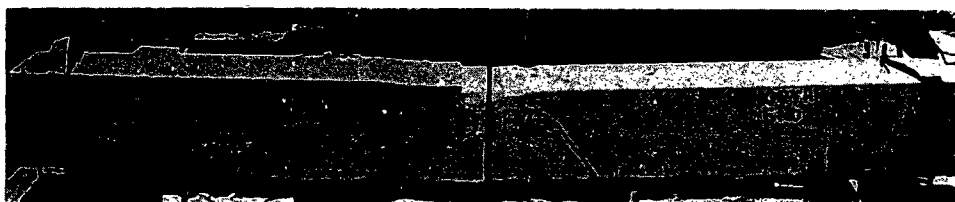
15D3B6

16D3A14

17D5A11

FIG. 4.11 CONTD.   MODES OF FAILURE OF DYNAMIC   TESTS,
BEAMS WITHOUT SHEAR REINFORCEMENT

60
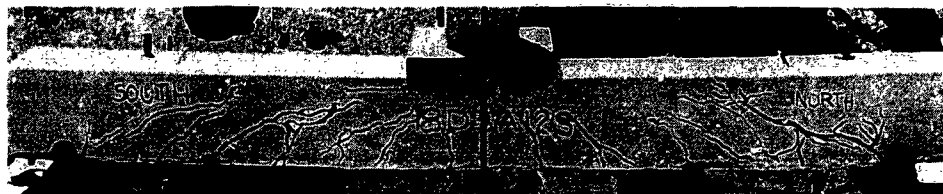
18 D 3 A 12   Shear reinforcement is only over the center region in this beam.

23 D 3 A 9

24 D 3 B 6

FIG. 4.12.   MODES OF FAILURE OF DYNAMIC TESTS, BEAMS WITH SHEAR REINFORCEMENT

SECTION 5. RESULTS OF PLATE-IN-COMPRESSION SERIES

5.1 General Remarks

This section contains the results of the eight beams tested with the steel plate acting as compressive reinforcement. The two beams tested without a plate are also included in this section.

Because of the way compressive reinforcement and concrete in the top of a beam share the total compressive force, it is not convenient to present the results in the form of force per stud versus center-line deflection as was done in the plate-in-tension series. Therefore, the results are presented in the form of load-deflection curves. The load is the total load on the beam as determined from accelerometer measurements on the falling mass.

When looking at the results of the plate-in-compression series, it should be kept in mind that these beams as reinforced without the steel plate were already close to being balanced beams for 3000-psi concrete. Concrete compressive strengths in excess of 4000 psi, as well as the addition of compression steel, caused this size of beam to be greatly under-reinforced as far as tension reinforcement was concerned.

5.2 Response of Beams with and without Steel Plates

Static tests. A comparison between the force-deflection relationships between two companion beams tested statically with and without a

steel plate acting as compressive reinforcement, is shown in the left portion of Fig. 5.1. Notice that the plate has the effect of giving the beam a slightly higher resistance for a given deflection. Also, the plate gives the beam an increase in ultimate capacity, and ductility.

Dynamic tests. Beams No. 21 and 22 were tested dynamically to investigate the effect of a plate acting as compressive reinforcement. The force-deflection curves for these beams are shown on the right side of Fig. 5.1. The beam resistance was increased considerably by the plate. The plate also caused the ductility to be considerably increased over the static tests. Very ductile members are usually desirable when they are expected to resist dynamic loads because ductile members can dissipate large amounts of energy before collapse. When these members are to be used in buried structures, ductility is essential to permit the structural deformations required to take full advantage of the inherent strength of the soil that surrounds the structure. Soil resistance can be mobilized only after deformations are imposed upon it.[6]

5.3 Effect of Concrete Strength and Stud Size

Even though the specimens tested in the plate-in-compression series do not permit a complete comparative study of the effects of concrete strength and stud size, these variables should affect beam response approximately the same way as in the plate-in-tension series. More specifically, the stud capacities should vary in the same way as

63
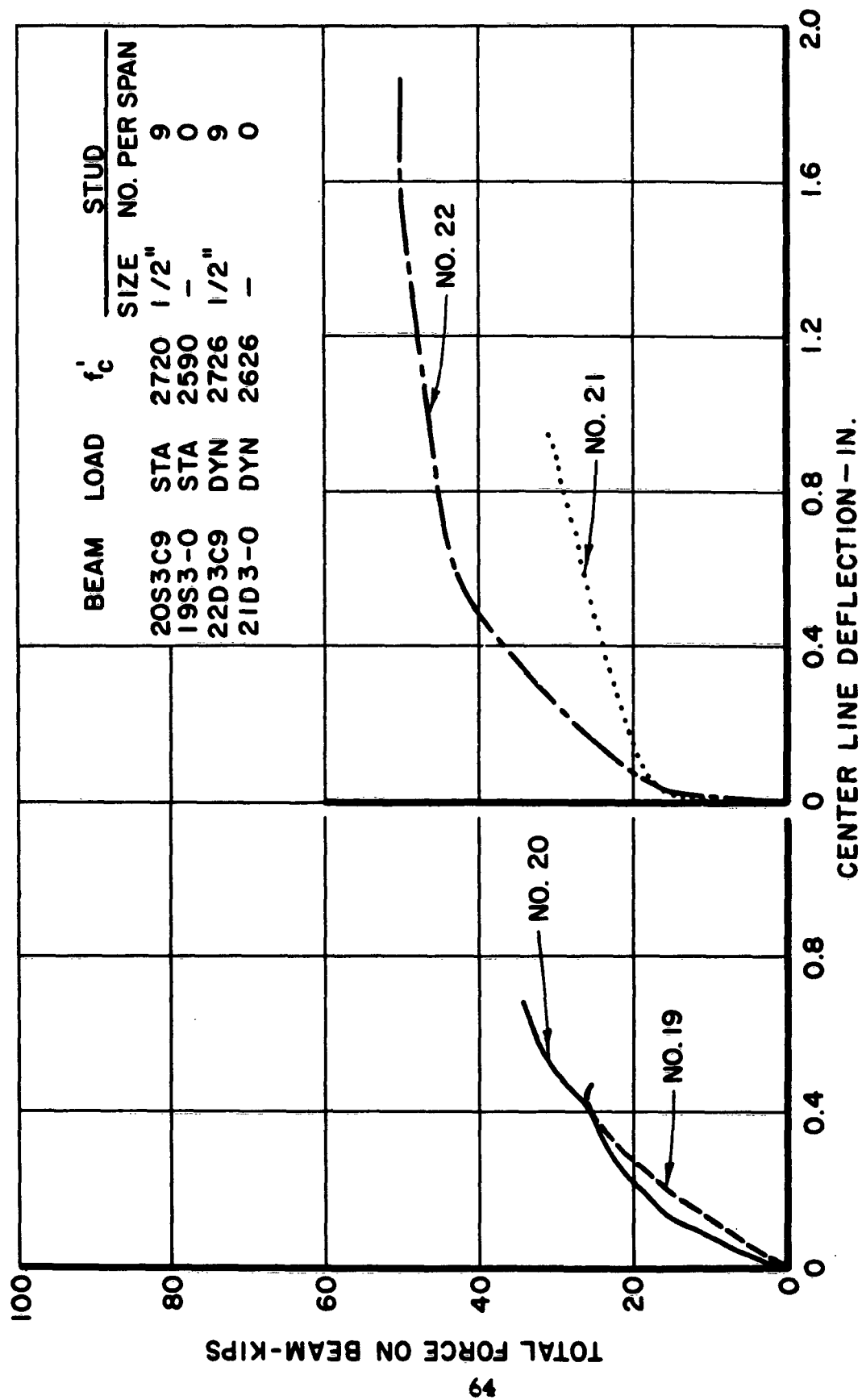
FIG. 5.1. FORCE-DEFLECTION RESPONSE OF BEAMS WITH AND WITHOUT A STEEL PLATE IN COMPRESSION

64

in the push-out specimens (discussed in Section 6 of this report). The studs are acting in a compression zone of the concrete in both the plate-in-compression beams and push-out specimens.

5.4 Effect of Number of Studs per Shear Span

In the plate-in-tension series, the studs were assumed to share equally in the shear between the concrete and steel plate. Beams in the plate-in-compression series require their studs to assume loads in proportion to the compressive force in the top of the beam. This force changes directly with the moment diagram along the beam which results in constant shear for a concentrated load. This suggests that the studs in the plate-in-compression series also have equal shear forces on them. However, in the dynamic tests, it is believed that slip starts near the center of the beam which causes the studs near the center to assume more load than the others initially.

Companion beams having 6, 9, and 12 studs per shear span are represented by their force-deflection curves in Fig. 5.2. In general, by increasing the number of studs per shear span, the beam capacity was also increased. Notice the large deflections encountered by beams No. 29 and 30. Beam 22 was prevented from deflecting more than 2 in. when it was stopped by the blocks under the center line of the beam.

5.5 Effect of Type of Loading

Figure 5.3 shows force-deflection relationships for beams both with and without a plate acting in compression loaded statically and

65

BEAM	LOAD		f'_c	STUD	
				SIZE	NO. PER SPAN
29D3C12	DYN		2945	1/2"	12
22D3C9	DYN		2726	1/2"	9
30D3C6	DYN		3226	1/2"	6

NO. 22 (OVER-ALL AVERAGE)

NO. 29

NO. 30

CENTER LINE DEFLECTION – IN.

TOTAL FORCE ON BEAM – KIPS
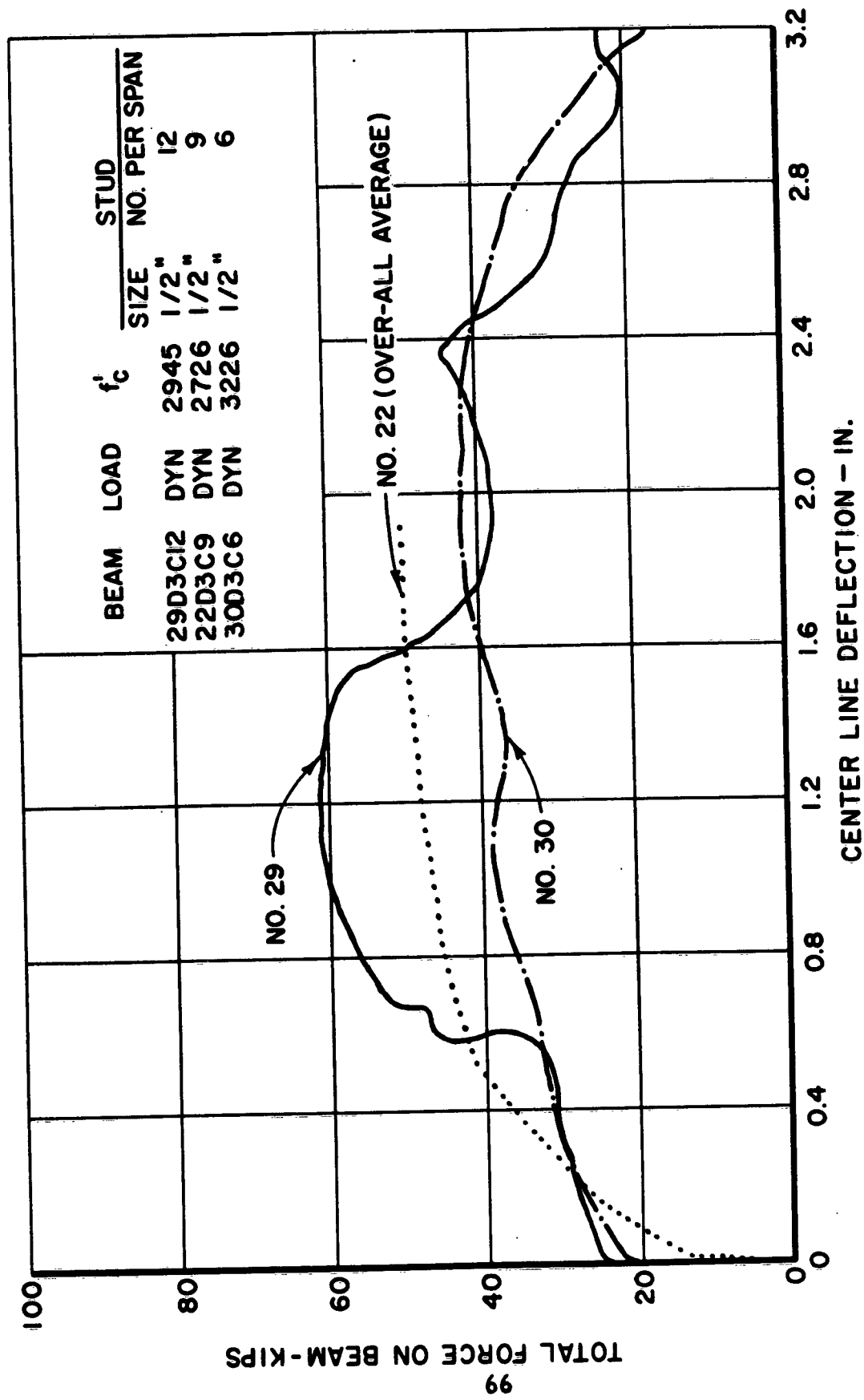
FIG. 5.2. EFFECT OF NUMBER OF STUDS PER SHEAR SPAN, PLATE IN COMPRESSION
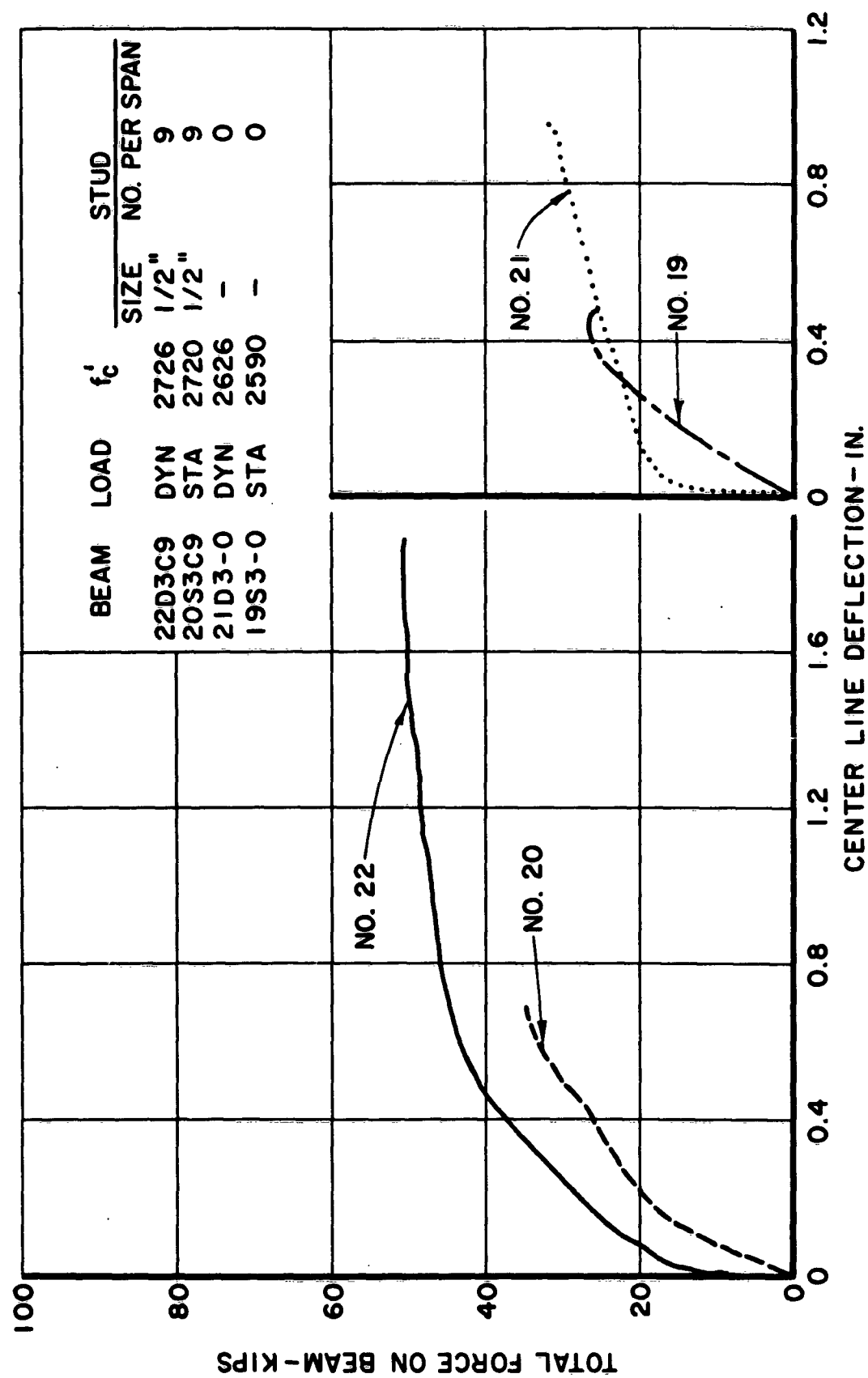
FIG. 5.3. EFFECT OF TYPE OF LOADING, PLATE IN COMPRESSION

dynamically. In general, the beams loaded dynamically showed a higher resistance for a specified deflection. Also, beams loaded dynamically showed more deflection before collapse than beams loaded statically. After the collapse stresses were reached, a small amount of time was required for beam collapse to take place, during which time the beam continued to deflect. It is believed that this time factor is partially the cause for larger deflections in the dynamic tests before collapse than in the static test.

Figure 5.4, which compares the force-deflection relationships of two companion beams loaded statically and dynamically, is included to demonstrate the effect of progressive damage (see Section 4.6) on beams loaded dynamically. Notice that beam No. 26 finally failed at a load less than a previous load (see Fig. 5.6) and even less than a companion beam loaded statically. Concrete strength probably had some effect here also. It is believed that the repeated loadings on beam No. 26 also had a great effect here.

5.6 Effect of Successive Dynamic Loadings

Figure 5.5 shows the force-deflection curves for two successive drops on beam No. 22. After the first drop, more than one-half of the deflection was recovered when the load was removed. Again, a sharp rise was noticed on the second drop until a load approximately equal to the maximum reached in the first drop was obtained. The second drop may be used to continue the upper resistance envelope started by the first drop. (See Fig. 4.8 for an example of how the envelope is drawn.)

68

BEAM	LOAD	f'_c	STUD	
			SIZE	NO. PER SPAN
27S5D4	STA	4716	5/8"	4
26D5D4	DYN	4053	5/8"	4

NO. 26

NO. 27

CENTER LINE DEFLECTION–IN.

TOTAL FORCE ON BEAM–KIPS

FIG. 5.4.   FORCE – DEFLECTION CURVES FOR TWO COMPANION BEAMS, LOADED STATICALLY AND DYNAMICALLY, PLATE IN COMPRESSION
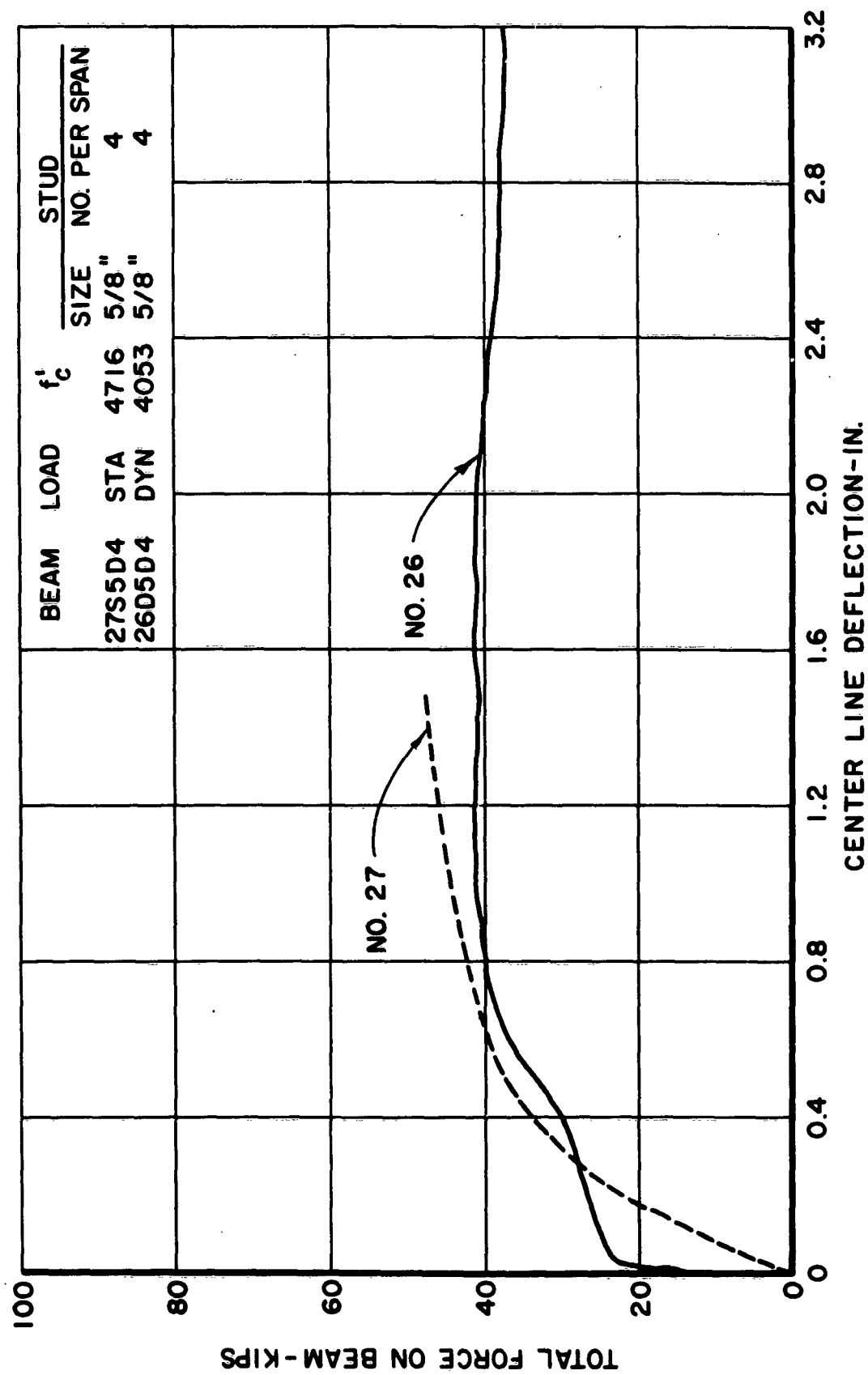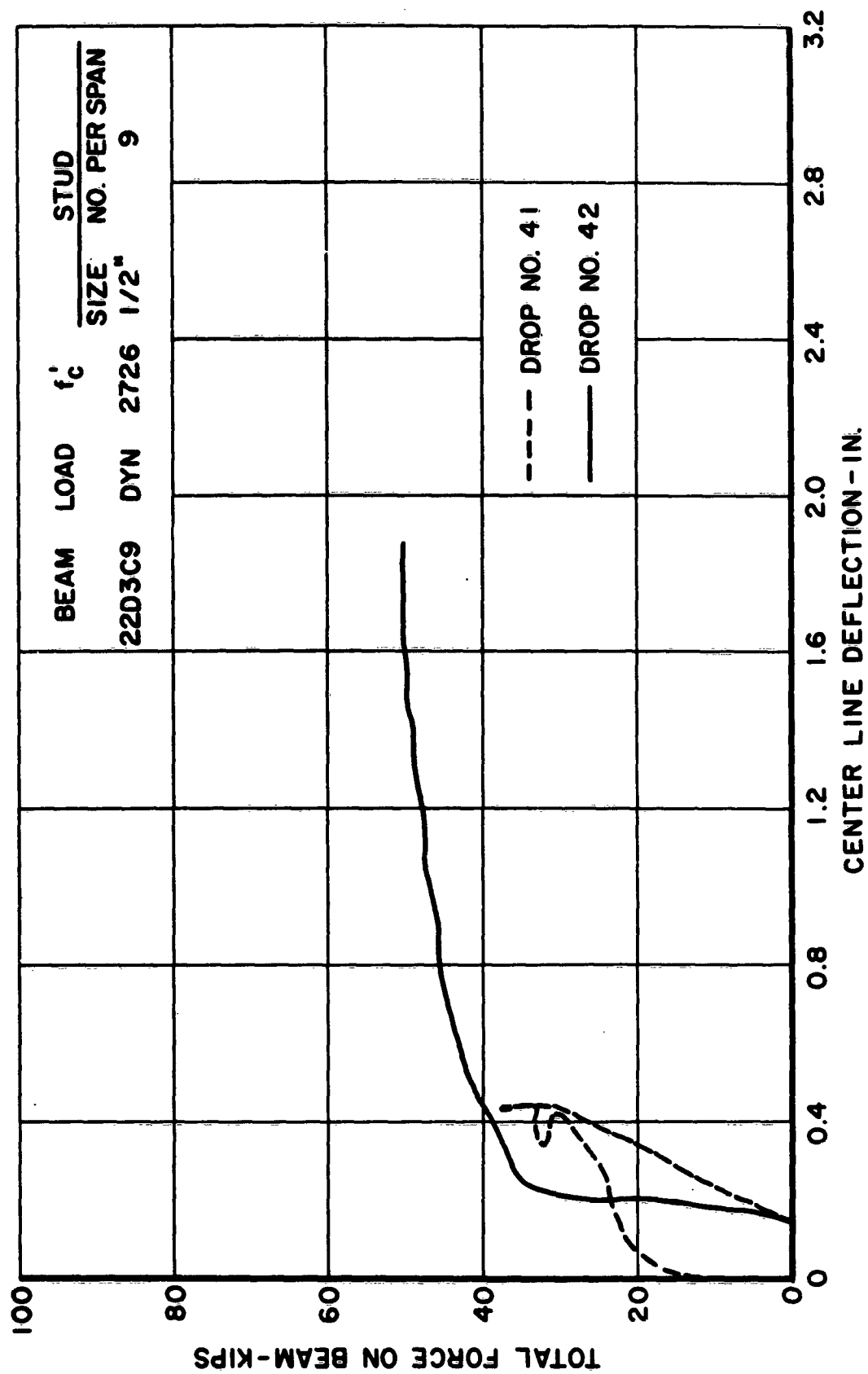
FIG. 5.5. EFFECT OF SUCCESSIVE DYNAMIC LOADINGS ON BEAM 22D3C9, PLATE IN COMPRESSION

70

Three drops were necessary to cause beam No. 26 to collapse completely. The force-deflection curves for all three drops are shown in Fig. 5.6. The unusual form of the curves shown in Fig. 5.6 is due to the beam deflections decreasing at certain times while the load was increasing, or the deflections increasing while the load was decreasing. Such is possible when the load values and beam deflections oscillate at different frequencies simultaneously as was true in this case.

5.7 Behavior of Beams During Testing

Static tests. Since all beams tested in the plate-in-compression series were reinforced with closely spaced closed welded stirrups, all cracks that opened wide were essentially vertical. As load was applied to the beams, cracks started to develop at a low value of load (usually at a load of approximately 4 kips). The first cracks observed were near the center of the beam and these cracks were usually about 3 or 4 in. high when first noticed. These cracks, along with others which developed as the load was increased, propagated very fast until they extended almost completely to the top of the concrete. In all beams tested statically, cracks in the concrete had extended up to within 1/2 in. of the top steel plate when only about 75 per cent of the ultimate load had been reached. As load was further increased, crushing of the concrete at the top fiber directly under the steel plate became visible near the center line of the beam.

Strain gages on the tensile reinforcing bars at the center line of the beams indicated that the bar force increased linearly with load on

71

CONTINUED BELOW

STUD

BEAM	LOAD	f'_c	SIZE	NO. PER SPAN
26D5D4	DYN	4053	5/8"	4

- - - - DROP NO. 50
- · - · DROP NO. 51
———— DROP NO. 52

CENTER LINE DEFLECTION - IN.
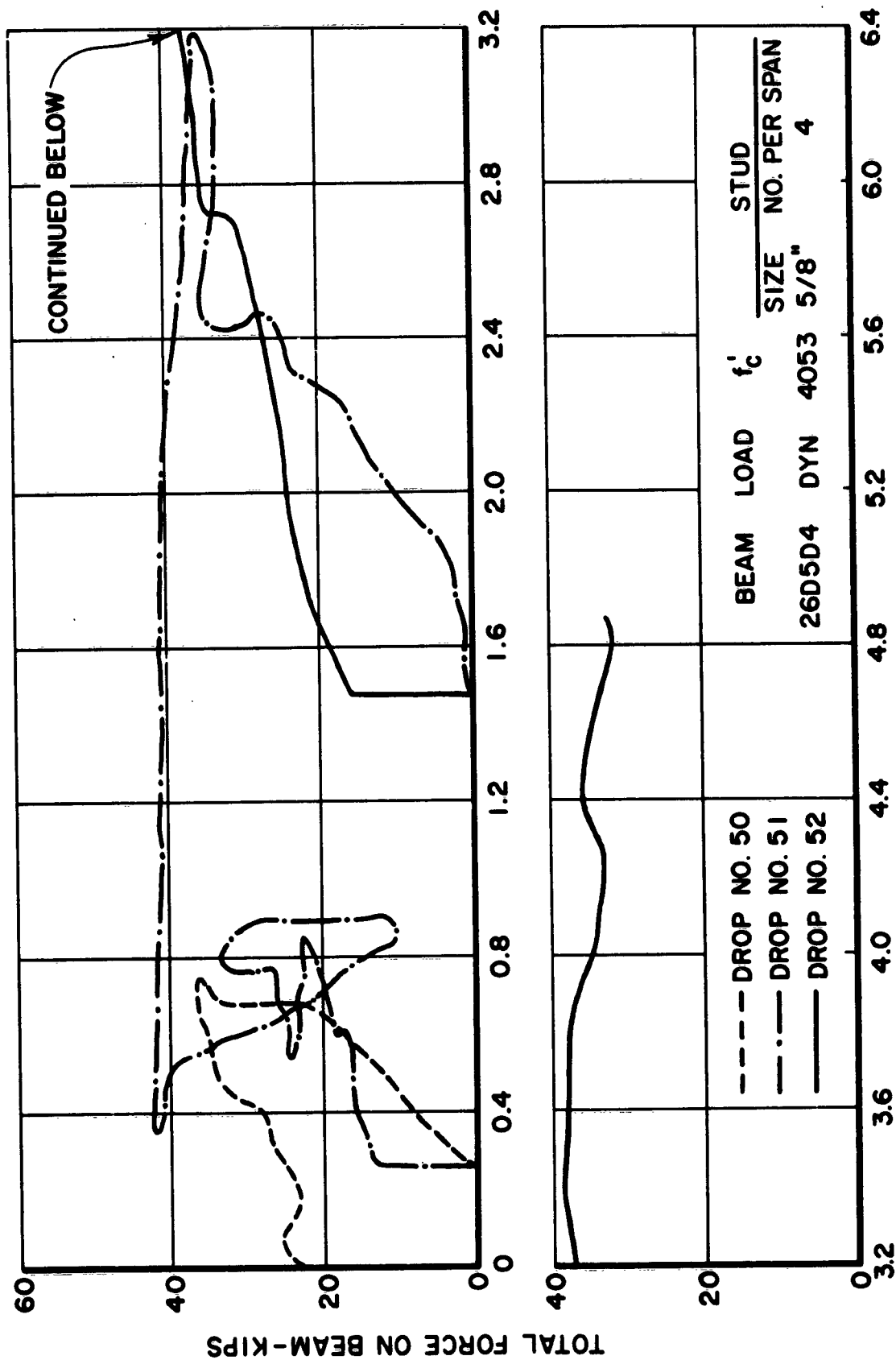
TOTAL FORCE ON BEAM-KIPS

FIG. 5.6.   EFFECT OF SUCCESSIVE DYNAMIC LOADINGS ON BEAM 26D5D4, PLATE IN COMPRESSION

72

the beam after the first crack. Before the first crack, the bar force was not linear with increase in load, indicating the concrete was helping with the tensile force.

Slip between the concrete and steel plate was small (less than 0.03 in.) as measured by the slip devices 6 in. inside of the support. The slip values fluctuated during loading as cracks developed near the slip devices.

The steel anchor plates welded to the ends of the reinforcing bars, combined with the action of the studs welded to the top steel plate near the supports complicated the beam action just inside of the supports near ultimate load. The anchorage effects near the end of the beam and the deterioration of the beam between the load and the supports, caused the steel plate on top of the beam to possess a reversed curvature a few inches inside of the supports. That is, tension was induced in the top plate just inside of the support near the ultimate load on the beam. This can be seen in Fig. 5.7. Strain gages were mounted on the steel plate between the studs. The difference in the forces obtained from the strains in the plate at the gage location give a close approximation of the load carried by a particular stud. This difference in force between two adjacent gage locations was not all carried by the stud or studs between them. Friction between plate and concrete was responsible for some of it. Nevertheless, it can be seen that a 1/2-in.-dia. stud carried approximately 15 kips or more. Similar measurements on beam No. 27 show forces carried by a 5/8-in.-dia. stud of at least 20 kips.

73
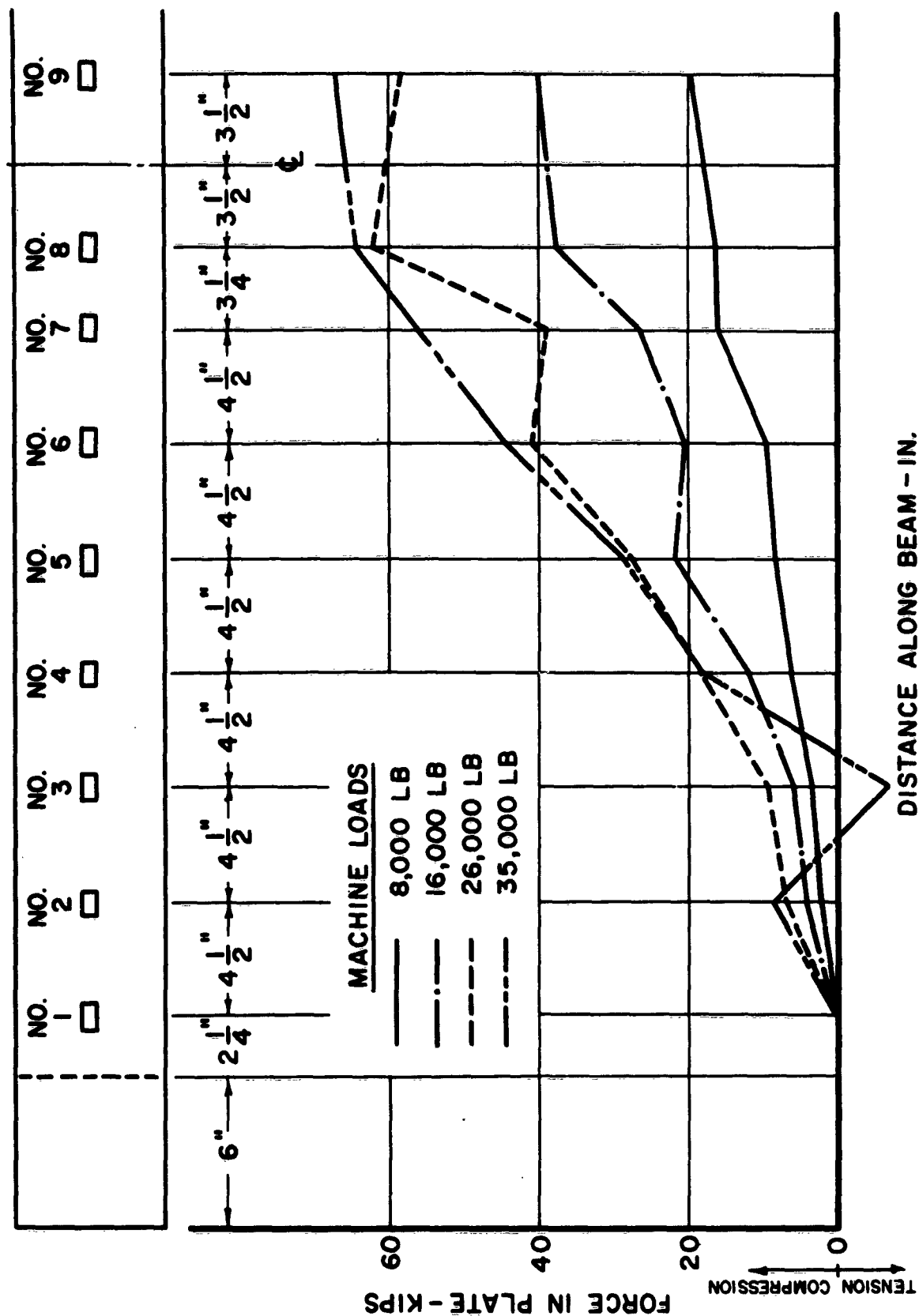
FIG. 5.7. FORCE IN PLATE ALONG BEAM 28S3CI2

74

Near beam collapse, the concrete near the top of the beam outside of the closed stirrups tended to bulge out laterally and spall off. The closed stirrups formed an internal core which remained intact.

Dynamic tests. The beams tested dynamically acted essentially the same as those in the static tests. The different stages of behavior could not be observed directly, but observation of the beams after collapse suggested the same type of behavior. The only major difference was the magnitudes of the collapse loads. The beams in the dynamic tests, of course, had higher resistances.

5.8 Modes of Failure

In general, the final failure of all of the beams tested in the plate-in-compression series was due to yielding of the tensile reinforcing bars. The anchor plate on one end of beam No. 20 came off during testing, causing that beam to fail by bond between the concrete and reinforcing bars.[*]

Photographs after collapse of beams tested statically, are shown in Fig. 5.8; and those tested dynamically are shown in Fig. 5.9. The core formed by the stirrups can be seen after the outside concrete spalled off in Fig. 5.9.

---

[*]Beam No. 20 has been used in the comparisons in this report because the anchor plate did not pull off until the very end of the test. The expected ultimate capacity of this beam had already been reached.

19S3-0
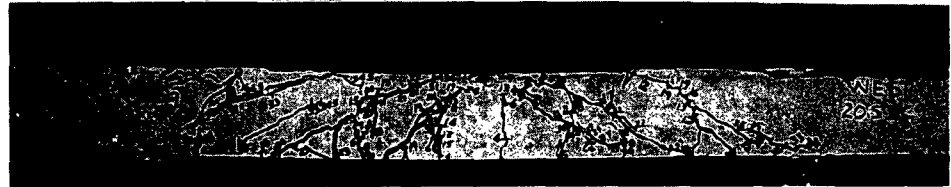
20S3C9

27S5D4
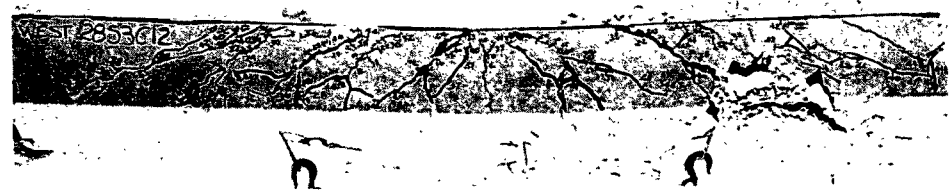
28S3C12

FIG. 5.8.   MODES OF FAILURE OF STATIC TESTS, PLATE
            IN COMPRESSION

21D3-O
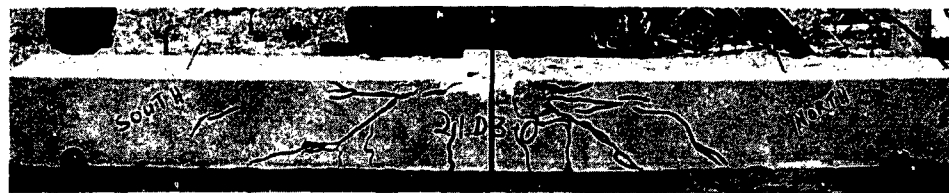
22 D3C9

25D3C6

26D5D4
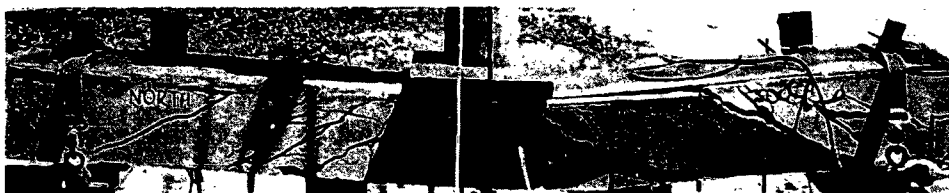
29D3C12

30D3C6

FIG. 5.9.   MODES OF FAILURE OF DYNAMIC TESTS,   PLATE
IN COMPRESSION.

SECTION 6. RESULTS OF PUSH-OUT TESTS

6.1 General Remarks

As mentioned previously, the push-out tests were included in
this investigation to determine dynamic stud capacities and the behavior
of the studs loaded at a fast rate. The type and size of specimens were
discussed in Section 2 of this report.

This section contains a summary of the data obtained from the
push-out tests. Also, a comparison is made between the maximum
dynamic stud capacities and the static critical capacities.

6.2 Summary of Data Obtained

Table 6.1 gives a compilation of the data obtained concerning stud
capacities from both static and dynamic tests. Stud sizes of 1/2 in. and
5/8 in. in diameter, and concrete compressive strengths of 3000 psi
and 5000 psi were the variables involved. Since the stud capacities in
the push-out tests performed by Viest[3] and in the beam tests discussed
herein seemed to vary with $d^2\sqrt{f_c'}$ this approach was tried for the
dynamic tests. To study this effect, the maximum stud capacities
measured were first corrected to 3000 psi and 5000 psi concretes.
The capacities followed by a double plus sign in Table 6.1 probably do
not indicate the absolute maximum capacities. The studs were not
completely sheared off in the tests so indicated. However, upon breaking

78

TABLE 6.1

SUMMARY OF DATA FROM PUSH-OUT TESTS

| 1/2-In.-Dia.-Studs | | | $f'_c \approx 3000$ psi | |

Specimen No.	f'_c	Measured Max Stud Capacity-lb	Corrected Max Stud Capacity*	$d^2\sqrt{f'_c}$
5S3A4P	2680	8,250	8,730	13.00
6D3A4P	3350	9,000++	8,520++	
22D3A4P	2726	8,000++	8,400++	
25D3A4P	3740	14,600	13,100	15.27
29D3A4P	2947	14,600	14,700	13.30
30D3A4P	3226	18,700	18,000	14.16
		Average	15,260	14.24

| 1/2-In.-Dia.-Studs | | | $f'_c \approx 5000$ psi | |

Specimen No.	f'_c	Measured Max Stud Capacity-lb	Corrected Max Stud Capacity*	$d^2\sqrt{f'_c}$
2S5A4P	6150	8,750	7,120	19.60
10D5A4P	4163	14,900	16,300	16.10
33D5A4P	3770	15,800	18,200	15.35
		Average	17,250	15.77

| 5/8-In.-Dia.-Studs | | | $f'_c \approx 3000$ psi | |

Specimen No.	f'_c	Measured Max Stud Capacity-lb	Corrected Max Stud Capacity*	$d^2\sqrt{f'_c}$
15D3B4P	2700	17,000++	18,000++	20.30
28D3B4P	2710	13,900++	14,600++	20.35
		Average	16,300	20.32

| 5/8-In.-Dia.-Studs | | | $f'_c \approx 5000$ psi | |

Specimen No.	f'_c	Measured Max Stud Capacity-lb	Corrected Max Stud Capacity*	$d^2\sqrt{f'_c}$
27D5B4P	4716	16,400	16,900	26.80
31D5B4P	4733	23,600	24,300	26.90
32D5B4P	4607	21,900	22,800	26.75
		Average	21,300	26.82

*These values were obtained by multiplying the maximum stud capacity by $\sqrt{3000/f'_c}$ and $\sqrt{5000/f'_c}$ for specimens with f'_c being approximately 3000 psi and 5000 psi respectively.

++Studs did not shear off completely on these tests.

up the concrete around the studs, the studs were definitely somewhat bent, which verified that some slip had taken place. Also, some crushing of the concrete adjacent to and near the base of the studs was observed.

6.3 Summary of Force-Slip Data

Force-slip curves were plotted for each test. Figure 6.1 shows a summary of the average force-slip curves. Each curve represents the average of two or more test results. It is evident from these curves that the force per stud did increase proportionately as the slip increased. Apparently, slip was necessary to make the studs utilize their full capacity. It appears, however, that a slip of about 0.06 in. is a good maximum value to use in design when based on ultimate capacities, in order to have some reserve left in both force capacity and slip capacity.

Another point shown by Fig. 6.1 is the definite increase in stud capacities at various slip values for the higher concrete strength and larger stud diameter.

6.4 Ultimate Stud Capacities

The maximum stud capacities as found in the dynamic push-out tests are listed in Table 6.1. Specimens No. 2 and No. 5 were tested statically and are also included in Table 6.1. A straight-line fit using a least squares technique was applied to the average values of the dynamic tests and it is shown by the solid line in Fig. 6.2. The solid line is a fit to only the three points closest to the line. The broken line is a straight-line fit to all four points. It is believed that all four points
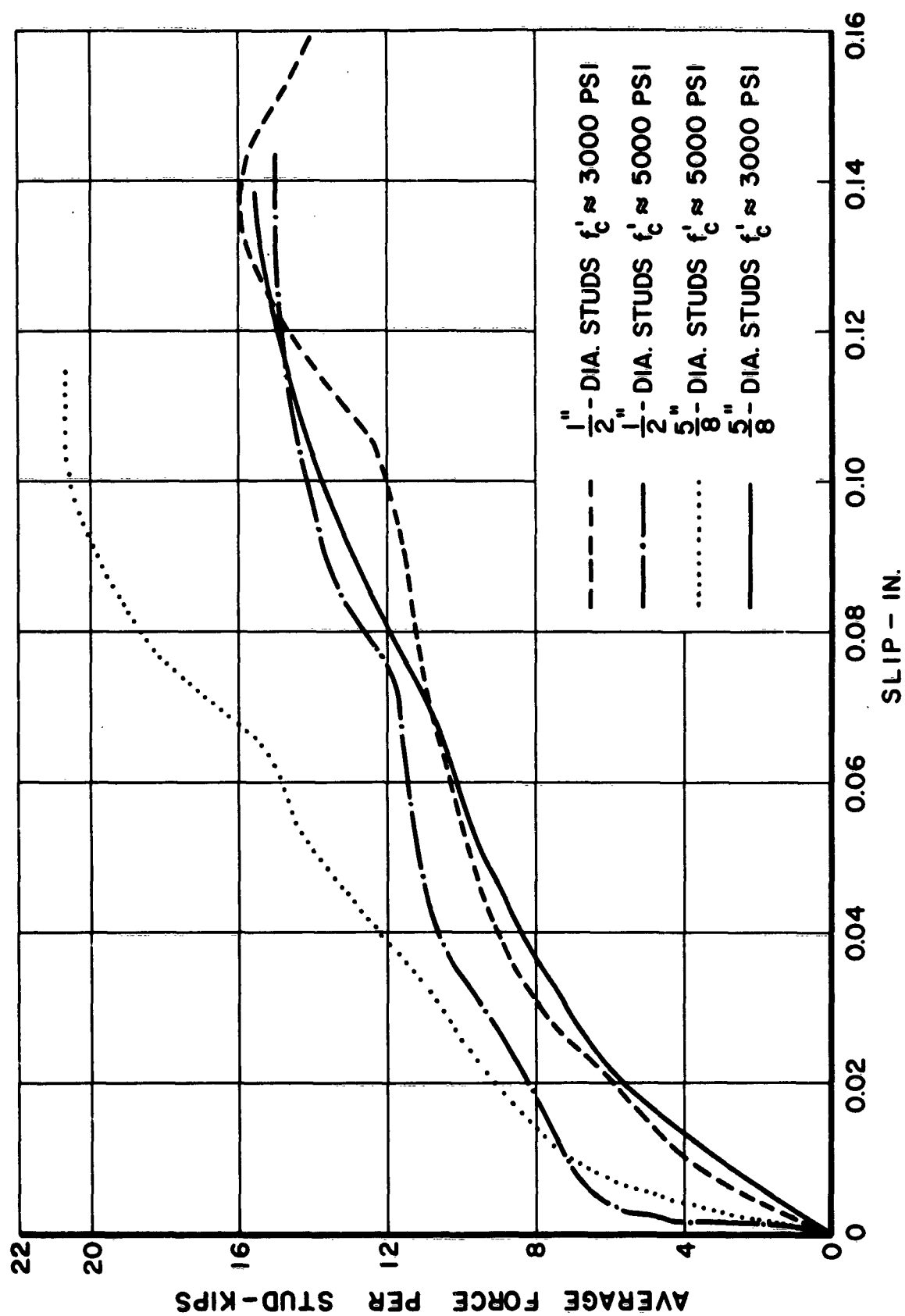
FIG. 6.I. SUMMARY OF AVERAGE FORCE SLIP CURVES FOR PUSH OUT SPECIMENS
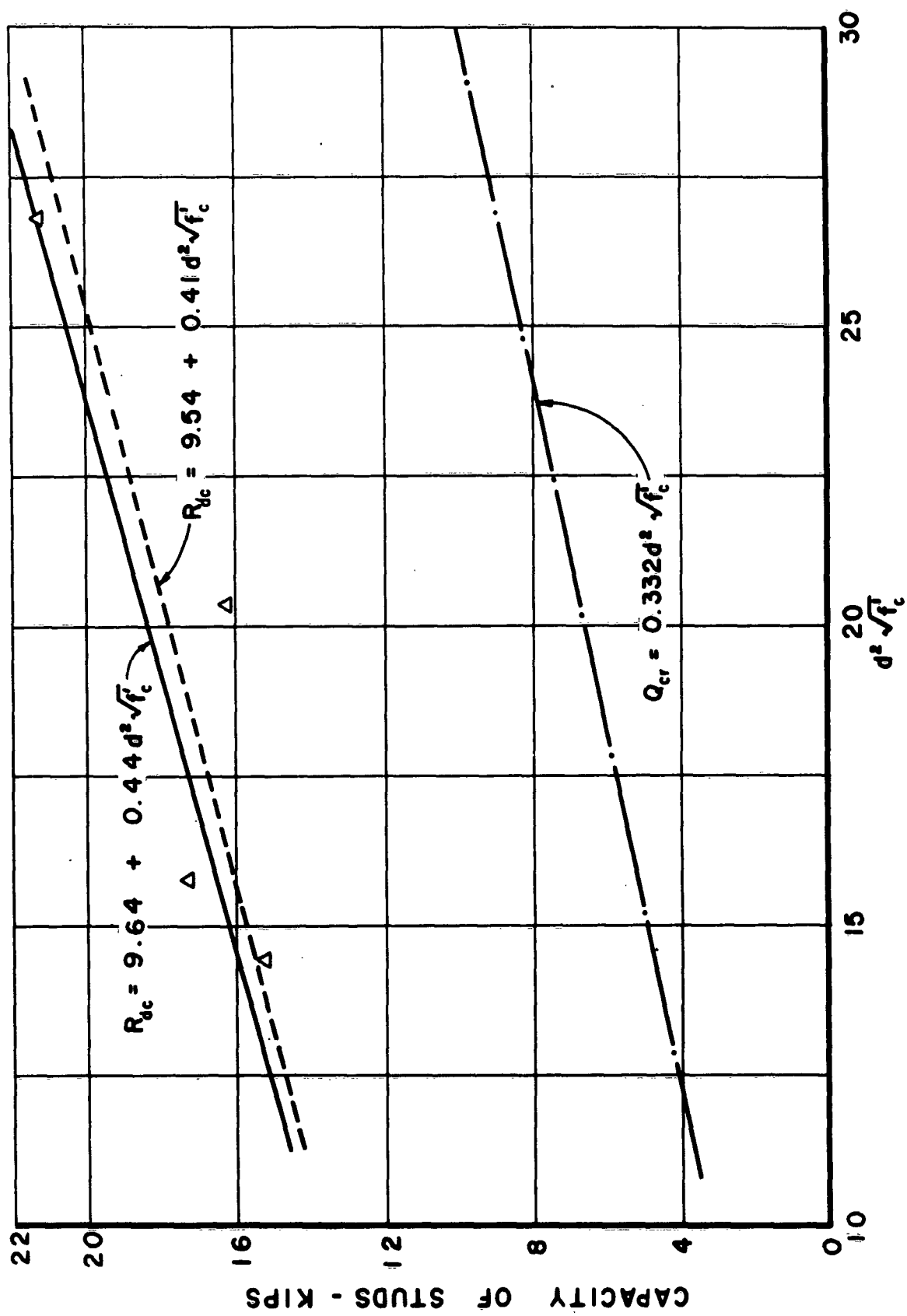
FIG. 6.2. STRAIGHT-LINE FIT OF STUD CAPACITY DATA

The chart plots CAPACITY OF STUDS - KIPS (vertical axis, 0 to 22) against $d^2\sqrt{f'_c}$ (horizontal axis, 0 to 30), showing the following relations:

$$R_{dc} = 9.54 + 0.41d^2\sqrt{f'_c}$$

$$R_{dc} = 9.64 + 0.44d^2\sqrt{f'_c}$$

$$Q_{cr} = 0.332d^2\sqrt{f'_c}$$

82

would have fallen almost exactly on the solid line if the studs in specimens No. 15 and 28 had sheared off completely as they did in all other tests making up the solid line. In order to demonstrate the extreme difference between the ultimate dynamic capacity and the statical critical capacity, the line for Q_{cr} from static tests as given in the Illinois report[1] is also included. From the static tests performed in the investigation reported herein, the maximum statical capacity was approximately 35 to 60 per cent above the critical capacity. The critical capacity per stud has been selected as that at which there is an abrupt change in the rate of slip; that is, the load at which the third stage of behavior of the shear connection begins.[1] (See Section 4 of this report on Behavior of Beams During Testing.)

SECTION 7.   DISCUSSION OF STUD CAPACITIES

7.1 General Remarks

The force-slip curves shown in Fig. 6.1 of the previous section showed the force that a given stud can carry depends to a great extent upon the slip involved. This was true in the beam tests as well as the push-out test. This section contains a discussion and comparison of the stud-capacity data obtained from both the beam tests with the plate in tension and the push-out tests.

It was mentioned in Section 6 that some slip was necessary in the push-out tests to mobilize the capacity of a stud. Because of the assumptions involved in the calculation of the force per stud in the plate-in-tension tests, the calculations indicate a sizeable force per stud even before any slip occurs. Before the beam becomes cracked, the concrete carries some of the tension, which causes this difference. Admittedly, the assumptions are not correct during this stage of loading. However, this action does suggest complete composite action and perfectly elastic action. The plotted points in Fig. 7.1 are points of maximum computed force per stud of dynamic tests before slip started, which in most cases, was probably before any cracking. A least squares technique was used to fit a straight line to these plotted points. The straight line in Fig. 7.1, therefore, represents the maximum force per stud which existed in the beams with the plate in tension at zero slip.
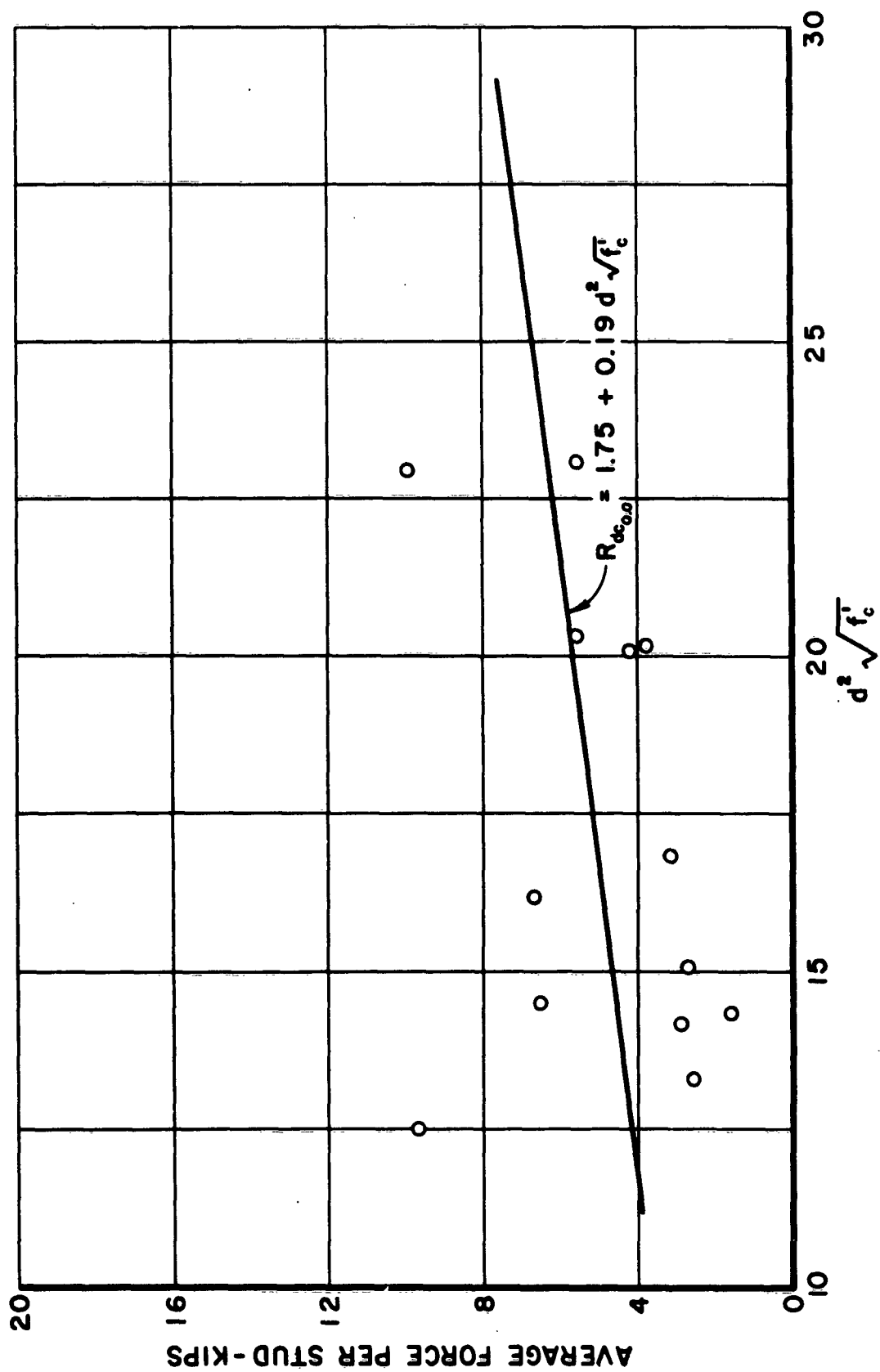
84

FIG. 7.1. FORCE PER STUD FROM BEAMS WITH THE PLATE IN TENSION AT ZERO SLIP

7.2 Comparison of Ultimate Dynamic Forces per Stud

A comparison between the maximum forces per stud obtained from beams and push-out tests is made in Fig. 7.2. None of the studs were sheared off in the beam tests which resulted in lower forces per stud. The solid line is a fit of the points for beams tested without stirrups. All of these beams failed in shear. The two points represented by the small triangles were not included in the straight-line fit represented by the solid line. These two points represent forces per stud from two beams tested in this series with stirrups. Even though the studs were not sheared off completely, the forces per stud came very close to the broken line representing the maximum capacities of studs from the push-out specimens. It is assumed, therefore, that the ultimate forces per stud from all beam tests would have been very close to the solid line if shear failures had been prevented.

7.3 Comparison of Forces per Stud at Various Slips

Comparisons of forces per stud from push-out tests and beam tests for slips of 0.02, 0.04, and 0.06 in. are shown in Figs. 7.3, 7.4, and 7.5, respectively. Again, straight lines were fitted to the data points. Since none of the beams collapsed before a slip of 0.06 in. had been reached, the forces were probably not seriously affected by the absence or presence of stirrups. Therefore, all beams in the plate-in-tension series were included.

For the range of concrete strengths and stud diameters studied, the forces per stud at the various slips for beams and push-out specimens

86
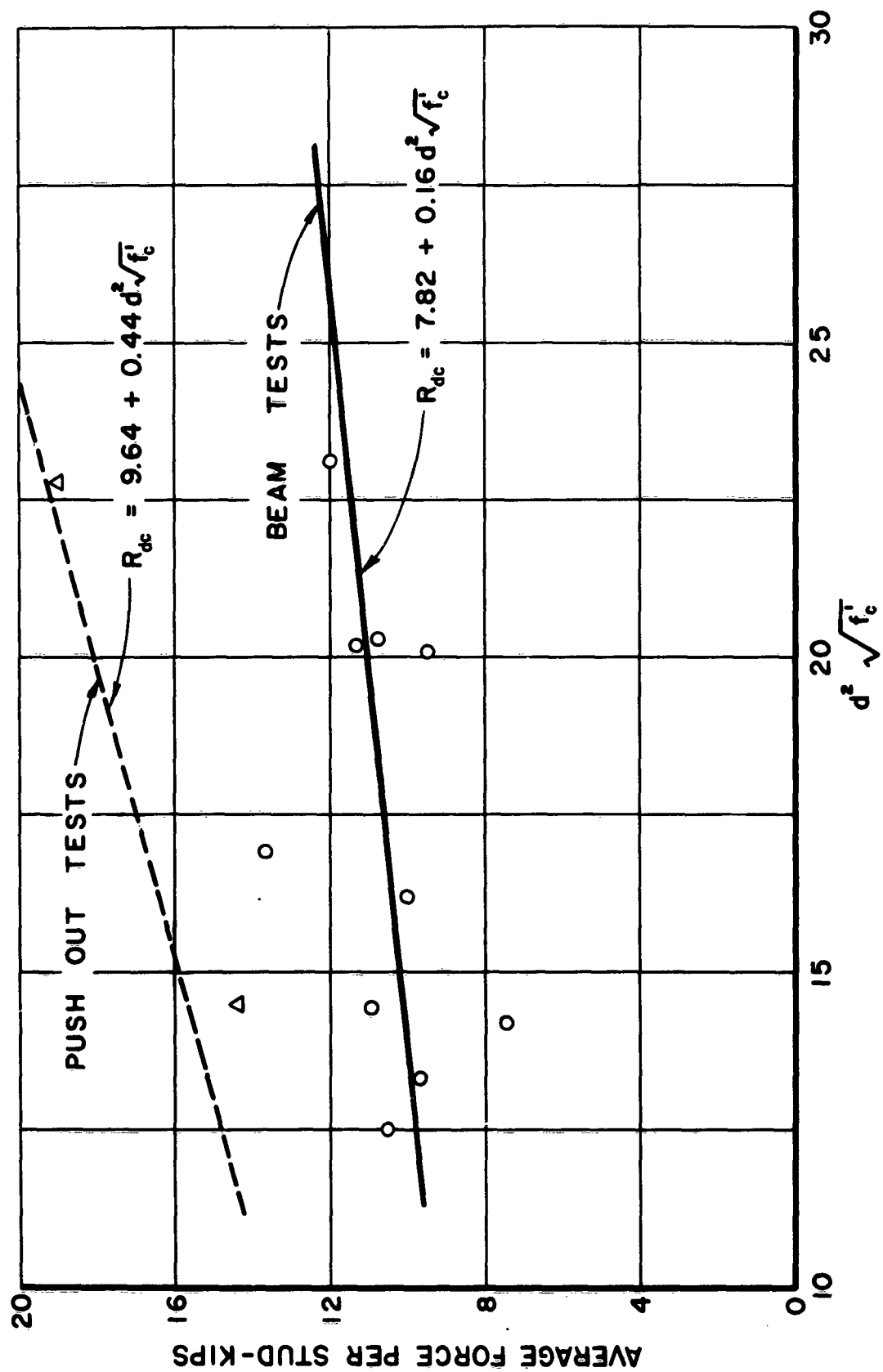
FIG. 7.2. COMPARISON OF ULTIMATE DYNAMIC FORCES PER STUD FROM BEAM AND PUSH OUT SPECIMENS

FIG. 7.3. COMPARISON OF FORCES PER STUD FROM PUSH OUT TESTS AND BEAM TESTS FOR A SLIP = 0.02 IN.

Legend within figure:

○ --- PUSH OUT TESTS
△ ——— BEAM TESTS

$R_{d_{0.02}} = 3.0 + 0.27 d^2 \sqrt{f'_c}$

$R_{d_{0.02}} = 5.3 + 0.11 d^2 \sqrt{f'_c}$

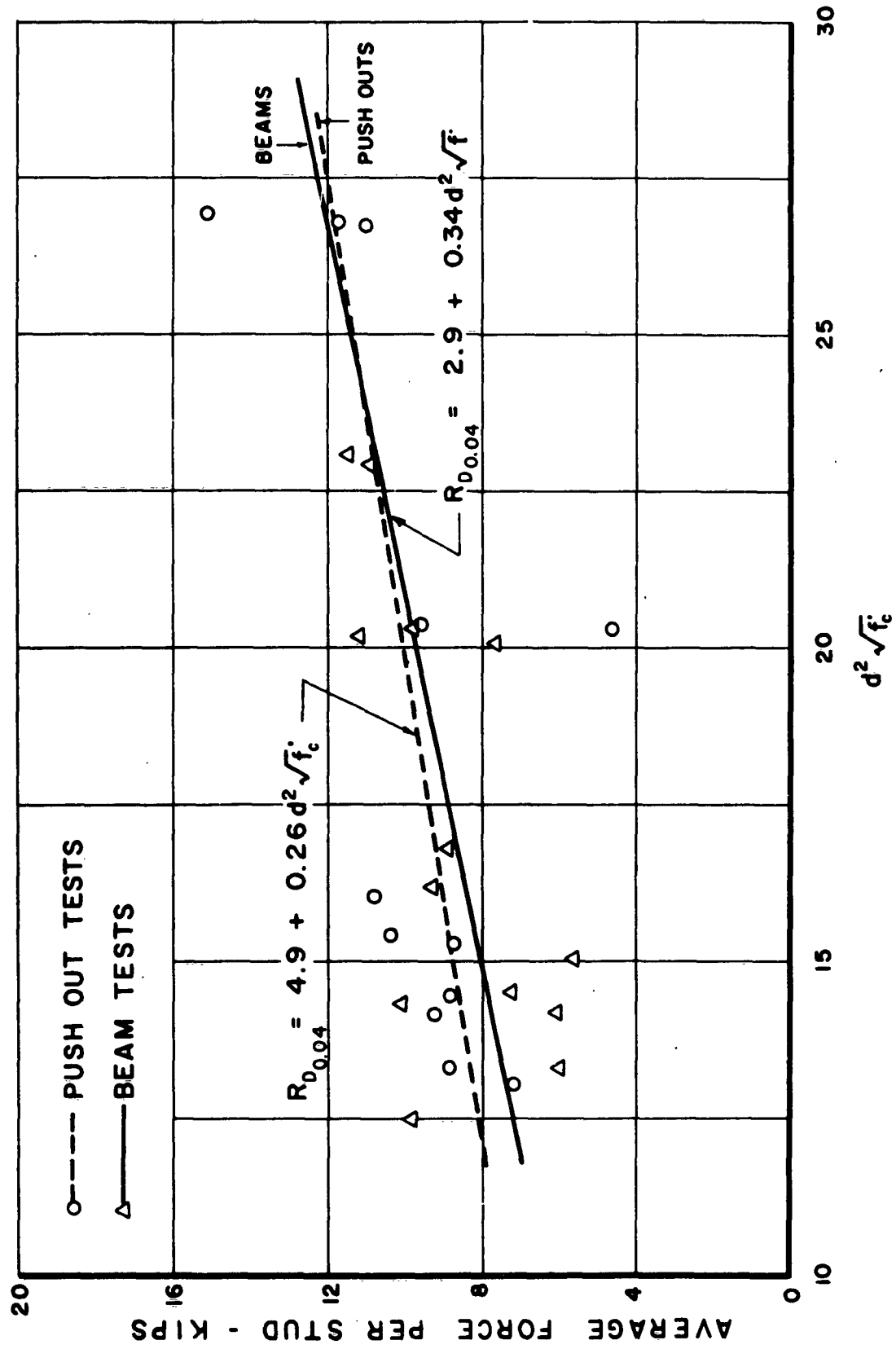Y-axis: AVERAGE FORCE PER STUD-KIPS

X-axis: $d^2 \sqrt{f'_c}$
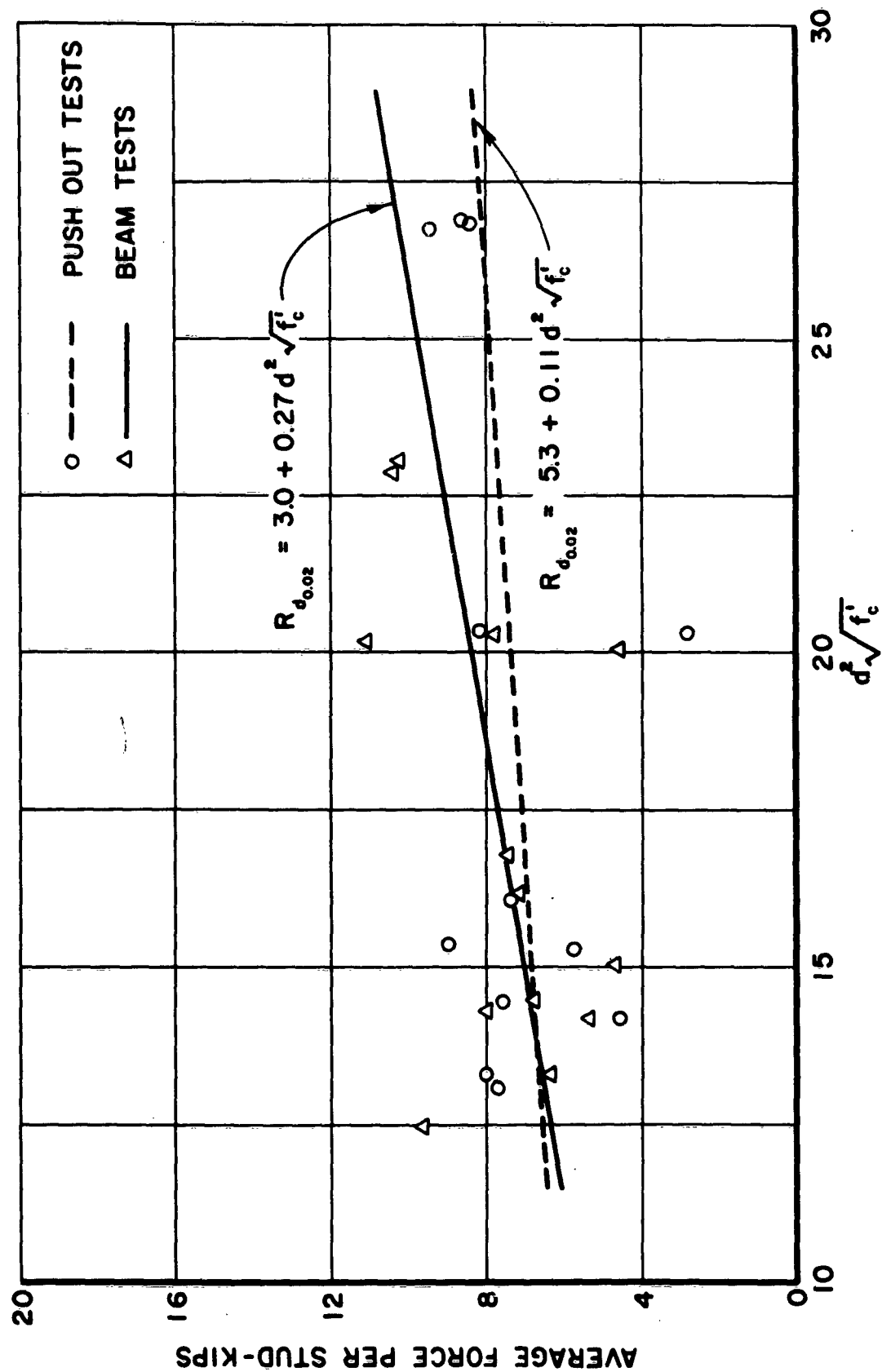
FIG. 7.4. COMPARISON OF FORCES PER STUD FROM PUSH OUT TESTS AND BEAM TESTS FOR A SLIP = 0.04 IN.
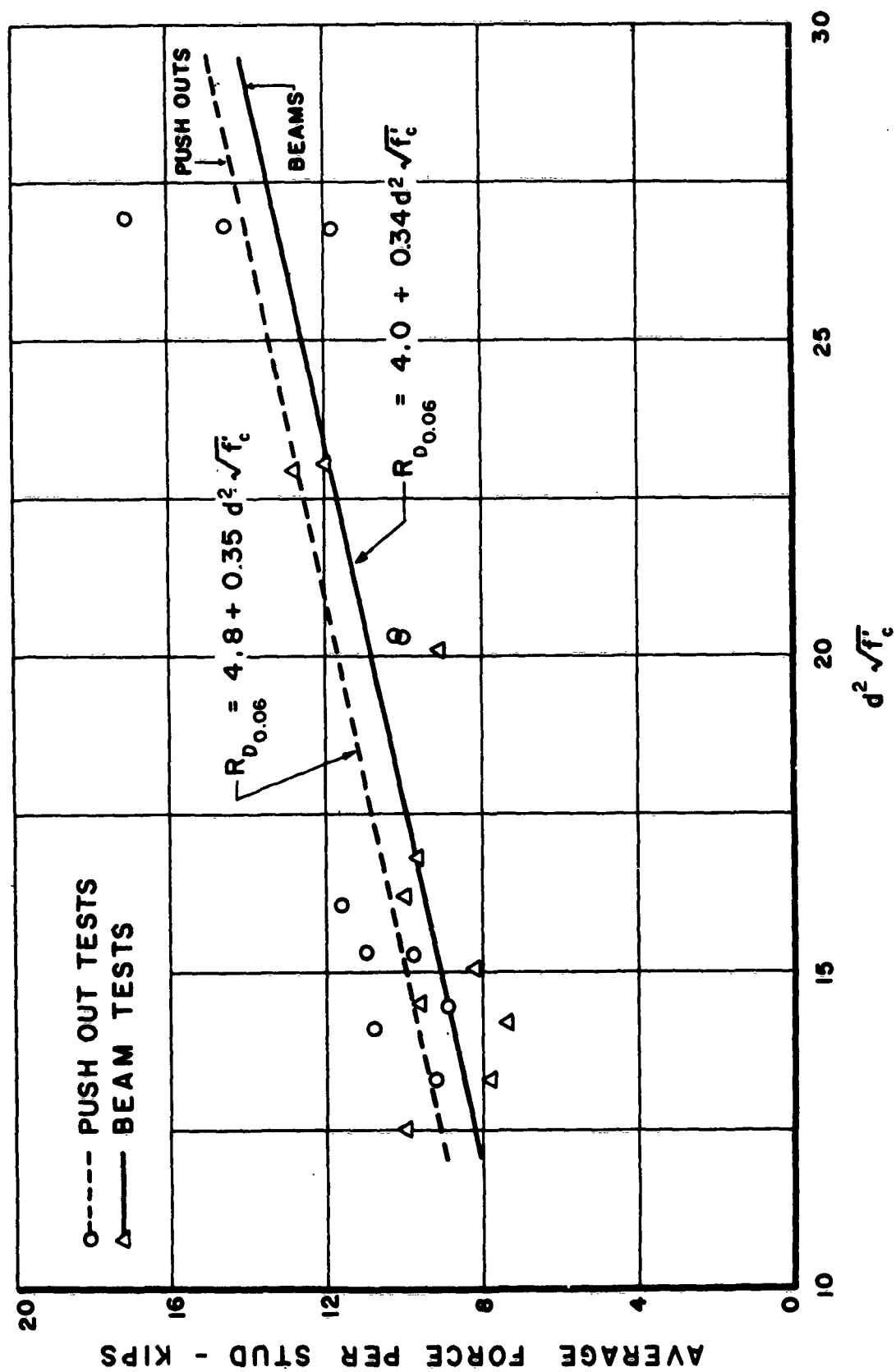
FIG. 7.5. COMPARISON OF FORCES PER STUD FROM PUSH OUT TESTS AND BEAM TESTS FOR A SLIP = 0.06 IN.

90

compare favorably even though some scatter in the data points is present. The variance of forces per stud with $d^2\sqrt{f'_c}$ for different values of slip is further indicated by these figures, particularly at the larger slips.

7.4 Slip Rates

Some of the scatter in data points seen in Figs. 7.3, 7.4, and 7.5, might be explained by different rates of slip. It is conceivable that a stud subjected to a higher slip rate will show a higher force for a certain value of slip. A study of the various slip rates for each specimen at the values of slip indicated was made. However, the slip-rate data were too erratic to be conclusive. In general, data points falling far above the line of fit were from tests having higher slip rates than most of the other tests. The converse was true for points falling far below the line of fit.

SECTION 8. DISCUSSION OF MEASURED AND COMPUTED RESPONSE

8.1 Theoretical Deflection Response

The elastic deflection response as computed by Kilgore[2] is restated in Eq. (8.1).

$$y(x,t) = \frac{4L}{\pi^4 \sqrt{EI\rho A}} \sum_{n=1,2,3}^{\infty} \sin\left(\frac{n\pi x}{L}\right) \sin\left(\frac{n\pi x'}{L}\right) \cdot Q \quad - - - - - \quad (8.1)$$

where

$$Q = \frac{1}{n^2} \sum_{m=1,2,3}^{\infty} \left\{ \frac{t_d}{m^2}(k - k_1) \cdot \sin\left(\frac{m\pi t_r}{t_d}\right) \right.$$

$$\left. - \frac{(-1)^m}{m} \pi \left[t_r(k - k_1) + t_d k_1 \right] \right\}$$

$$\cdot \left[\frac{\frac{m\pi}{t_d} \sin\left(\frac{n^2\pi^2}{L^2}\sqrt{\frac{EI}{\rho A}}\, t\right) - \frac{n^2\pi^2}{L^2}\sqrt{\frac{EI}{\rho A}} \sin\left(\frac{m\pi}{t_d}\, t\right)}{\frac{m^2\pi^2}{t_d^2} - \frac{n^4\pi^4 EI}{L^4 \rho A}} \right]$$

Equation (8.1) neglects rotatory inertia effects, deflection due to shear, and the effects of damping. All of these effects are comparatively small in most truly elastic long slender beams. The type of composite beams studied herein does not remain elastic after cracks begin to form in the

92

concrete. Therefore, Eq. (8.1) is valid only during the early stages of most of the beams tested in this investigation. As was seen in the previous sections, cracks started to form in the beams at very low values of load. This was particularly true for the beams with the plate in compression.

The inelastic deflection response of composite beams of the types discussed herein cannot be so simply determined as by Eq. (8.1). The inelastic response is dependent upon a variable beam stiffness which is virtually impossible to write algebraically. Therefore, the determination of an expression for the inelastic deflection response of composite beams will not be attempted herein.

8.2 Beam Stiffness

Beam stiffness as used herein refers to the product of modulus of elasticity and moment of inertia. The stiffness of the composite beams was dependent upon the height of cracks in the concrete and amount of slip which took place between the concrete and steel plate. Further, the beam stiffness was usually not constant along the beam due to the nonuniform distribution of cracks. In most of the beams tested in this investigation, the cracks formed near the center of the beam, (point of load) and this behavior concentrated the reduced stiffness near the center.
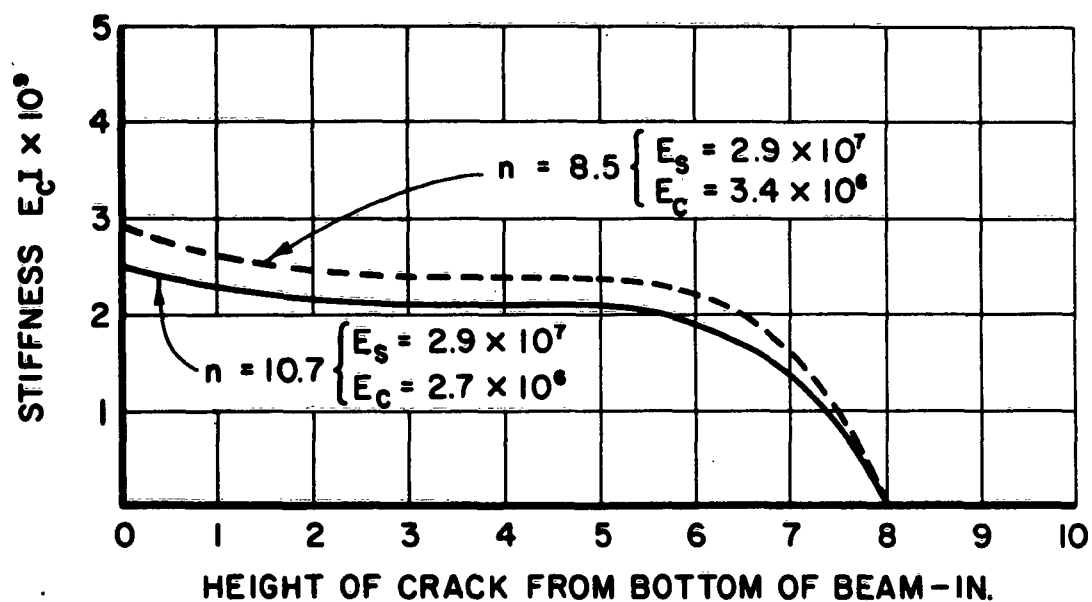
Beam stiffnesses for various crack heights were computed using the transformed-area method for two concrete strengths in both the plate-in-tension beams and the plate-in-compression beams. Curves

93

for stiffness as a function of crack heights are presented in Fig. 8.1. These stiffnesses refer only to sections of the beam where such cracks formed. Notice that after the concrete becomes cracked for 1 or 2 in. in the beams with the plate in tension, there is very little change in stiffness until the crack becomes about 6 in. high. In the beams with a plate in compression, the beam stiffness becomes approximately constant after a crack of approximately 4 in. is reached. Since the plate was on the top of the beam, the stiffness does not decrease to zero. This accounts for the observed cracks propagating very near to the top of the beams with the plate in compression without producing beam failure.

To illustrate the effect that beam stiffness had on elastic deflections, Eq. (8.1) was used to compute center-line deflections of a simply supported beam under the same concentrated load pulse for various stiffnesses. These deflections are shown in Fig. 8.2. Notice that as the stiffness decreased, the deflection and the fundamental period increased. Figure 8.2b shows how the first peak deflection varied with stiffness.

8.3 Comparison of Measured and Computed Deflections

A comparison was made by Kilgore[2] of the measured and computed deflections of a composite beam. Using Eq. (8.1) with several load pulses as measured in tests in this investigation, several additional comparisons were made between the measured deflections and the computed elastic deflections. All comparisons were on beams with the
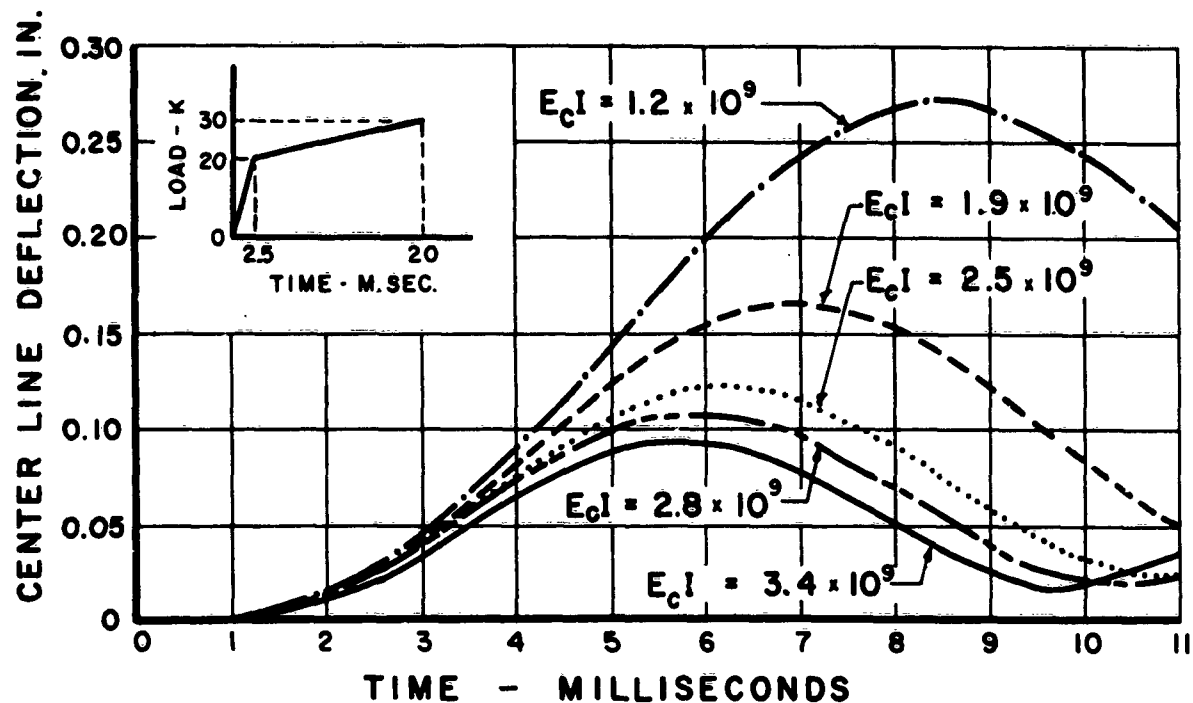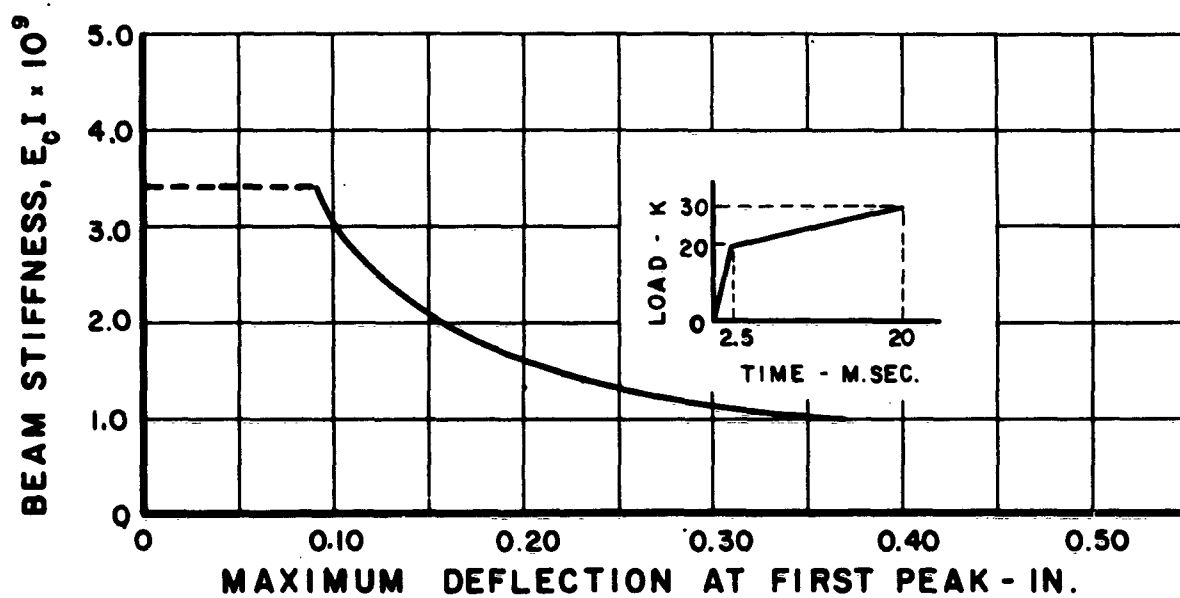
94

a.) BEAMS WITH PLATE IN TENSION
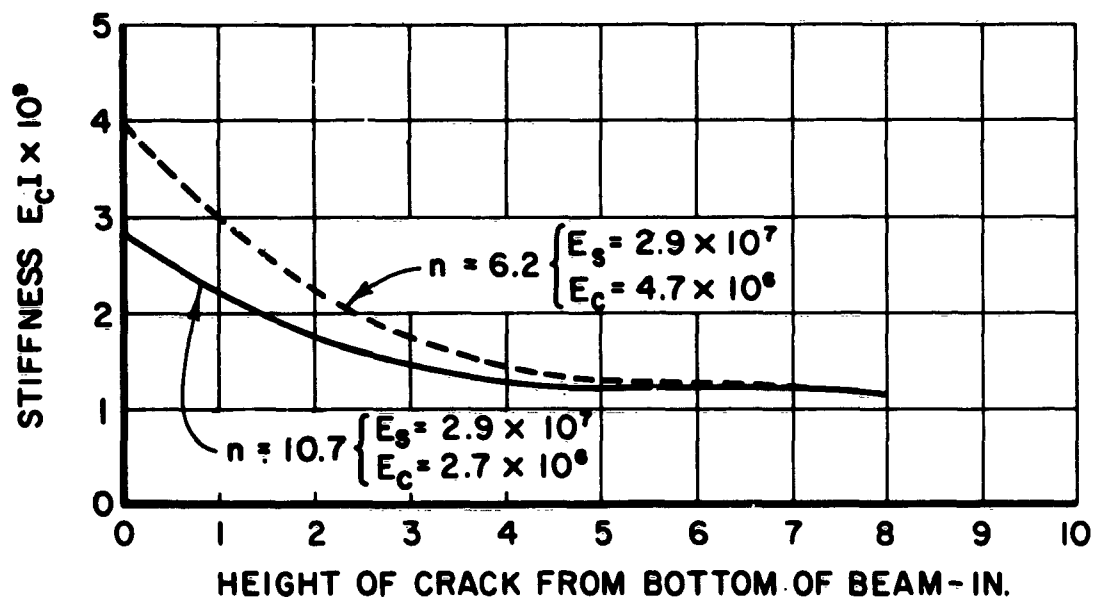
b.) BEAMS WITH PLATE IN COMPRESSION

FIG. 8.1 COMPUTED BEAM STIFFNESS AS A FUNCTION OF CRACK HEIGHTS

95

A) DEFLECTION RESPONSE FOR VARIOUS STIFFNESSES

B) FIRST PEAK DEFLECTION AS A FUNCTION OF STIFFNESS

FIG. 8.2. EFFECT OF STIFFNESS ON COMPUTED
DEFLECTIONS

96

plate-in-tension series. In each case, the measured and computed deflections were exactly the same until a deflection of approximately 0.08 to 0.10 in. was reached. In Fig. 8.2b, the beam stiffness does not change until a center-line deflection of about 0.09 in. is reached because the concrete does not become cracked until then. Therefore, for complete elastic action, the center-line deflections should be limited to approximately 1/1000 of the span. Figure 8.3 is included to show a comparison between measured deflections and elastic computed deflections for a particular beam and loading. The measured and computed deflection responses of all beams compared were the same up to approximately 0.08-in. deflection regardless of the number of studs per shear span. This suggests that the range of elastic action is mostly dependent upon the tensile strength of the concrete.

8.4 Slope, Moment, and Shear Relationships

Equation (8.1) can be differentiated successively with respect to x to determine expressions for slope, moment, and shear. These expressions are given by Eqs. (8.2), (8.3), and (8.4), respectively.

$$\theta(x, t) = \frac{\partial y\,(x, t)}{\partial x} = \frac{4L}{\pi^4 \sqrt{EI\rho A}} \sum_{n=1}^{\infty} \qquad\qquad\qquad\qquad \cdots\cdots\,(8.2)$$

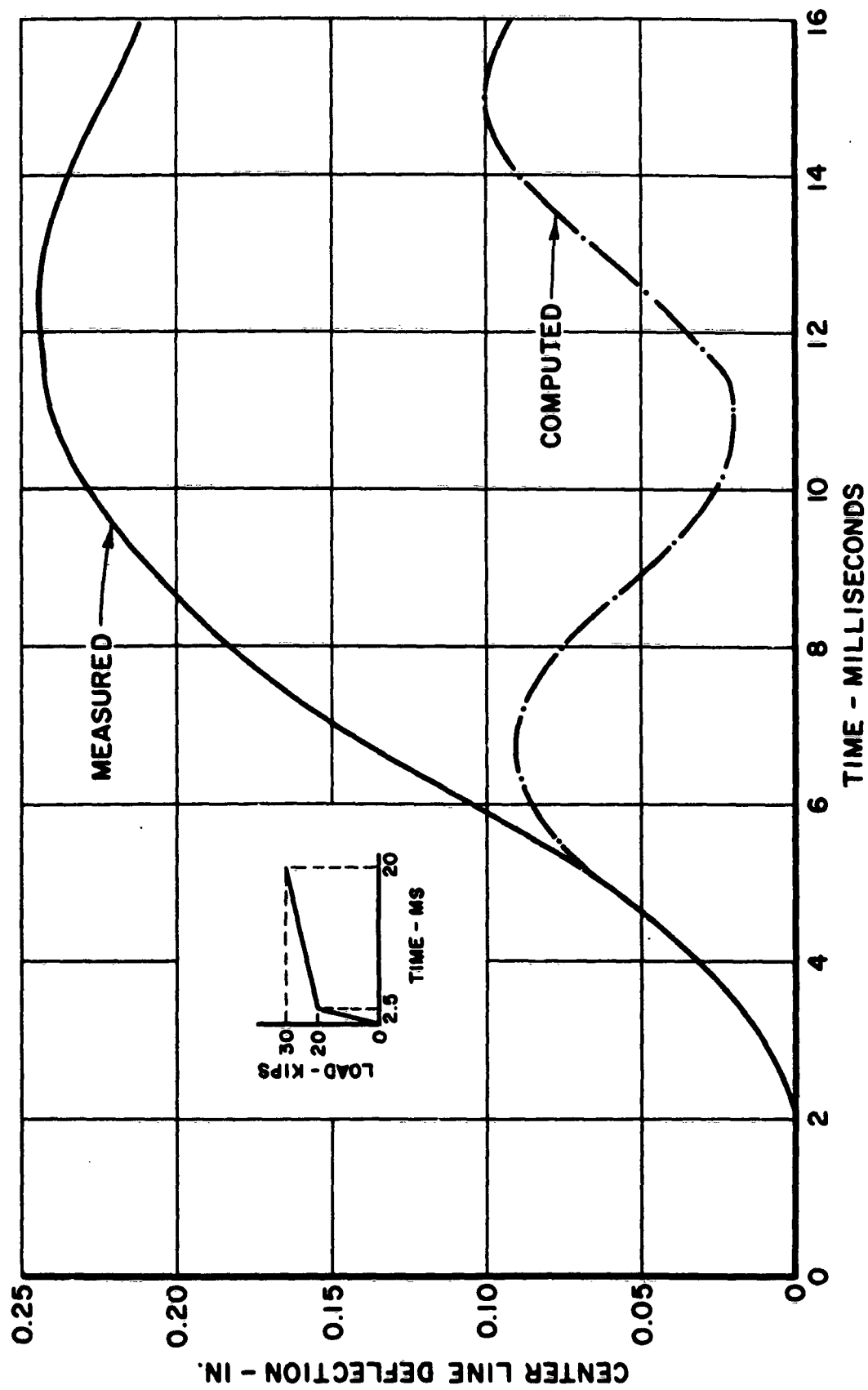$$\frac{n\pi}{L}\,\cos\left(\frac{n\pi x}{L}\right)\,\sin\left(\frac{n\pi x'}{L}\right)\,\cdot\,Q$$

97

FIG. 8.3. COMPARISON BETWEEN A MEASURED AND COMPUTED DEFLECTION RESPONSE

$$M(x,t) = \frac{\partial^2 y(x,t)}{\partial x^2} = \frac{4L}{\pi^4 \sqrt{EI\rho A}} \sum_{n=1}^{\infty}$$

$$\left. -\frac{n^2 \pi^2}{L^2} \sin\left(\frac{n\pi x}{L}\right) \sin\left(\frac{n\pi x'}{L}\right) \cdot Q \right\} \quad ----- \quad (8.3)$$

$$V(x,t) = \frac{\partial^3 y(x,t)}{\partial x^3} = \frac{4L}{\pi^4 \sqrt{EI\rho A}} \sum_{n=1}^{\infty}$$

$$\left. -\frac{n^3 \pi^3}{L^3} \cos\left(\frac{n\pi x}{L}\right) \sin\left(\frac{n\pi x'}{L}\right) \cdot Q \right\} \quad ----- \quad (8.4)$$

Notice that the value of Q is not affected by the differentiations except, in effect, a change in the powers of n. Unfortunately, the change in n is in the direction which makes convergence more difficult. Equations (8.2), (8.3), and (8.4) were programmed in Fortran-60 language for the Control Data Corporation 1604 digital computer for $m = 100$ terms and $n = 30$ terms. After a preliminary run on the computer to compute the slope and shear at the end of a beam, it appeared that the solution was diverging with increasing n. Definitely, the study indicated that it is not feasible to try to determine shear along the beam by this method.

A simple method of computing the shear in these beams was tried which assumes that the beam vibrates essentially in the first mode. A plot of deflections along the elastic beam at various times showed that this assumption is reasonable. That is, higher modes have little influence on the deflections. Using this assumption and the statical deflection equation (Eq. (8.5)), the reactions $(P/2)$ can be approximated from the known dynamical deflections.

99

$$\Delta_{\xi} = \frac{PL^3}{48EI} \qquad \qquad ----- (8.5)$$

This method was applied to an elastic steel beam which had a stiffness of 1.47×10^9 lb-inches^2. Notice the close comparison represented in Fig. 8.4a. A similar comparison was made for a composite beam tested in this study, and it is presented in Fig. 8.4b. Again the comparison is only good through the range before cracks form in the concrete. The study does indicate, however, that composite beams with the dimensions studied herein are affected very little by higher modes of vibration than the first.

If an average value of stiffness can be accurately estimated for composite beams, a closer comparison than that shown in Fig. 8.4b will result. This average stiffness should be slightly less than the uncracked beam stiffness. A good value to use appears to be that which corresponds to the horizontal portion of the stiffness-crack-height curve shown in Fig. 8.1. This value does result, however, in a nonagreement of the beginning portions of the measured and computed deflection responses.
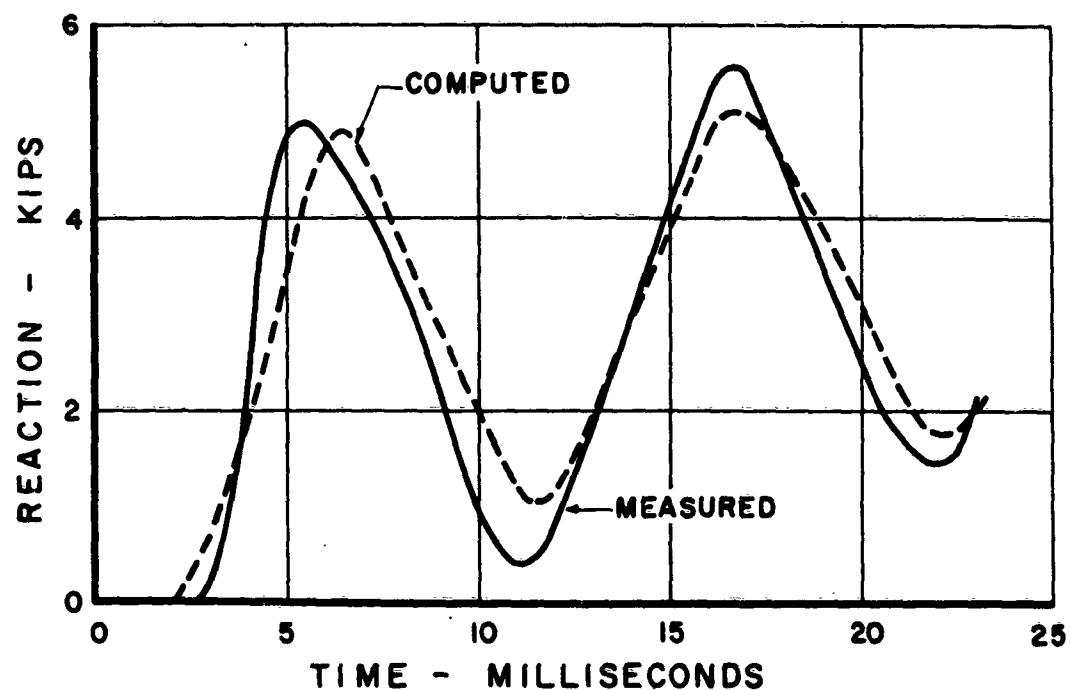
A) STEEL BEAM
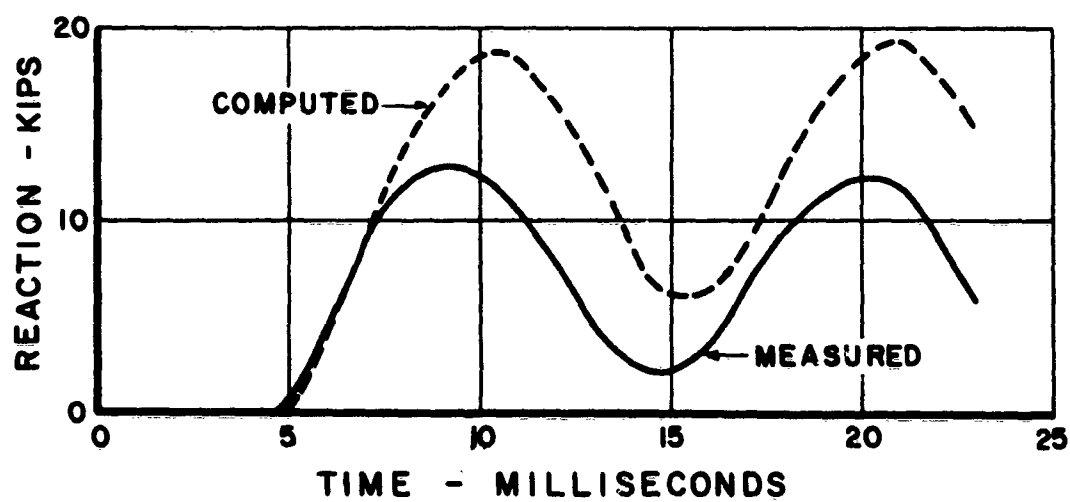
B) COMPOSITE BEAM

FIG. 8.4. COMPARISON OF MEASURED AND
COMPUTED REACTIONS

101

SECTION 9. CONCLUSIONS

The results from a study of composite steel and concrete beams
loaded statically and dynamically at their center lines have been presented.
The dynamic load pulse consisted of forces ranging up to 80 kips and
durations up to 120 milliseconds. The pulse was made up of two positive
slopes with rise times to the end of the first slope ranging from 3 to 9
milliseconds. The beams in this study were reinforced with steel plates
either at the bottom of the beams to serve as tensile reinforcement or
at the top of the beam to serve as compressive reinforcement. The
steel plates and concrete were connected to each other by steel studs
which were welded to the plates. Thus, the action of these composite
beams depended to a great extent upon the action and capacities of the
studs. Stud action and capacities were determined from push-out tests.
The action of composite beams was also studied along with the resulting
stud capacities. Comparisons were made of stud capacities obtained
from beams and push-out specimens. Within the scope of this study,
the following conclusions appear to be valid:

> 1. Concrete beams with steel plates connected to the
>   concrete by welded stud shear connectors at the
>   concrete-steel interface respond satisfactorily as
>   composite members under both static and dynamic
>   loadings, for slips up to 0.06 in. at the interface.

102

2. Dynamic tests of composite beams with a plate serving as tensile reinforcement show approximately a 50-percent increase in flexural resistance over companion beams tested statically. This increase in flexural resistance is due mainly to the increase in strengths of the separate materials resulting from high straining rates.

3. Dynamic capacities of stud shear connectors as found from dynamic push-out tests compare favorably with those from beam tests for various slips. Therefore, when only dynamic stud capacities are desired, they may be determined from simple dynamic push-out tests.

4. Slip between the concrete and steel is necessary to mobilize the full dynamic capacity of a stud.

5. Stud diameter and concrete compressive strength are critical parameters in the determination of dynamic stud capacities. Stud capacities vary approximately with $d^2\sqrt{f'_c}$.

6. Ultimate dynamic stud capacities can be reached only if sufficient shear strength is provided to prevent the beams from failing prematurely in shear. For beams of the type tested in this program, shear reinforcement was required for the stud capacities to be reached.

7. Ductility is increased slightly in beams with a plate in tension by increasing the concrete strength. Beams with a plate in compression have considerably more ductility than beams with a plate in tension. Beams loaded dynamically show more ductility than companion beams loaded statically.

8. Composite beams may be loaded repeatedly with dynamic loading without causing failure if the loads are well within the elastic capacities of the beams. Repeated loads at or greater than the elastic capacities would cause progressive damage which would ultimately lead to failure.

9. The deflection response of the type of composite beams studied in this investigation is affected very little by higher modes of vibration than the first mode.

10. Stud capacities and beam shear capacities are two of the major parameters to consider in the design of composite beams.

SECTION 10. RECOMMENDATIONS

10.1 General Remarks

Based on the data obtained in this investigation, certain recommendations can be made regarding beam design. It is assumed that composite beams of the type mentioned herein will be designed considering that the sole structural purpose of the steel plate is to carry either tension or compression forces. That is, the capacity of the plate to resist shear in a direction normal to the plate is negligible. Therefore, the major objective is to design for a proper horizontal shear connection between the concrete and steel plate.

When designing composite beams to resist dynamic loads, it is recommended that ultimate strengths of the materials be used. A few simple design suggestions and stud capacities are suggested in the following paragraphs.

10.2 Plate as Tensile Reinforcement

Beams with a steel plate acting as tensile reinforcement may be designed under the following assumptions:

a. The steel plate carries all of the tension, i.e., the concrete is not effective in tension.

b. Studs in a constant shear zone share the horizontal shear equally.

105

c. Studs in a variable shear zone carry horizontal shear in proportion to the shear diagram.

Based on the above assumptions, studs should be spaced according to the vertical shear diagram. Presumably, any combination of stud sizes may be used so long as their capacities satisfy the force requirements dictated by the shear diagram. For continuity of action between the steel plate and concrete, a minimum of one stud per square foot of plate area is recommended.

Repeated loads. A study was made on all beams which were tested with repeated loads to determine the highest load per stud that would permit essentially all beam deflection to be recovered when the load was removed. Figure 10.1 shows the procedure used.
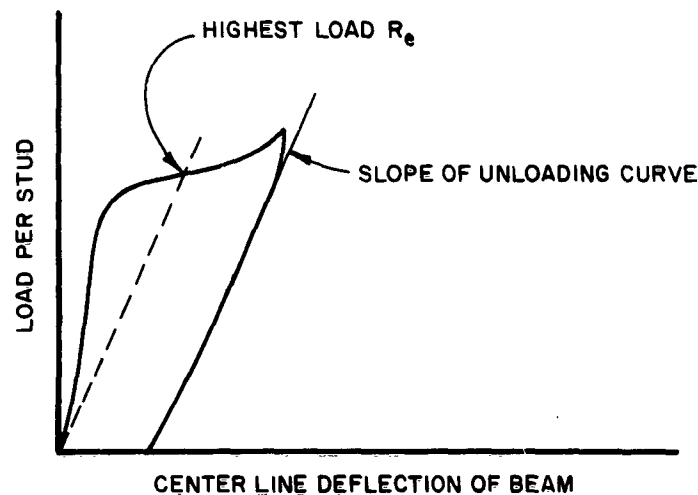

FIG. 10.1   PROCEDURE USED TO DETERMINE R_e

A line was drawn with the same slope as the unloading curve but through zero deflection. It was assumed that the slope of all unloading curves for a particular member would be the same as that determined in the

106

tests. The point where this line intersected the loading curve was chosen as the highest load per stud that permitted essentially all deflection to be recovered when the load was removed. This load corresponded to a slip slightly more than 0.02 in. in all cases. Therefore, a slip of 0.02 in. is recommended as the maximum slip to be permitted in design when a few repeated loads (say less than 10) are expected.

If more than 10 repeated loads are expected, stud capacities for zero slip are recommended. This would ensure complete elastic action. If only one load is expected, a slip of 0.06 in. can be tolerated without total collapse.

The following stud capacities are recommended for use in design of composite members with a steel plate acting as tensile reinforcement:

$$R_{dc_{0.00}} = 1.75 + 0.19 \; d^2\sqrt{f'_c} \quad - - - \text{ Elastic (many repeated loads)}$$

$$R_{dc_{0.02}} = 3.0 \; + 0.27 \; d^2\sqrt{f'_c} \quad - - - \text{ Less than 10 repeated loads}$$

$$R_{dc_{0.06}} = 4.0 \; + 0.34 \; d^2\sqrt{f'_c} \quad - - - \text{ Only one load expected}$$

Beam shear. The average ultimate dynamic beam shearing stress was computed for all beams which failed in shear. The values of shearing stress ranged from $2.60\sqrt{f'_c}$ to $5.54\sqrt{f'_c}$ with an average value of $3.77\sqrt{f'_c}$. It appears that an ultimate dynamic shearing stress in the concrete of $2.0\sqrt{f'_c}$ can easily be tolerated without beam collapse.

It is recommended that web reinforcement be provided for all shearing stresses in excess of a value of $2.0\sqrt{f_c'}$.

10.3 Plate as Compressive Reinforcement

The main assumption that should be made in designing beams with a plate acting as compressive reinforcement, is that the change in compressive force in the plate along the beam is caused only by the studs. Therefore, it is recommended that the studs be designed and spaced according to the change in plate-force diagram along the beam. The stud capacities recommended above for the various slips and repeated loading conditions are also recommended for beams with the plate acting as compressive reinforcement. Using these capacities, beams with a plate serving as compressive reinforcement may be designed simply as doubly reinforced beams. Again it is recommended that at least one stud per square foot of plate be used as a minimum whether it is needed or not for the transfer of shear. If in certain cases, buckling of the plate is quite possible, the stud spacing might be dictated by the requirement to prevent buckling.

10.4 Future Research

In this investigation, certain information has been found which should extend the understanding of composite beam design and construction. Experience gained during this investigation dictated certain aspects of composite beam design which were outside of the scope herein, but which might increase understanding. Therefore, the following recommendations which might be of concern to future researchers are made.

108

1. Since shear strength of the concrete was so critical in the tests reported herein, a comprehensive study of the dynamic shear strength of concrete should be made. To supplement the study of dynamic shear strength as well as to afford other information pertinent to beam design, a study of the dynamic tensile strength of concrete should be made.

2. A study should be made using both static and dynamic tests of composite beams composed of concrete and steel plates on both the top and bottom faces of the concrete. In addition, a study should be made of the action of beams where reinforcing bars and a steel plate are both used either as tension or compression reinforcement.

3. Since lightweight concrete is being used more and more in construction, a study similar to the type reported herein should be made using lightweight concrete.

4. It is suggested that an analytical study of beam action be made which includes the inelastic action of the beam. In this study, both slip at the concrete-steel interface and reduced stiffness of the beam as a result of cracking of the concrete should be included.

5. In any future tests of the type reported herein, it is recommended that slip at the concrete-steel interface be measured at several points along the beam. This is

109

needed more at low values of load than at ultimate load.
A better understanding of slip distribution at low loads
might serve to predict failure mechanisms.

SECTION 11. REFERENCES

1. Juan Casillas G. de Leon, et al, Study of Reinforced Concrete Beams and Slabs Reinforced with Steel Plates, Contract AF 33(600)-31319, Urbana, University of Illinois, May 1957.

2. Kilgore, Larry, The Response of an Elastic Beam, Simply Supported Subjected to Dynamic Loads at Its Center Line, Master's Thesis, Austin, The University of Texas, January 1964.

3. Viest, I. M., "Investigation of Stud Shear Connectors for Composite Concrete and Steel T-Beams," Proceedings, Journal of American Concrete Institute, Vol. 53, April 1956, pp. 875-891.

4. Howland, F. L., and W. Egger, Correlation of Results of Dynamic Tests of Beams and Model Frames, Civil Engineering Studies, Urbana, Structural Research Series No. 109, University of Illinois, September 1955.

5. Matlock, Hudson, et al, High-Velocity Impact Cushioning, Part I, Drop-Test Facilities and Instrumentation, Austin, Structural Mechanics Research Laboratory, The University of Texas, August 1957, pp. 9-12.

6. Air Force Design Manual, Principles and Practices for Design of Hardened Structures, Research Directorate, AF SWC - TDR 62-138, Air Force Special Weapons Center, Air Force Systems Command, Kirtland Air Force Base, New Mexico, December 1962.

7. Smith, E. F., and J. Neils Thompson, A Study of Vermiculite Concrete as a Shock-Isolating Material, Austin, Structural Mechanics Research Laboratory, The University of Texas, January 1964, (Contract DA 22-079-eng-342).

APPENDIX

APPENDIX A. DETAILS OF TEST SPECIMENS

A. 1 General Remarks

This appendix contains a compilation of the details of the test specimens. Table A-1 contains a summary of pertinent information concerning the test program. Dimensions of the various specimens are given in Figs. A-1 through A-3.

113

TABLE A-1

Summary of Information Concerning Test Program

Plate-in-Tension-Series

Specimen No.	f'_c (psi)	Drop No.	Drop Height (ft)	Cushioning Material	Remarks
13S5	5574				Static Test
14S5	5977				Static Test
17S3	3515				Static Test
8D3B9	2706	14	10'-0"	V.C.*	
9D3A6	2500	16	6'-0"	V.C.	
10D5A9	4315	17	12'-6"	S.G.**	
11D5B9	3505	21	13'-0"	V.C.	
12D3A12	3216	22	11'-6"	V.C.	
13D3A9	2823	25	10'-0"	V.C.	
14D3B12	2643	29	16'-0"	V.C.	
15D3B6	2665	30	8'-0"	V.C.	
16D3A14	3300	32	11'-6"	V.C.	
17D5A11	4326	33	4'-6"	S.G.	
17D5A11	4526	34	11'-6"	V.C.	2nd Drop
18D3A12	3623	35	10'-0"	V.C.	Stirrups
18D3A12	3623	36	14'-0"	V.C.	2nd Drop
23D3A9	3390	44	13'-0"	S.G.	Color Fastax
23D3A9	3390	45	11'-0"	V.C.	2nd Drop

TABLE A-1 (Cont'd)

Summary of Information Concerning Test Program

Plate-in-Tension Series (Cont'd)

Specimen No.	f'_c (psi)	Drop No.	Drop Height (ft)	Cushioning Material	Remarks
24D3B6	3463	46	13'-0"	S. G.	
24D3B6	3463	47	12'-0"	V. C.	2nd Drop

Plate-in-Compression Series

Specimen No.	f'_c (psi)	Drop No.	Drop Height (ft)	Cushioning Material	Remarks
19S3-0	2590				Static Test
20S3C9	2720				Static Test
21D3-0	2626	40	10'-0"	V. C.	
22D3C9	2726^+	41	13'-0"	V. C.	
22D3C9	2726^+	42	14'-0"	V. C.	2nd Drop
26D5D4	4053	50	13'-0"	V. C.	1st Drop
26D5D4	4053	51	16'-6"	V. C.	2nd Drop
26D5D4	4053	52	13'-0"	V. C.	3rd Drop
27S5D4	4716				Static Test
28S3C12	2710				Static Test
29D3C12	2945	54	13'-0"	V. C.	
30D3C6	3226	60	16'-6"	V. C.	

115

Summary of Information Concerning Test Program

Push-Out Test Series

Specimen No.	f'_c (psi)	Drop No.	Drop Height (ft)	Cushioning Material	Remarks
2S5A4P	6497				
5S3A4P	2680				
6D3B4P	3350	6	7'-0"	V.C.	1st Drop
6D3B4P	3350	7	7'-6"	V.C.	2nd Drop
6D3B4P	3350	8	9'-6"	V.C.	3rd Drop
10D5A4P	4163$^+$	18	8'-0"	V.C.	
10D5A4P	4163$^+$	19	14'-0"	V.C.	2nd Drop
15D3B4P	2665$^+$	31	14'-0"	V.C.	
22D3A4P	2726$^+$	43	13'-0"	V.C.	
25D3A4P	3740	49	13'-0"	V.C.	
27D5B4P	4716	53	20'-0"	V.C.	
28D3B4P	2710$^+$	58	20'-0"	V.C.	
29D3A4P	2945	57	20'-0"	V.C.	
30D3A4P	3226	59	15'-0"	V.C.	
31D5B4P	4733	63	20'-0"	V.C.	
32D5B4P	4607	64	18'-0"	V.C.	
33D5A4P	3770	65	18'-0"	V.C.	

$^+$Concrete strengths were slightly higher in specimen due to testing one day after testing control cylinders.

*V.C. Vermiculite Concrete (see Appendix B)

**S.G. Spiralgrid (see Appendix B)
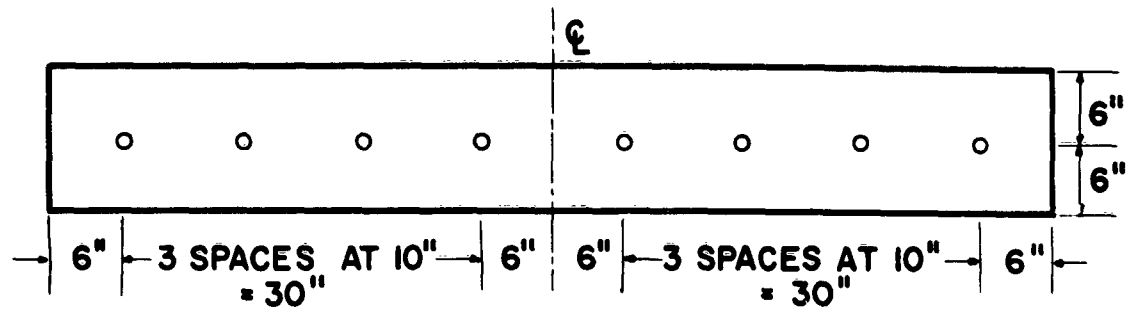
4 STUDS PER SHEAR SPAN
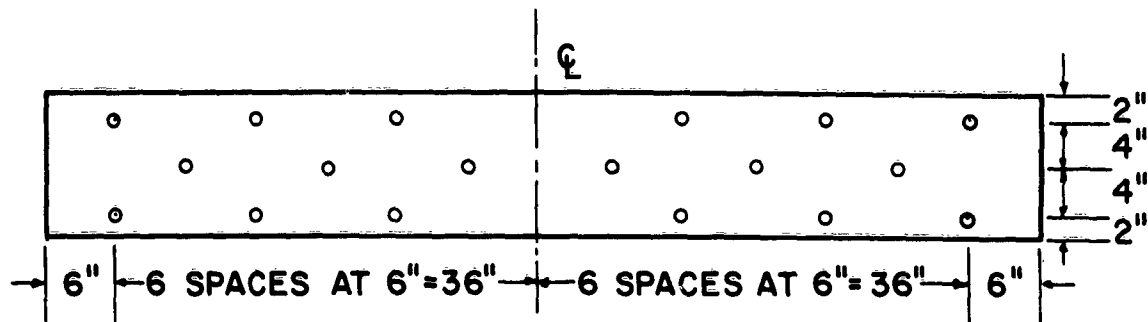
26D5D4   27S5D4
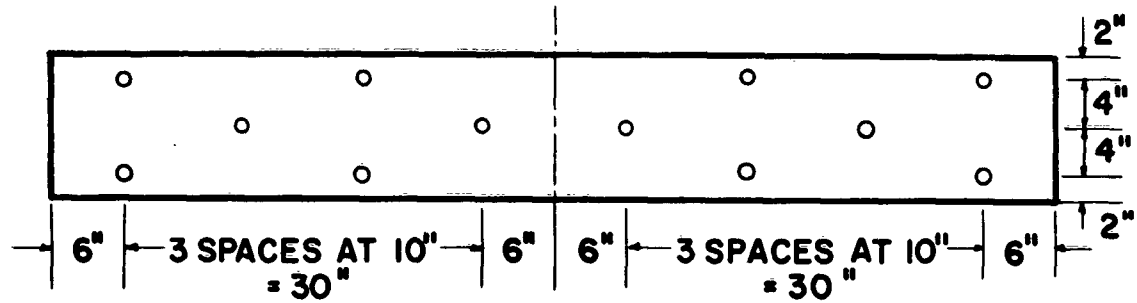
6 STUDS PER SHEAR SPAN
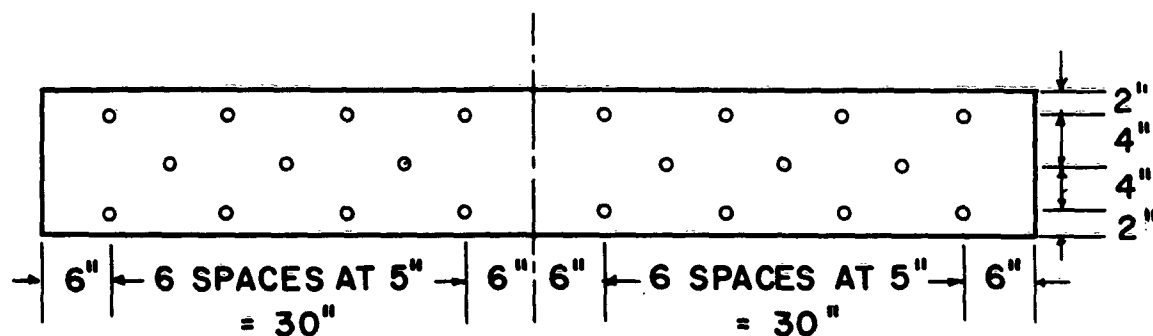
15D3B6   25D3C6
24D3B6   30D3C6
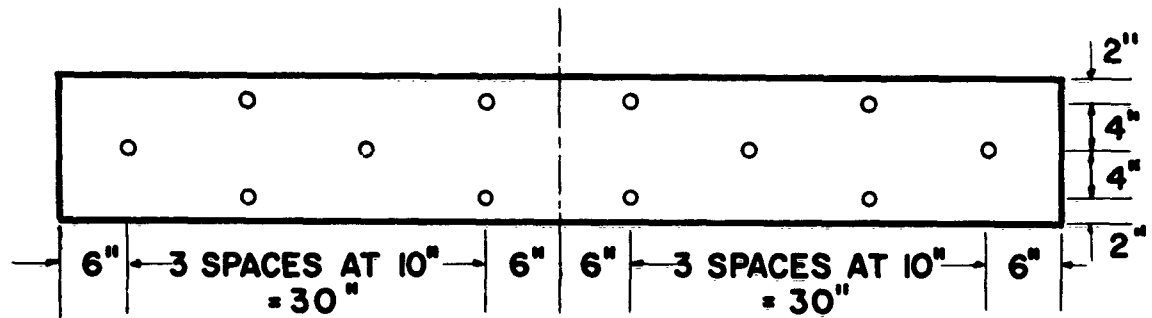
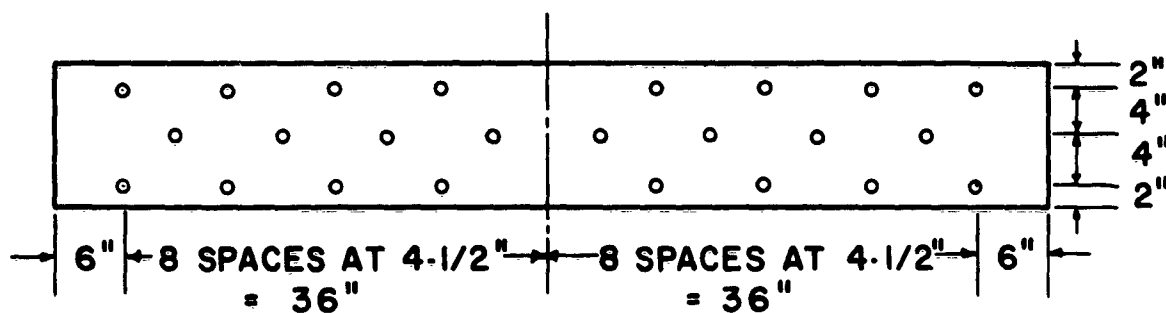6 STUDS PER SHEAR SPAN

9D3A6

FIG. A-I. STUD PATTERN AND SPACING

117

9 STUDS PER SHEAR SPAN

4S5A9	10D5A9	20S3C9
7S3B9	11D5B9	22D3C9
8D3B9	13D3A9	23D3A9

11 STUDS PER SHEAR SPAN

17D5A11

12 STUDS PER SHEAR SPAN

18D3A12S   28S3C12   29D3C12

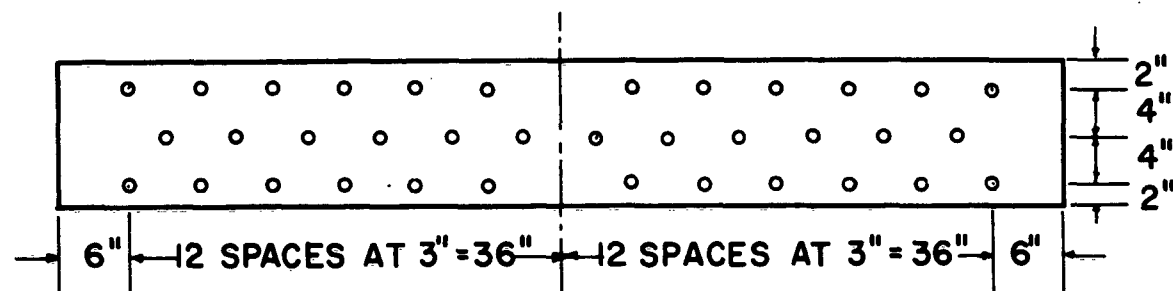FIG. A-1 (CONTD.). STUD PATTERNS AND SPACINGS
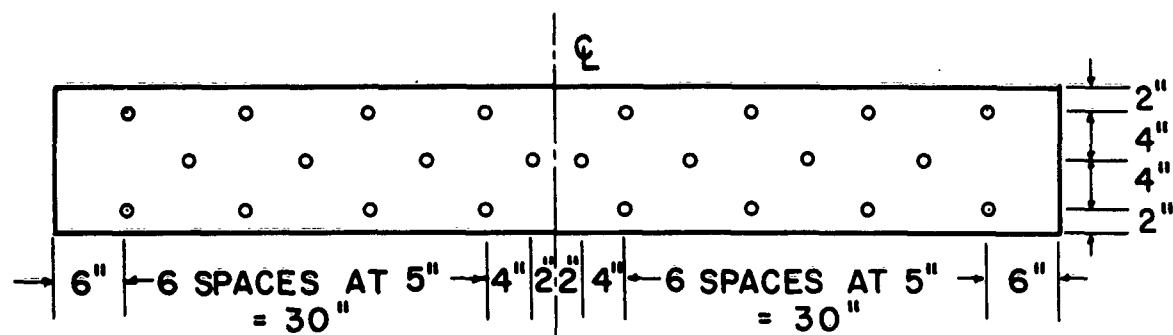
12 STUDS PER SHEAR SPAN

12D3A12   14D3B12
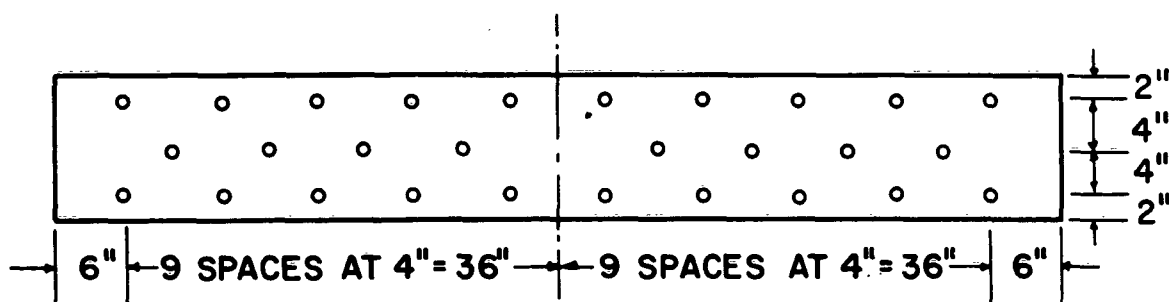
14 STUDS PER SHEAR SPAN

16 D3A14

18 STUDS PER SHEAR SPAN

3S5A18

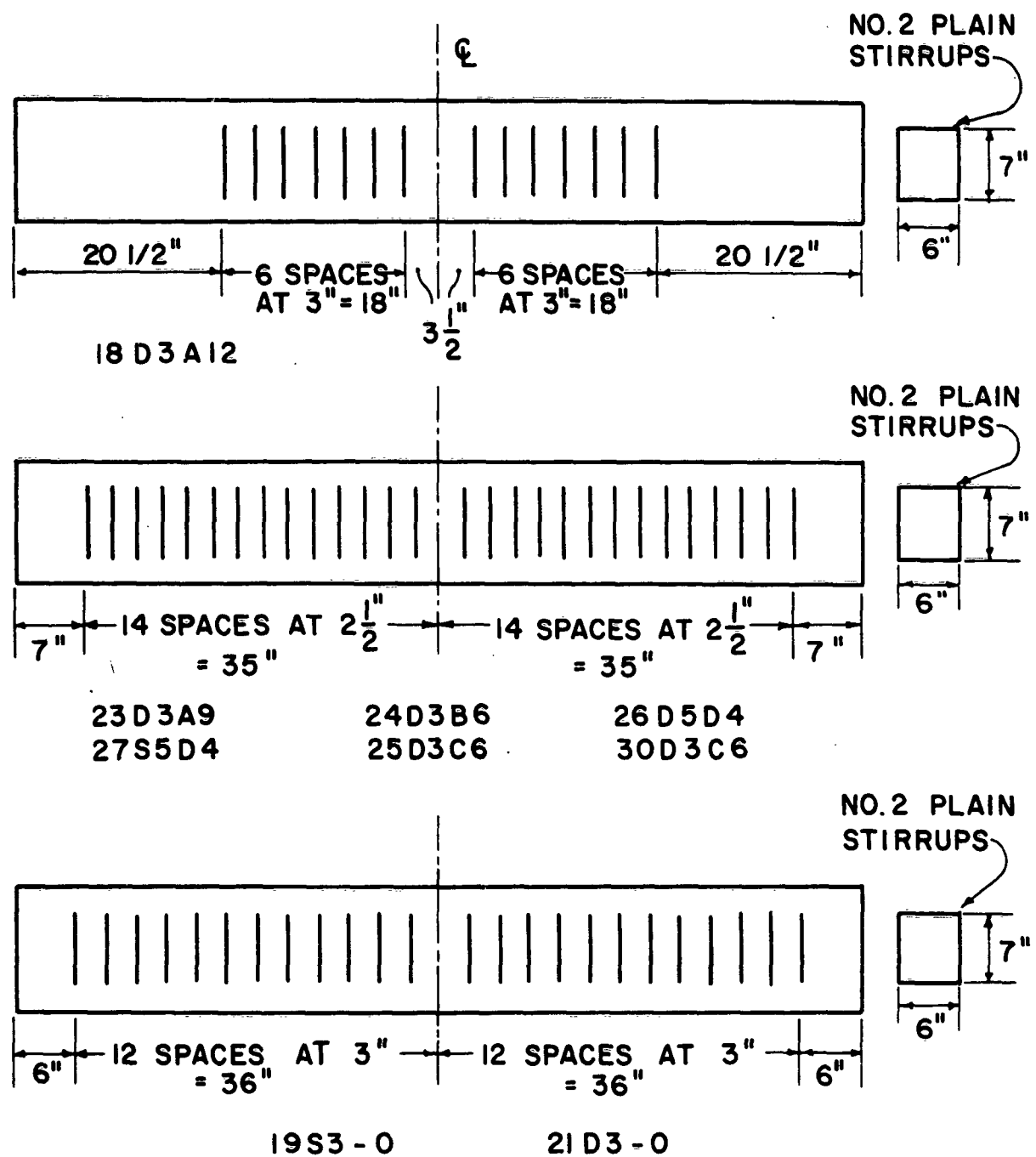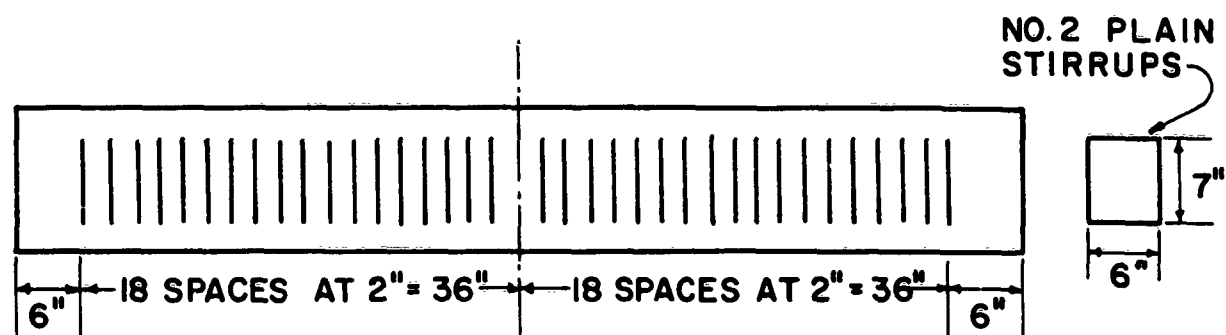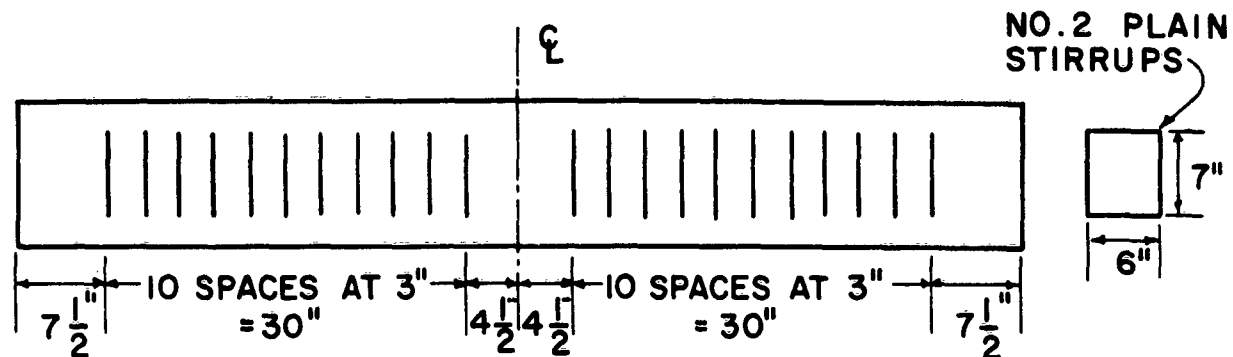FIG. A-1 (CONTD.). STUD PATTERNS AND SPACINGS

NO. 2 PLAIN STIRRUPS

7"

6"

20 1/2" 6 SPACES AT 3"= 18" $3\frac{1}{2}$" 6 SPACES AT 3"= 18" 20 1/2"

18 D 3 A 12

NO. 2 PLAIN STIRRUPS

7"

6"

7" 14 SPACES AT $2\frac{1}{2}$" = 35" 14 SPACES AT $2\frac{1}{2}$" = 35" 7"

23 D 3 A 9   24 D 3 B 6   26 D 5 D 4
27 S 5 D 4   25 D 3 C 6   30 D 3 C 6

NO. 2 PLAIN STIRRUPS

7"

6"

6" 12 SPACES AT 3" = 36" 12 SPACES AT 3" = 36" 6"

19 S 3 - 0   21 D 3 - 0

FIG. A-2.   STIRRUP   PATTERNS   AND   SPACING

NO.2 PLAIN STIRRUPS

7"

6"

7½" | 10 SPACES AT 3" = 30" | 4½" 4½" | 10 SPACES AT 3" = 30" | 7½"

20 S 3 C 9   22 D 3 C 9

NO.2 PLAIN STIRRUPS

7"

6"

6" | 18 SPACES AT 2" = 36" | 18 SPACES AT 2" = 36" | 6"

28 S 3 C 12   29 D 3 C 12

FIG. A - 2 (CONTD.). STIRRUP PATTERNS AND SPACING
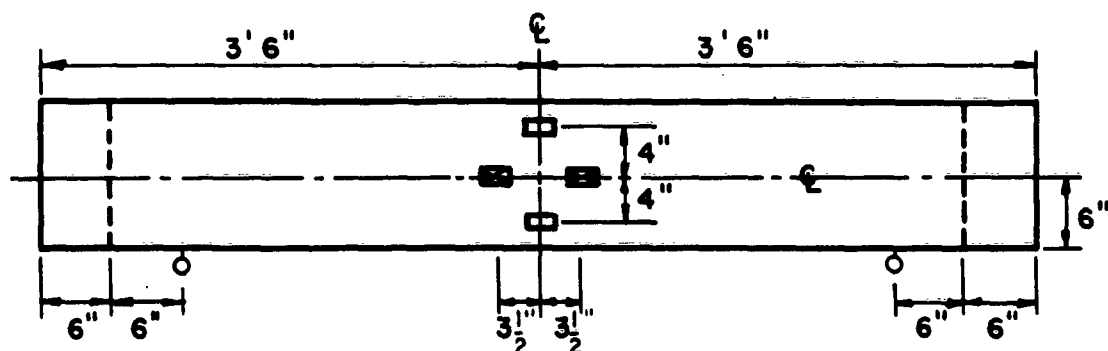
121

3'6" | 3'6"

4"
4"
6"

6" 6" | 3½" 3½" | 6" 6"

3S5A18   4S5A9   7S3B9
8D3B9   9D3A6   10D5A9
11D5B9   12D3A12   13D3A9
14D3B12   15D3B6   16D3A14
17D5A11   18D3A12S   23D3A9
24D3B6

3'6"

6"

6" 6" | 3½" 3½" | 6" 6"
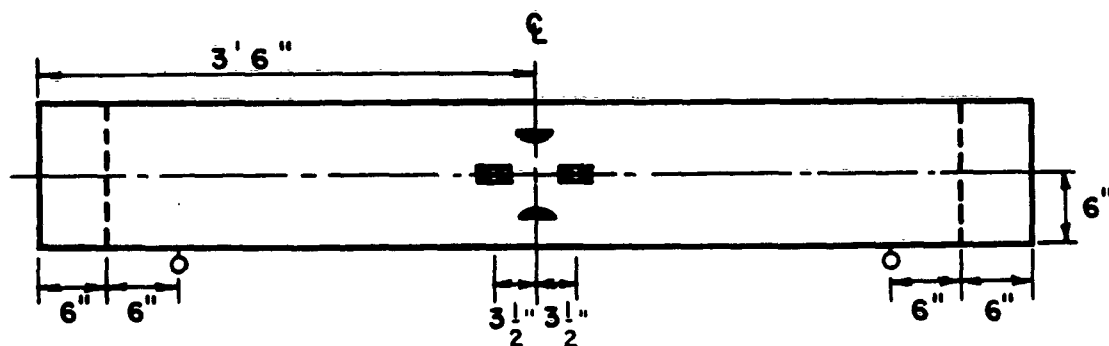
19S3-0(NO SLIP GAGES)   22D3C9   28S3C12   25 D3C6
21D3-0(NO SLIP GAGES)   26D5D4   29D3C12   30 D3C6
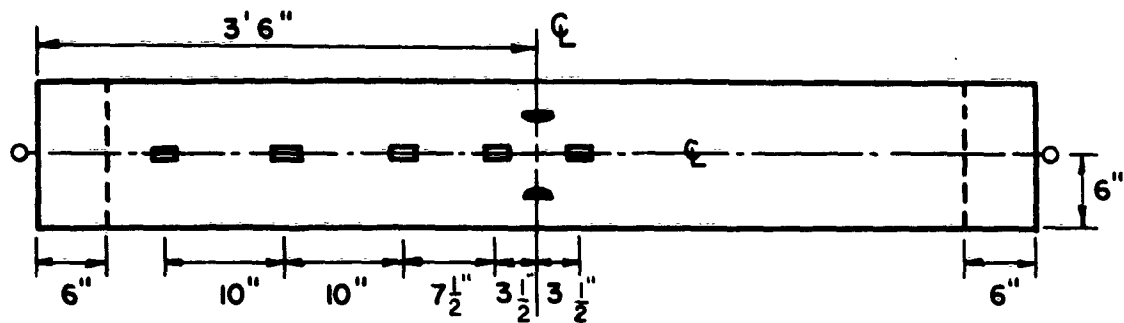
FIG. A-3.   POSITION OF GAGES
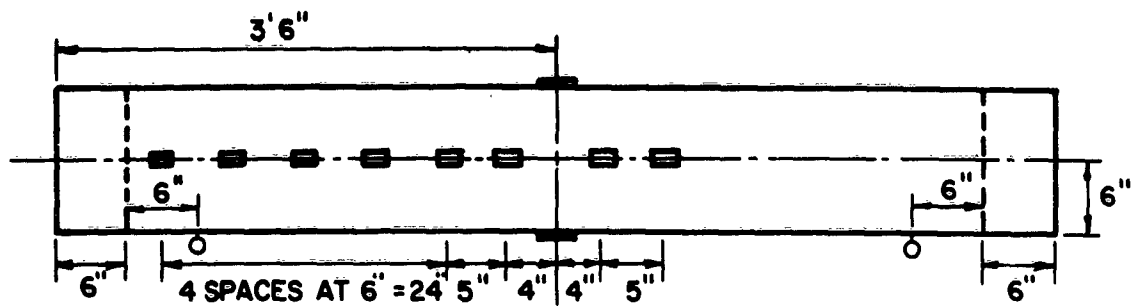
20S3C9 -CONCRETE STRAIN GAGES 3/4" FROM TOP
OF BEAM

27S5D4

IDENTIFICATION KEY FOR GAGES

▭ — STRAIN GAGE ON STEEL PLATE

▨ — STRAIN GAGE ON CONCRETE

◖ — STRAIN GAGE ON STEEL BAR

φ — SLIP GAGE

FIG. A-3 (CONTD.).   POSITION   OF   GAGES

APPENDIX B. DESCRIPTION OF MATERIAL PROPERTIES AND MEASURING EQUIPMENT

B.1 Remarks

This appendix contains descriptions of the properties of the materials used in this investigation. The equipment not described in the body of this report is also briefly described in this appendix.

B.2 Materials

Cement. All cement used in the beams and push-out specimens was high early-strength Type III cement. This permitted the specimens to obtain the desired strengths and they could be tested in approximately five to seven days after casting.

Some of the cement used in casting the lightweight vermiculite aggregate concrete used for cushioning and shaping the load pulse was Type I cement.

Aggregate. Washed Colorado sand and gravel was used in all beams and push-out specimens. The maximum size of coarse aggregate used in the first 9 beams and first 3 push-out specimens was 3/4 inch. The maximum size of aggregate used in all other specimens was 1 inch. The fineness modulus for all of the sand used was approximately 3.0. The saturated-surface-dry absorption was about one per cent by weight for the fine aggregate and about 2 per cent for the coarse aggregate.

The aggregate used in the lightweight concrete which was used for cushioning the falling mass is identified as vermiculite No. 3. This aggregate is graded so that almost all of the material passes a No. 8 sieve and all of it is retained on a No. 50 sieve. This material is used commercially in insulating plaster.

Concrete. Concrete compressive strengths of 3000 psi and 5000 psi were desired for this investigation. The average concrete strengths obtained were approximately 2900 psi and 4700 psi, respectively, at the time of test. Actual concrete compressive strengths for the individual specimens may be found in Table A-1. Slumps ranged from 1-3/4 to 6 in. with an average of 4 inches.

Steel plate. The steel plates used in all of the beams were cut from stock plate 1/4-in. thick. No information was known on the direction of roll on any of the plates, and all of the plates did not come from the same ingot. This probably accounts for some of the differences in properties. To determine various properties of the plates, a coupon 2 in. wide and 12. long was cut from the end of each of the plates. This area of the plates was not strained at all during the beam tests. Each coupon was milled down to 1 in. wide in the center and load-deformation characteristics were obtained. A mechanical extensometer was used to obtain deformations. Table B-1 gives the material properties thus found.

Shear connectors. All of the shear connectors used were Nelson studs obtained from Gregory Industries, Incorporated. Two sizes of studs were used with diameters of 1/2 and 5/8 inch. All studs were

TABLE B-1

Properties of Steel Plates

Specimen No.	Yield Stress psi	Ultimate Stress psi	Modulus of Elasticity psi
4S5A9	35,700	56,600	27,000,000
7S3B9	37,650	58,400	28,500,000
8D3B9	42,000	63,000	29,700,000
9D3A6	34,200	55,000	---
10D5A9	37,900	59,068	27,750,000
11D5B9	37,600	56,800	32,350,000
12D3A12	37,300	57,100	---
13D3A9	38,000	58,300	---
14D3B12	38,300	57,800	28,700,000
16D3A14	36,000	63,700	31,000,000
17D5A11	38,000	62,900	28,800,000
18D3A12	38,000	62,400	29,400,000
20S3C9	39,000	54,300	28,000,000
22D3C9	39,000	61,200	28,500,000
23D3A9	40,000	62,500	---
24D3B6	39,000	62,500	29,000,000
25D3C6	41,000	63,800	29,400,000
26D5D4	40,000	63,500	30,000,000
27S5D4	39,000	62,800	27,500,000
28S3C12	41,000	63,200	29,500,000
29D3C12	34,000	55,700	---
30D3C6	40,000	62,200	28,000,000

126

approximately 4 in. long except those used in the first static beam test and the first push-out test, which were approximately 5-1/2 in. long. The dimensions of the 4-in.-length studs are shown in Fig. B-1. According to the stud manufacturer, the studs are made from low carbon steel with a minimum yield strength of 60,000 psi and minimum ultimate tensile strength of 70,000 psi.
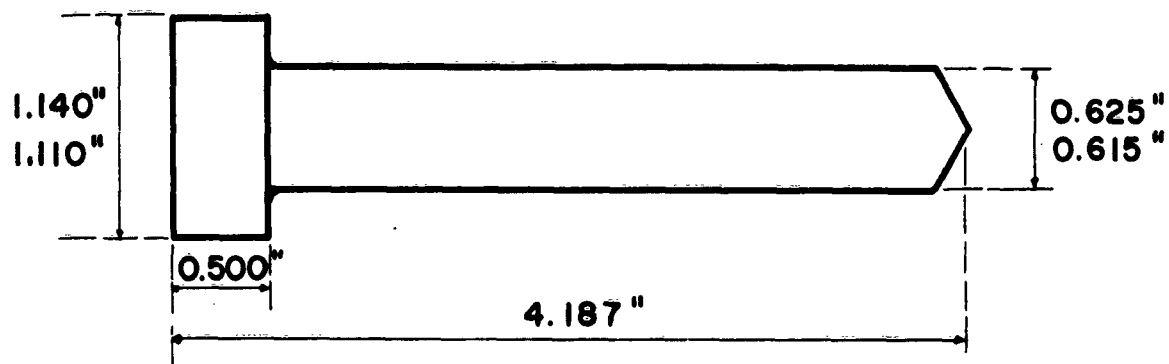
Reinforcing bars. Two high-strength deformed No. 8 bars were used as tension reinforcement in all of the beams in the plate-in-compression series. A typical static stress-strain curve for these bars is shown in Fig. B-2.

Shear reinforcement. Closed welded stirrups were used in all beams with an identification number larger than 17. Both No. 2 plain bars and No. 3 deformed bars made from mild steel were used in making the stirrups. (See Fig. A-2 for stirrups size and spacing.)

Vermiculite concrete. The vermiculite concrete which was used as a cushioning material was made with mix proportions of 1:4, 1:6, and 1:8 loose volume of cement to aggregate. Typical mix proportions for a 1:8 mix follow:

Expanded vermiculite aggregate	2 cu ft
Type I portland cement	0.25 cu ft
Water	0.84 cu ft
Admixture (AEA)	200 grams

For further information concerning mix proportions and mixing techniques, see Ref. 7.

5/8 IN.-DIA. STUD
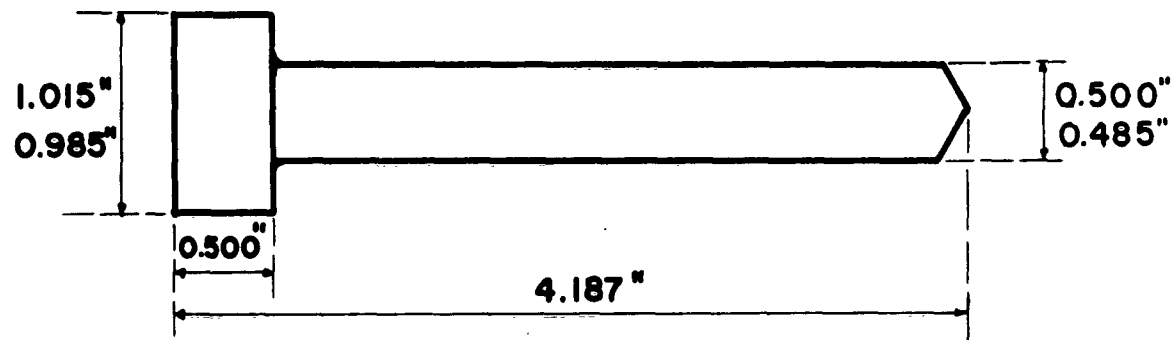
1/2 IN.-DIA. STUD
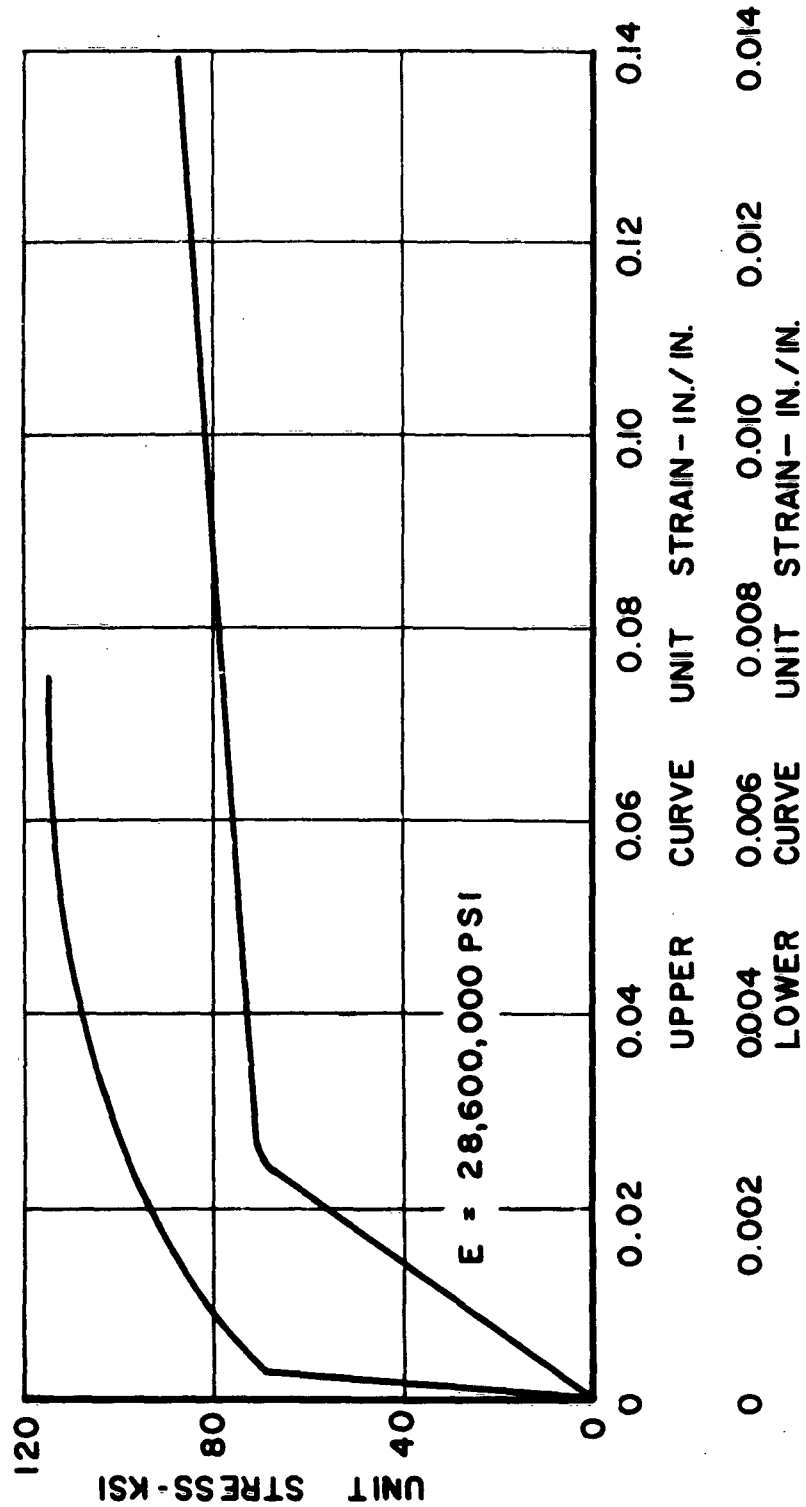
FIG. B-I.   DIMENSIONS OF STUDS

128

FIG. B-2. TYPICAL STATIC STRESS-STRAIN CURVE FOR NO. 8 DEFORMED REINFORCING BAR

E = 28,600,000 PSI

UNIT STRESS - KSI

| UPPER CURVE | UNIT STRAIN - IN./IN. | 0 | 0.002 | 0.04 | 0.06 | 0.08 | 0.10 | 0.12 | 0.14 |
| LOWER CURVE | UNIT STRAIN - IN./IN. | 0 | 0.002 | 0.004 | 0.006 | 0.008 | 0.010 | 0.012 | 0.014 |

Some of the early batches were made with high early-strength Type III cement. The average dynamic crushing stress of the vermiculite concrete ranged from approximately 400 psi to 2500 psi, in which the concrete made with the Type III cement gave the higher crushing stresses.

Spiralgrid. A material designated as Spiralgrid which was manufactured by the General Grid Corporation was used for three of the beam tests. Figure B-3 shows a static force-deformation curve for this material. Figure B-4 shows a cylinder of tapered Spiralgrid before and after crushing. Spiralgrid is made by wrapping a combination of plain aluminum foil and an aluminum corrugation into a cylindrical shape. From tests performed by the General Grid Corporation, Spiralgrid was superior to both Trussgrid and regular honeycomb-type cores for long columns, since it is symmetrical about its axis and crushes uniformly.

B.3 Equipment

Visicorder. A Honeywell Model 906A Visicorder oscillograph was used to record six of the measurements in the dynamic beam tests and all of the measurements in the dynamic push-out tests. The electrical signals from the various measuring devices were amplified before being fed into the Visicorder. The Visicorder is an oscillograph which utilizes high sensitivity subminiature plug-in galvanometers. The galvanometers reflect light beams on light-sensitive paper running through the Visicorder. Thus the signal is recorded. The frequency response for this model ranges from 0 to 3000 cps.
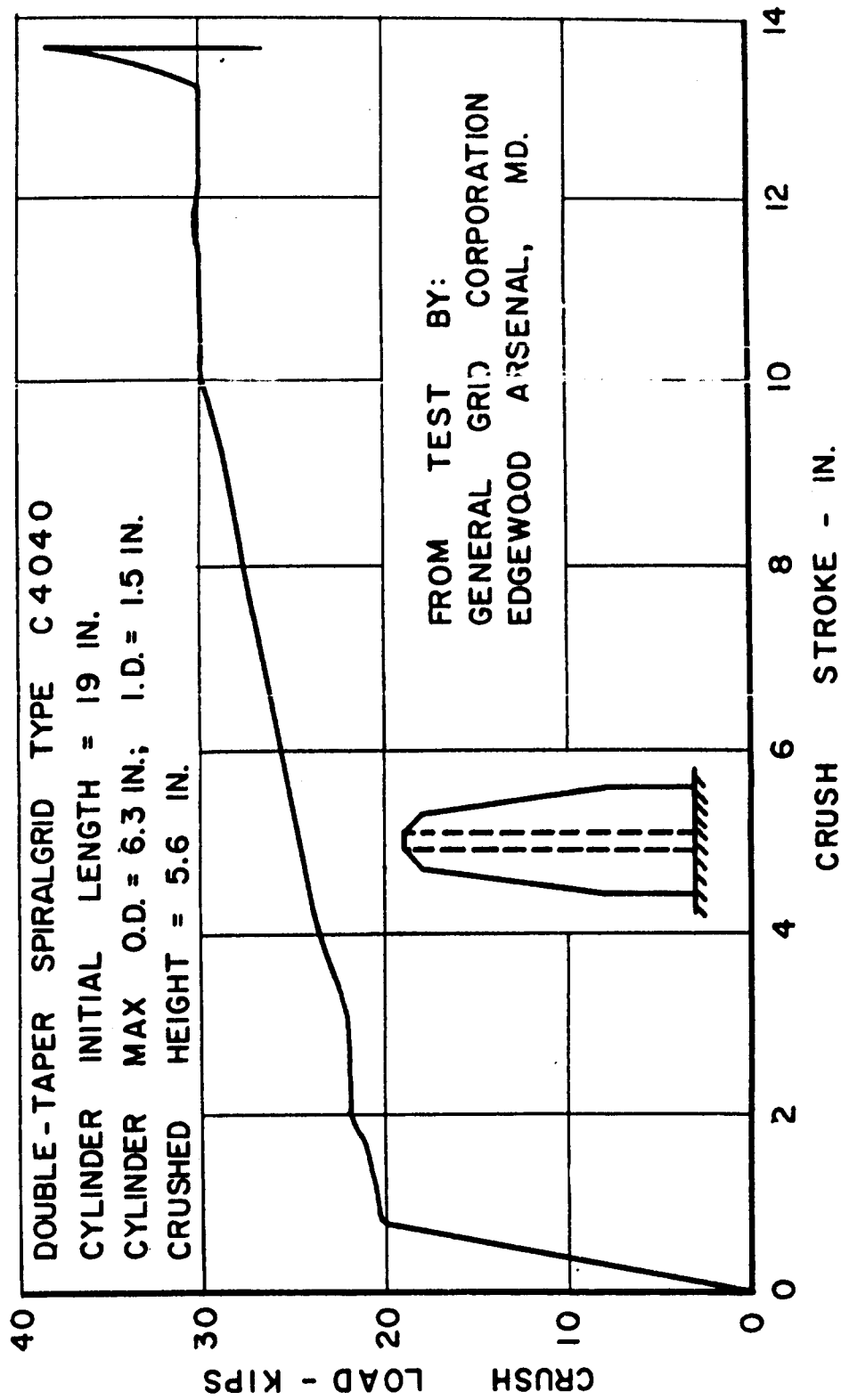
DOUBLE-TAPER SPIRALGRID TYPE C4040
CYLINDER INITIAL LENGTH = 19 IN.
CYLINDER MAX O.D. = 6.3 IN.;   I.D. = 1.5 IN.
CRUSHED HEIGHT = 5.6 IN.

FROM TEST BY:
GENERAL GRID CORPORATION
EDGEWOOD ARSENAL, MD.

LOAD - KIPS

CRUSH

CRUSH STROKE - IN.

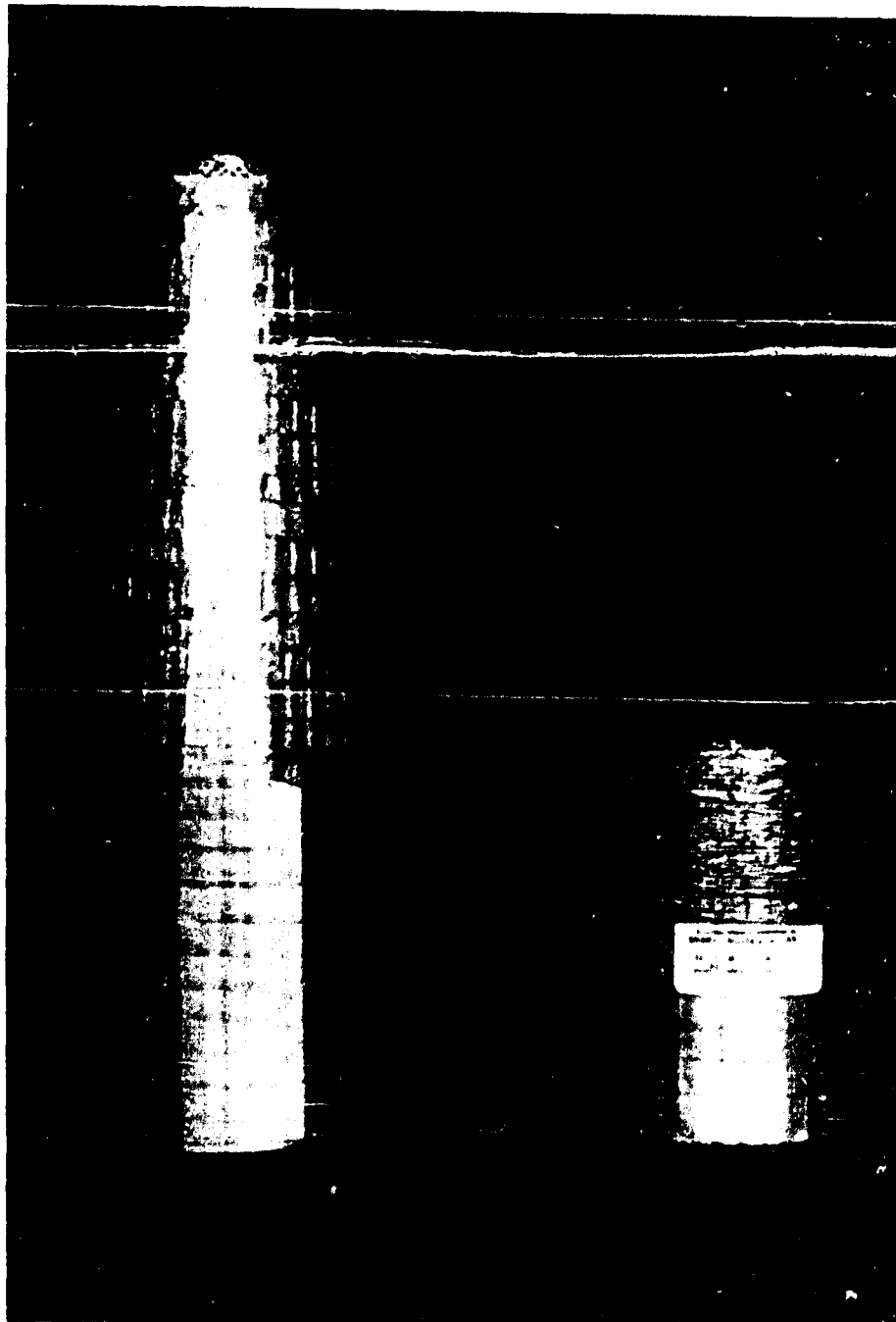FIG. B-3.   STATIC FORCE DEFORMATION CURVE OF SPIRALGRID

FIG. B.4.   PHOTOGRAPH OF SPIRALGRID BEFORE AND
AFTER CRUSHING

132

Oscilloscopes and camera. The measurements not recorded by the Visicorder were recorded either by a Tektronix Type 551 dual-beam cathode-ray oscilloscope or a Hewlett-Packard Model 130B oscilloscope. The traces were photographed as they moved across the screens by Polaroid cameras attached to the oscilloscopes.

Fastax movie camera. A 16-mm Fastax movie camera made by the Wollensak Optical Company was used to record most of the tests during impact. This camera has the ability to take up to 8000 frames per second. However, only about 6200 frames per second was the maximum taken during this investigation.

Accelerometer. A strain-gage-type accelerometer made by the Consolidated Electrodynamics Corporation was mounted on the top of the mass to measure the acceleration of the mass. This accelerometer had a maximum acceleration response of 50g. The data necessary for calibration of the accelerometer was given by the manufacturer.

The following equation was used for calibration.

$$N = \frac{10^6}{4F} \left(\frac{R}{R_c + 0.5R} \right) \qquad\qquad ----- \text{(B-1)}$$

where

N = Number of units of acceleration

R = Transducer bridge resistance

F = Calibration factor

R_c = Calibrating resistor

The above equation yielded a calibration of 10. 1g for the calibrating resistor used in this investigation.

Strain gages. Three types of electrical-resistance-type strain gages were used in this investigation. All gages were obtained from the Baldwin Lima Hamilton Company. The gages used on the slip devices were Baldwin Type FA-25-12, S-6. All gages used on the steel plates and reinforcing bars were Baldwin Type FA-50-12, S-6. The gages used on the concrete were wire Type A-12 gages.

The gages used on the steel plate, concrete, and steel reinforcing were all used in pairs. Calibration of the strain gages was accomplished by using Eq. (B-2).

$$\varepsilon = \frac{R}{S \times GF} \qquad \text{- - - - - (B-2)}$$

where

ε = Units of strain in inches per inch

R = Total resistance of the two strain gages

S = Resistance of the shunt used

GF = Gage factor of the gages

Potentiometer. A precision potentiometer made by the Technology Instrument Corporation in Acton, Massachusetts, was mounted on a stationary stand underneath the center of the beam to measure the deflection of the beam. This potentiometer was a slide-wire type with a travel of 2-1/2 inches. It produced linear response throughout its range. A

134

lever-fulcrum device was made to use with the potentiometer on some tests to measure deflections more than 2-1/2 inches. This device was also rigged to produce linear response. Accurate resolutions of 1/100 of an inch could be obtained.

Dynamometers. Four dynamometers which were made in the Structural Mechanics Research Laboratory at The University of Texas were used under the ends of the beams to measure the end reactions. Each dynamometer was instrumented with eight electric-resistance foil strain gages mounted on a reduced area section of the dynamometer. Four of the strain gages were longitudinal and four were transverse, mounted diametrically opposite to each other to eliminate bending effects. Two dynamometers mounted side by side under each end of the beam were wired into a single bridge to measure the total reaction at each end. Each dynamometer had an ultimate capacity of 61 kips giving an end reaction capacity of 122 kips. With the hookup arrangements and preamplification used, resolutions as small as 100 lb were easily accomplished.

DISTRIBUTION

No. cys

HEADQUARTERS USAF

1   Hq USAF (AFOCE-KA), Wash, DC 20330

1   Hq USAF (AFRNE-B, Maj Lowry), Wash, DC 20330

1   Hq USAF (AFTAC), Wash, DC 20330

MAJOR AIR COMMANDS

1   AFSC (SCT), Andrews AFB, Wash, DC 20331

1   SAC (OA), Offutt AFB, Nebr 68113

1   AFLC (MCSW), Wright-Patterson AFB, Ohio 45433

1   ADC (Ops Anlys), Ent AFB, Colorado Springs, Colo 80912

1   AUL, Maxwell AFB, Ala 36112

2   USAFIT, Wright-Patterson AFB, Ohio 45433

1   USAFA, Colo 80840

AFSC ORGANIZATIONS

1   AF Materials Laboratory, Wright-Patterson AFB, Ohio 45433

    ASD, Wright-Patterson AFB, Ohio 45433

1   (SEPIR)

1   (ASAMCC)

    RTD, Bolling AFB, Wash, DC 20332

1   (RTN-W, Lt Col Munyon)

1   (RTS)

1   BSD (BSSF), Norton AFB, Calif 92409

    ESD, L. G. Hanscom Fld., Bedford, Mass 01731

1   (CRRA)

1   (CRZG)

KIRTLAND AFB ORGANIZATIONS

1   AFSWC (SWEH), Kirtland AFB, NM 87117

10   AFWL, Kirtland AFB, NM 87117

5   (WLR)

        (WLIL)

OTHER AIR FORCE AGENCIES

1   Director, USAF Project RAND, via: Air Force Liaison Office, The RAND Corporation, ATTN: RAND Library, 1700 Main Street, Santa Monica, Calif 90406

DISTRIBUTION (cont'd)

ARMY ACTIVITIES

1   Chief of Research and Development, Department of the Army
(Special Weapons and Air Defense Division), Wash, DC 20310

2   Chief of Engineers (ENGMC-EM), Department of the Army, Wash,
DC 20315

1   Director, Army Research Office 3045 Columbia Pike, Arlington, Va
22204

Director, US Army Waterways Experiment Sta, P.O. Box 631,
Vicksburg, Miss 39181

2   (WESRL)

2   (WESVC)

NAVY ACTIVITIES

1   Bureau of Yards and Docks, Department of the Navy, Code 22.102,
(Branch Manager, Code 42.330), Wash 25, DC

3   Commanding Officer and Director, Naval Civil Engineering
Laboratory, Port Hueneme, Calif

1   Officer-in-Charge, Naval Civil Engineering Corps Officers School,
US Naval Construction Battalion Center, Port Hueneme, Calif

OTHER DOD ACTIVITIES

2   Director, Defense Atomic Support Agency (Document Library Branch),
Wash, DC 20301

1   Commander, Field Command, Defense Atomic Support Agency
(FCAG3, Special Weapons Publication Distribution), Sandia Base,
NM 87115

1 . Office of Director of Defense Research and Engineering, ATTN:
John E. Jackson, Office of Atomic Programs, Room 3E 1071,
The Pentagon, Wash, DC 20330

20   Hq Defense Documentation Center for Scientific and Technical
Information (DDC), Bldg 5, Cameron Sta, Alexandria, Va 22314

AEC ACTIVITIES

1   Sandia Corporation (Information Distribution Division) Box 5800,
Sandia Base, NM 87115

OTHER

1   Office of Assistant Secretary of Defense (Civil Defense), Wash, DC
20301

1   OTS, Department of Commerce, Wash 25, DC

1   General American Transportation Corp., MRD Division, ATTN:
Dr. G. L. Neidhardt, 7501 N. Natchez Ave., Niles, Ill

DISTRIBUTION (cont'd)